



National Aeronautics and
Space Administration

P-170
#304584

Energy Efficient Engine

Flight Propulsion System Final Design and Analysis

by

D.Y. Davis
E.M. Stearns

General Electric Company

August 1985

Prepared for

National Aeronautics and Space Administration


N90-28558

Uncl. as
0304584

63/07

(NASA-CR-168219) ENERGY EFFICIENT ENGINE:
FLIGHT PROPULSION SYSTEM FINAL DESIGN AND
ANALYSIS Report, Nov. 1973 - Aug. 1983 (GE)
CSCL 21E
170 P

These limitations shall be considered void after two (2) years after date of such data.

1. Report No. NASA CR-168219		2. Government Accession No.		3. Recipient's Catalog No.	
4. Title and Subtitle Energy Efficient Engine - Flight Propulsion System Final Design and Analysis				5. Report Date August 1985	
				6. Performing Organization Code	
7. Author(s) D.Y. Davis E.M. Stearns				8. Performing Organization Report No. R83AEB488	
				10. Work Unit No.	
9. Performing Organization Name and Address General Electric Company Aircraft Engine Business Group Evendale, Ohio 45215				11. Contract or Grant No. NAS3-20643	
				13. Type of Report and Period Covered Nov. 1978 - Aug. 1983	
12. Sponsoring Agency Name and Address National Aeronautics and Space Administration Lewis Research Center 21000 Brookpark Rd. Cleveland, Ohio 44135				14. Sponsoring Agency Code	
15. Supplementary Notes Project Manager: Mr. C.C. Ciepluch NASA-Lewis Research Center Cleveland, Ohio 44135					
16. Abstract <p>The Energy Efficient Engine (E³) is a NASA program to create fuel saving technology for future transport engines. The Flight Propulsion System (FPS) is the engine designed to achieve E³ goals.</p> <p>Achieving these goals required aerodynamic, mechanical and system technologies advanced beyond that of current production engines. These technologies have been successfully demonstrated in component rigs, a core engine and a turbofan ground test engine. The design and benefits of the FPS are presented in this report.</p> <p>All goals for efficiency, environmental considerations, and economic payoff were met. The FPS has, at maximum cruise, 10.67 km (35,000 ft), M0.8, standard day, a 16.9% lower installed specific fuel consumption than a CF6-50C. It provides an 8.6% reduction in direct operating cost for a short haul domestic transport and a 16.2% reduction for an international long distance transport.</p>					
17. Key Words (Suggested by Author(s)) Energy Conservation Subsonic Transport Turbine Engine Aircraft Turbine Engine Energy Efficient Engine			18. Distribution Statement 		
19. Security Classif. (of this report) Unclassified		20. Security Classif. (of this page) Unclassified		21. No. of Pages	22. Price*



[REDACTED]

[REDACTED]

FOREWORD

This report presents the final preliminary analysis and design of an advanced Flight Propulsion System (FPS) conducted by the General Electric Company. This work was performed for the National Aeronautics and Space Administration (NASA), Lewis Research Center, under Contract NAS3-20643 as part of the Aircraft Energy Efficiency (ACEE) Program, Energy Efficient Engine (E³) Project. Mr. Carl C. Ciepluch was the NASA E³ Project Manager; Mr. Peter G. Batterton was the NASA Assistant Project Manager. Mr. Roger Chamberlin was the NASA Project Engineer responsible for the effort associated with the Flight Propulsion System - Final Analysis and Design reported herein. Mr. Donald Y. Davis was Manager of the E³ Project for the General Electric Company.

PRECEDING PAGE BLANK NOT FILMED

TABLE OF CONTENTS

<u>Section</u>	<u>Page</u>
1.0 SUMMARY	1
2.0 INTRODUCTION	6
3.0 FLIGHT PROPULSION SYSTEM DESIGN AND ANALYSIS	9
3.1 Features	9
3.2 Maintainability	12
3.3 Durability	16
3.4 Growth	18
3.5 Performance Retention	21
3.6 Acoustics	22
3.7 System Compatibility	25
4.0 CYCLE AND ENGINE PERFORMANCE	30
4.1 Cycle History and Selection Criteria	30
4.2 Initial FPS Cycle Selection Process	30
4.3 Final Cycle Refinement	32
4.4 Cycle Definition	33
4.5 Reference Engine Comparison	36
4.6 Starting	36
5.0 COMPONENT AND SYSTEM DESIGN AND PERFORMANCE	37
5.1 Fan	37
5.1.1 Aerodynamic Design	41
5.1.2 Mechanical Design	45
5.1.3 Performance	45
5.2 Compressor	45
5.2.1 Aerodynamic Design	48
5.2.2 Mechanical Design	52
5.2.3 Performance	56
5.3 Combustor	57
5.3.1 Aerodynamic Design	57
5.3.2 Mechanical Design	61
5.3.3 Performance	62
5.4 High Pressure Turbine	65
5.4.1 Aerodynamic Design	65
5.4.2 Mechanical Design	71
5.4.3 Cooling Design	73
5.4.4 Performance	76

TABLE OF CONTENTS (Concluded)

<u>Section</u>	<u>Page</u>
5.5 Low Pressure Turbine	82
5.5.1 Aerodynamic Design	85
5.5.2 Mechanical Design	87
5.5.3 Cooling Design	88
5.5.4 Performance	90
5.6 Turbine Frame	90
5.7 Sumps, Drives, Configuration, and Lube System	96
5.7.1 Bearing System	96
5.7.2 Forward Sump	96
5.7.3 Aft Sump	98
5.7.4 Configuration	98
5.7.5 Lube System	100
5.8 Exhaust System	101
5.9 Nacelle	102
5.9.1 Fan Reverser	105
5.9.2 Mount System	110
5.9.3 Accessory Package	114
5.10 Control System	114
5.10.1 Design	114
5.10.2 Fuel Control System	125
5.10.3 Stator Control System	128
5.10.4 Active Clearance Control System	131
5.10.5 Fuel Heater/Regenerator System	133
5.10.6 Performance	133
5.11 Dynamic System	135
5.11.1 Design	135
5.11.2 Performance	137
5.12 Weight	139
5.13 Cost	139
6.0 ENGINE/AIRCRAFT INTEGRATION	142
6.1 Sensitivity Factors	142
6.2 Economic Evaluation	143
7.0 CONCLUSIONS	147
8.0 RECOMMENDATIONS	148
9.0 REFERENCES	149

LIST OF ILLUSTRATIONS

<u>Figure</u>		<u>Page</u>
1.	E ³ Flight Propulsion System (FPS) Design.	4
2.	E ³ Flight Propulsion System Features.	11
3.	FPS On-Wing Access Provisions.	13
4.	Energy Efficient Engine Modules.	14
5.	FPS Maintainability Features.	15
6.	E ³ Typical Flight Cycle.	17
7.	Performance Degradation Characteristics.	23
8.	E ³ Low Noise Design Features.	24
9.	Fan Frame Acoustic Design.	26
10.	Sample Stability Stack Crosswind - Fan at Takeoff Thrust.	28
11.	Sample Stability Stack Crosswind - Compressor at Takeoff Thrust.	28
12.	E ³ Cycle Selection.	31
13.	E ³ Fan Cross Section.	38
14.	E ³ Fan Component.	39
15.	Particle Trajectories.	40
16.	Typical Tests and Particle Size Distribution.	42
17.	Inner Outlet Guide Vane.	44
18.	E ³ Compressor Cross Section.	47
19.	High Pressure Compressor Rotor Design Features.	53
20.	Compressor Rotor Hardware.	54
21.	Compressor Stator Design Features.	55
22.	E ³ Combustor Cross Section.	59
23.	Combustor Liner/Dome Assembly - Aft Looking Forward.	60

LIST OF ILLUSTRATIONS (Continued)

<u>Figure</u>		<u>Page</u>
24.	E ³ High Pressure Turbine Cross Section.	66
25.	Stage 1 High Pressure Turbine Nozzle Assembly.	67
26.	High Pressure Turbine Rotor Assembly.	68
27.	High Pressure Turbine Active Clearance Control Manifolds.	69
28.	High Pressure Turbine Cooling Flow Supply Circuits.	74
29.	Stage 1 Blade-Tip Clearances.	77
30.	Interstage Seal Clearances.	78
31.	Stage 2 Blade-Tip Clearances.	79
32.	E ³ Low Pressure Turbine Cross Section.	83
33.	Low Pressure Turbine Rotor Assembly.	84
34.	Turbine Frame with Aft Sump Installed.	92
35.	E ³ Turbine Frame Cross Section.	93
36.	E ³ Turbine Frame Cross Section - End View.	94
37.	E ³ Forward Sump Design.	97
38.	E ³ Aft Sump Design.	99
39.	E ³ Mixer.	103
40.	Nacelle General Arrangement.	106
41.	Front View, Reverser Cross Section.	107
42.	E ³ FPS Thrust Reverser Actuation.	109
43.	Overall Engine Reverser Thrust Comparison.	111
44.	Mount Links.	112
45.	Forward Mount Brackets/Fan Frame.	113
46.	E ³ FPS Accessory Package.	117

LIST OF ILLUSTRATIONS (Concluded)

<u>Figure</u>		<u>Page</u>
47.	Full Authority Digital Electronic Control (FADEC).	119
48.	Control System Inputs.	121
49.	Control System Outputs.	123
50.	Hybrid Electronics.	124
51.	ICLS Full Authority Digital Electronic Control.	126
52.	E ³ Fuel System.	127
53.	Compressor Stator Vane Control.	129
54.	Clearance Control System.	132
55.	Fuel Heater/Regenerator Schematic.	134
56.	Core Rotor Soft Support and Squeeze-Film Damper System.	136
57.	Number 3 Bearing Soft Support and High Load Damper.	138
58.	DOC Improvement Relative to CF6-50C.	146

LIST OF TABLES

<u>Table</u>		<u>Page</u>
I.	E ³ FPS Program Goals and Status.	2
II.	Component Performance at Maximum Cruise Thrust.	5
III.	E ³ FPS Cycle Characteristics.	9
IV.	E ³ FPS Reliability Features.	16
V.	FPS Life.	18
VI.	E ³ Growth Capability.	19
VII.	Growth Component Changes.	20
VIII.	Estimated In-Service Performance Losses.	23
IX.	E ³ Noise Margin From FAR 36.	27
X.	E ³ FPS Stability Assessment.	29
XI.	FPS Component Performance - Maximum Cruise Conditions.	34
XII.	FPS Cycle Definition.	35
XIII.	Fan Performance.	46
XIV.	FPS Compressor Aerodynamic Cycle Match.	51
XV.	Compressor Performance.	58
XVI.	Combustor Performance.	63
XVII.	FPS Emissions.	64
XVIII.	HPT Aerothermodynamic Cycle Match Point.	70
XIX.	Active Clearance Control System Payoff.	80
XX.	High Pressure Turbine Performance.	81
XXI.	LP Turbine Cycle Match Point.	86
XXII.	Low Pressure Turbine Performance.	91
XXIII.	Mixer Performance at Maximum Cruise.	104

LIST OF TABLES (Concluded)

<u>Table</u>		<u>Page</u>
XXIV.	Accessory Gearbox Location Trade Study Results.	115
XXV.	Qualitative Factors in Accessory Package Selection.	116
XXVI.	FPS Weight Summary.	140
XXVII.	FPS Cost Summary.	141
XXVIII.	Direct Operating Cost Sensitivity Factors.	144
XXIX.	DOC Improvements.	145

LIST OF ABBREVIATIONS

ACC	Active Clearance Control
AMAC	Advanced Multistage Axial Flow Core Compressor
CD&I	Component Development and Integration
DOC	Direct Operating Cost
ECS	Environment Control System
EPNdB	Effective Perceived Noise Level, decibels
FADEC	Full Authority Digital Electronic Control
FICA	Failure Indication and Corrective Action
FOD	Foreign Objective Damage
FPS	Flight Propulsion System
G/B	Gearbox
GI	Ground Idle
HPT	High Pressure Turbine
ICLS	Integrated Core/Low Spool
IGV	Inlet Guide Vane
LPT	Low Pressure Turbine
M	Mach Number
MXCL	Maximum Climb
MXCR	Maximum Cruise
MZSOV	Main Zone Shutoff Valve
N_c	Core Physical Speed
N_f	Fan Physical Speed
N_1	Fan Physical Speed
N_2	Core Physical Speed
N/\sqrt{T}	Turbine Corrected Speed
OGV	Outlet Guide Vane
PD&I	Preliminary Design and Integration
PTO	Power Takeoff
P_{S3}	Static Pressure at Compressor Discharge
P_{T0}	Freestream Total Pressure
PZRV	Pilot Zone Reset Valve
sfc	Specific Fuel Consumption

LIST OF ABBREVIATIONS (Concluded)

T/O	Takeoff
T ₂₅	Total Temperature at Core Inlet
T ₃	Total Temperature at High Pressure Turbine
T ₁₂	Total Temperature at Fan Inlet
T ₄₁	High Pressure Turbine Rotor Inlet Temperature
T ₄₂	Total Temperature at High Pressure Turbine Discharge
T ₄₉	Low Pressure Turbine Inlet Temperature
VSV	Variable Stator Vane
W _f	Fuel Flow
W ₂₅	Physical Core Airflow at Core Inlet
$\frac{W\sqrt{T}}{P}$	Turbine Corrected Flow

1.0 SUMMARY

The Energy Efficient Engine (E³) program is part of the National Aeronautics and Space Administration (NASA) Aircraft Energy Efficiency program. The objective of this program is to substantially improve the efficiency of commercial transport aircraft which would enter service in the late 1980's and early 1990's.

NASA established specific performance, economic, and environmental goals for E³. The General Electric E³ Flight Propulsion System (FPS) meets these goals. These goals and the current status are shown in Table I. The FPS design was reported first in 1980 and updated in 1982. This report presents the final design and the economic benefits of the FPS.

The E³ FPS design is self-contained, ready to mount and interface with the aircraft pylon. It incorporates advances in technology beyond that employed for engines currently in service. To evaluate these new technologies, the E³ program included rig tests of each component, a core engine test, and a turbofan engine test.

The General Electric E³ FPS features include:

- A long duct, mixed-flow, acoustically treated bulk absorber nacelle incorporating a cascade-type thrust reverser.
- A core-mounted accessory drive module.
- A highly efficient, wide-chord, 32-blade fan and debris-separating booster module.
- A 10-stage, 23:1 pressure ratio compressor.
- A double annular combustor for low emissions.
- A highly efficient two-stage high pressure turbine and a five-stage low pressure turbine.
- A two-frame, five-bearing design.
- Spring-mounted bearing supports with viscous damping on the core thrust bearing.
- A full authority digital electronic control (FADEC).

Table I. E³ FPS Program Goals and Status.

FPS Characteristic	NASA Goal	FPS Status
<ul style="list-style-type: none"> ● Installed Specific Fuel Consumption (SFC) 	Minimum 12% Reduction From CF6-50C ⁽¹⁾	16.6% Reduction ⁽¹⁾ 16.9% Reduction ⁽²⁾
<ul style="list-style-type: none"> ● Direct Operating Cost (DOC) 	Minimum 5% Reduction From CF6-50C on Equivalent Aircraft	8.6% to 16.2% Reduction Depending on Aircraft and Distance
<ul style="list-style-type: none"> ● Noise 	Meet FAR 36 (1978) Provisions for Growth	Meets With Margin
<ul style="list-style-type: none"> ● Emissions 	Meet EPA Proposed 1981 Standards	Meets Goal
<ul style="list-style-type: none"> ● Performance Retention 	Minimum 50% Reduced Deterioration From CF6-50C Levels	Projected to Meet
<p>(1) Using E³ ground rules which specify maximum cruise thrust at M = 0.8, 10.67 km (35,000 ft) with zero bleed and power extraction.</p> <p>(2) Maximum cruise thrust at M = 0.8, 10.67 km (35,000 ft) with bleed and power extraction, using the bleed air/fuel heater system.</p>		

- A mixer to combine fan and core exhaust flows.
- Case cooling systems to actively control blade tip clearances in the compressor, high pressure turbine, and low pressure turbine.
- Composite materials and advanced manufacturing techniques.
- Component efficiency levels above previous state of the art.

The FPS engine is shown in Figure 1.

The component test program has been completed. Component performance results are shown in Table II.

The core engine and integrated core/low spool (ICLS) engine tests have been completed. The results of ICLS testing exceeded the performance goals established in the E³ program. During both core and ICLS tests, the engines operated without aerothermal or mechanical problems. At sea level static, standard day takeoff, specific fuel consumption of 0.0332 kg/hr-N (0.326 lbm/hr-lbf) was measured during testing of the heavily instrumented ICLS turbofan engine.

The specific fuel consumption projected for the FPS is based on improvement which can conservatively be expected during the development of a production engine. Because many components achieved performance levels significantly better than their goal levels, the component performance requirements for FPS have been increased. Final component requirements are shown in Table II. Based on these component performance levels, optimized cooling flow utilization and cycle rematching, the uninstalled (no nacelle drag) specific fuel consumption at standard day maximum cruise conditions projected for the E³ FPS is 0.0539 kg/hr-N (0.529 lbm/hr-lbf) at Mach 0.8/10.67 km (35,000 ft).

Fuel prices have increased from the 7.9¢ to 13.2¢ per liter (30¢ to 50¢ per gallon) range used initially in the E³ program to about \$0.396 per liter (\$1.50 per gallon) in the current market. The higher fuel price has substantially increased the economic payoff due to the more fuel-efficient E³.

E³ direct operating cost is now 8.6% to 16.2% lower than a typical current production engine, the CF6-50. This range covers a spectrum of aircraft size and flight lengths.

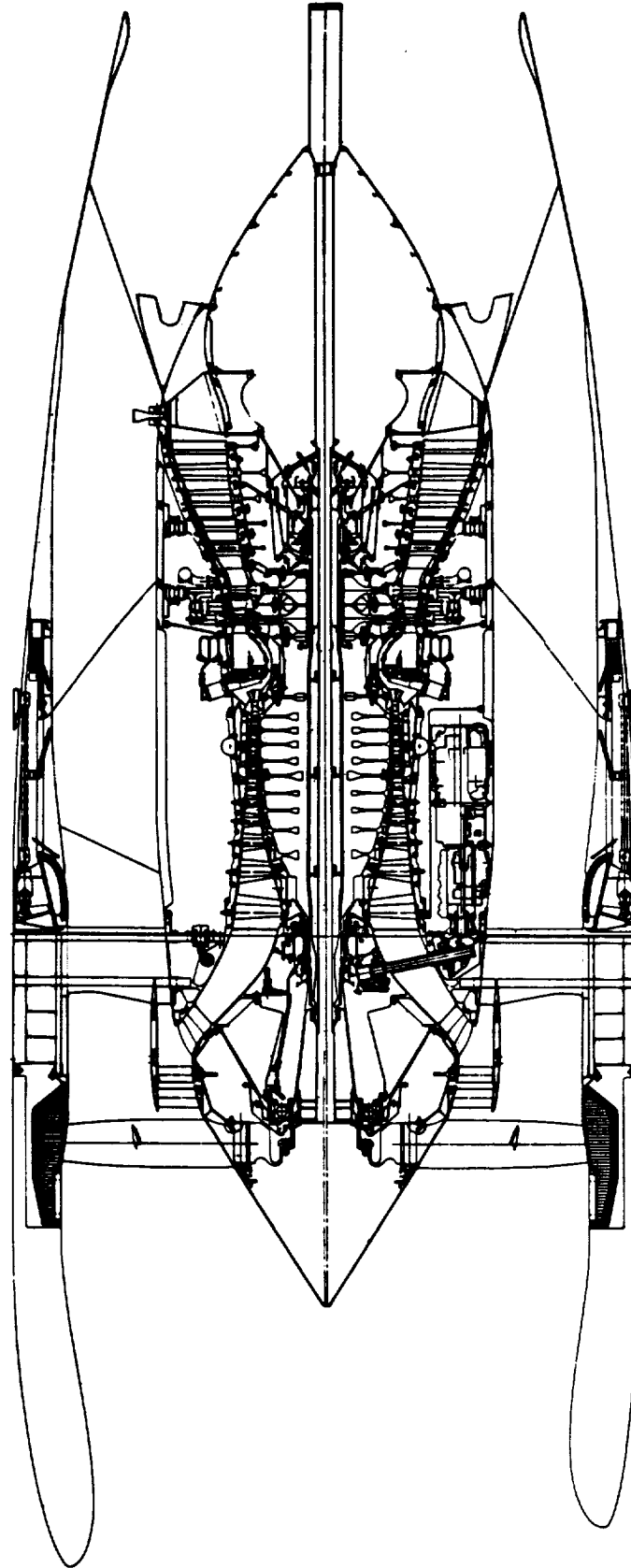


Figure 1. E³ Flight Propulsion System (FPS) Engine.

Table II. Component Performance at Maximum Cruise Thrust.

	Initial FPS Requirements	Component Test Results	Final FPS Requirements
Fan Efficiency	0.887	0.892	0.894
Fan Hub and Booster Efficiency	0.892	0.895	0.906
Compressor Efficiency	0.861	0.856	0.861
Combustor Efficiency	0.995	0.9995	0.999
Combustor Pressure Drop, %	5	4.8	5
Combustor Emissions	EPA Proposed 1981 Standards	Met Goal Except NO _x	EPA Proposed 1981 Standards
High Pressure Turbine Efficiency	0.924	0.925	0.927
Low Pressure Turbine Efficiency	0.917	0.916	0.925
Mixer, SFC Improvement, %	3.1	2.6 Demonstrated	2.9

2.0 INTRODUCTION

The objective of the E³ program is the development of technology to improve the energy efficiency of propulsion systems for subsonic commercial aircraft introduced in the late 1980's. The need for E³ type programs was established by shortages of petroleum-based fuels. Since the E³ program was launched, escalated fuel prices have made improved aircraft energy efficiency essential. The E³ program is a major element of the NASA Aircraft Energy Efficient Program.

The following technical goals were established by NASA for the fully developed E³ Flight Propulsion System:

- Fuel Consumption - Minimum of 12% reduction in installed sfc compared to a CF6-50C at maximum cruise thrust, Mach 0.8 at 10.67 km (35,000 ft) altitude on a standard day with no bleed or power extraction.
- Direct Operating Cost - Minimum of 5% reduction from CF6-50C on equivalent aircraft.
- Noise - Comply with FAR 36 (1978).
- Emissions - Comply with EPA Proposed 1981 Standards for new engines.
- Performance Retention - Minimum of 50% reduction in the rate of performance deterioration in service as compared to the CF6-50C.

To meet and demonstrate the program goals, the E³ program is structured into four major technical tasks.

- Task 1 addresses the design and evaluation of the E³ Flight Propulsion System. The FPS is a complete, fully developed production engine, including nacelle, and is intended to achieve program goals while in and during its commercial service. The design is executed in sufficient depth to evaluate performance, cost, weight, installation considerations, and economic payoff. The information developed in Task 1 establishes the design and performance requirements for hardware to be tested in component rigs, a core engine, and a turbofan engine. Following the component and engine test programs, the FPS is reevaluated. The final FPS is the subject of this report.
- Task 2 consists of the detailed design, fabrication, and rig testing of each engine component and includes supporting technology efforts. Task 2 has been completed.

- Task 3 involves the design, fabrication, and test evaluation of a core test vehicle, consisting of the compressor, combustor, and high pressure turbine. Task 3 has been completed.
- Task 4 integrates the core with the low pressure components to make the Integrated Core/Low Spool (ICLS) turbofan test vehicle. Task 4 has been completed.

The E³ is one of a series of joint technology programs between NASA, industry, and the United States scientific community. The E³ program was preceded by studies of conventional and unconventional engine cycles and by component technology studies.

Work on the E³ started in 1978. Initially, there was a thorough engine cycle optimization phase to evolve the optimum cycle for achieving program goals. The preliminary FPS design was then initiated. In parallel with this effort, aircraft/engine integration work with the Boeing, Lockheed, and Douglas aircraft companies was accomplished. The E³ FPS Preliminary Analysis and Design is reported in Reference 1, and the Aircraft/Engine Integration Evaluation is reported in Reference 2. There was an update of the FPS design reported in Reference 3.

Detail design work then proceeded on the engine system and components. Each component was fabricated, assembled, and rig tested, followed by a core engine test and testing of the ICLS test engine. This design work established the detailed flight designs of almost all of the FPS engine. The exceptions were the fan frame and nacelle which, for cost and timing reasons, were heavier nonflight designs. The test programs provided rigorous aerodynamic and mechanical evaluation of E³ technology.

This report describes the FPS design at the end of the contract period. The experience of the detailed design work and testing are reflected in this final FPS design. Also included in this report is an assessment of the economic benefits, in terms of reduced direct operating cost (DOC), attributable to this E³ FPS.

The established benefits of the E³ FPS will be the basis for future engine and aircraft studies for several years ahead. Important information required for conducting such studies will be the level of risk and actual technology advancement represented by the final E³ FPS design. The E³ FPS represents a

very conservative migration into the future, even though E³ technology is advanced compared to current engines.

3.0 FLIGHT PROPULSION SYSTEM DESIGN AND ANALYSIS

3.1 FEATURES

The NASA/General Electric Energy Efficient Flight Propulsion System achieves high propulsive efficiency by utilizing a low fan pressure ratio and a mixer than combines the fan and core streams prior to discharging them through a common exhaust nozzle. Higher thermal efficiency is achieved by using higher engine pressure ratio, increased high pressure turbine inlet temperatures, and improved component performance compared to engines such as the CF6-50C. Characteristic cycle parameters for the E³ FPS design are given in Table III.

Table III. E³ FPS Cycle Characteristics.

Cycle Pressure Ratio at Max Climb ⁽¹⁾	38.4
Bypass Ratio at Max Climb ⁽¹⁾	6.7
Fan Pressure Ratio at Max Climb ⁽¹⁾	1.68
Turbine Rotor Inlet Temperature at Sea Level Static Warm Day ² Takeoff Power	1365° C (2489° F)
Specific Fuel Consumption at Max Cruise ³ , Bare Engine	0.0540 kg/(hr-N) [(0.529 lbm/(hr-lbf))]
Specific Fuel Consumption at Max Cruise ³ , Installed Engine	0.0559 kg/(hr-N) [(0.548 lbm/(hr-lbf))]
(1) Maximum climb is the cycle match point, M = 0.8/10.7 km (35,000 ft), standard day plus 10° C (18° F).	
(2) Sea level static warm day refers to a standard day temperature +15° C (27° F).	
(3) Max cruise is the performance evaluation point, M = 0.8/10.7 km (35,000 ft), standard day temperature (15° C, 59° F).	

The FPS mechanical layout is compact, which is favorable to decreased deterioration, allowing simple frame and bearing arrangement and making the full length fan duct/mixer arrangement practical. Two frame components and five bearings are used. The front frame is made of composite materials and is integral with the fan outlet guide vanes. The rear frame is located behind the low pressure turbine. Two bearings carry the fan. The low pressure turbine (LPT) is supported by the rear frame. The core shaft is supported by a thrust bearing in the fan frame and by a differential roller bearing carried by the low pressure rotor within the LPT. Both shafts rotate in the same direction.

The nacelle is an integral part of the engine. The acoustic design is integrated into the nacelle and engine. Active clearance control (ACC) is used to improve performance and reduce deterioration in the compressor, high pressure turbine (HPT), and LPT. A unique double annular combustor is used to achieve low emissions. A full authority digital electronic control (FADEC) manages fuel flow and the other engine functions. The major engine features are illustrated in Figure 2.

Design technology improvements have been incorporated into the FPS since the preliminary design reported in Reference 3. The improvements are listed below.

- Reduced Turbine Heat Transfer Coefficients - The more efficient blading in E³ has lower heat transfer coefficients than current production engines, requiring less cooling flow.
- N4 Material for HPT Stage 1 Blade and Stage 2 Vane - Replaced René 150. N4 has improved high temperature chemical stability and metallurgical properties.
- Thermal Barrier Coating on Combustor, HPT Stage 1 Vane, Stage 1 Blade and Stage 2 Vane - Reduces required cooling air flow.
- DS Eutectic Noncooled HPT Stage 2 Blade - Eliminates the requirement for cooling air flow.
- Increased Mixer Penetration - Slightly increased penetration, providing higher mixer effectiveness and an additional reduction in sfc.
- Start Bleed Eliminated - Not needed, as demonstrated during core and ICLS testing.

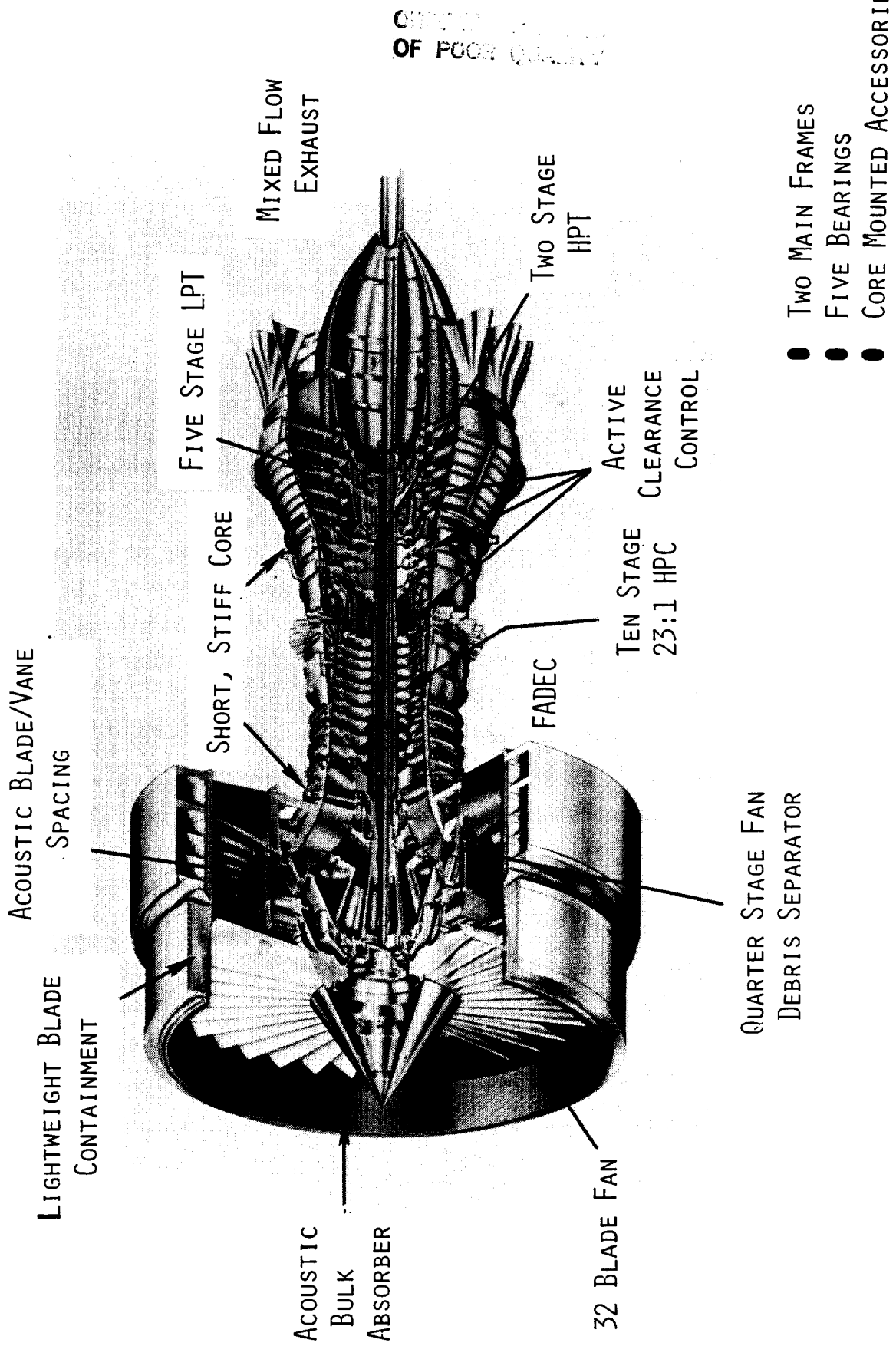


Figure 2. E³ Flight Propulsion System Features

- Start Range Turbine Cooling - Not needed, as demonstrated during core and ICLS testing.
- Improved Component Performance - Based on rig, core and ICLS testing.
- Cycle Rematch - The cycle was rematched to better utilize the more efficient components and the speed/flow characteristic of the compressor, which resulted in improved sfc and increased takeoff thrust. The cycle changes are discussed in Section 4.3.

3.2 MAINTAINABILITY

An important aspect of commercial engine operation is the maintainability of the engine as related both to maintenance costs and to aircraft utilization. Maintainability has been a prime design and configuration consideration for the FPS.

Figure 3 illustrates the access feature of the FPS. Both the outer fan cowl/reverser and inner cowl cover are swung up to permit access to the core engine. Since the FPS uses core-mounted accessories, this quick access to the core cowl cavity is more important than on some current commercial engines using fan-case-mounted accessories. The oil tank is located on the outer fan case to permit quick inspection and servicing when required.

The FPS engine design is based on the modular concept for ease of maintenance. Individual modules containing the major engine components can be built and stored separately for quick replacement and consequent quick shop turnaround times. Figure 4 illustrates the major modules as they could exist in a maintenance facility.

Some of the important maintainability features of the FPS are illustrated in Figure 5. These features have been retained because General Electric experience in the commercial engine business has shown that they enhance the serviceability of commercial engines and reduce maintenance costs.

Another aspect of the maintainability effort was the estimation of expected maintenance costs for the fully developed FPS. The estimate was based on the CF6-50C commercial engine service data base, with scaling factors applied for thrust, mission, and design life. In addition, such parameters as operating temperatures and speeds, configuration differences, and

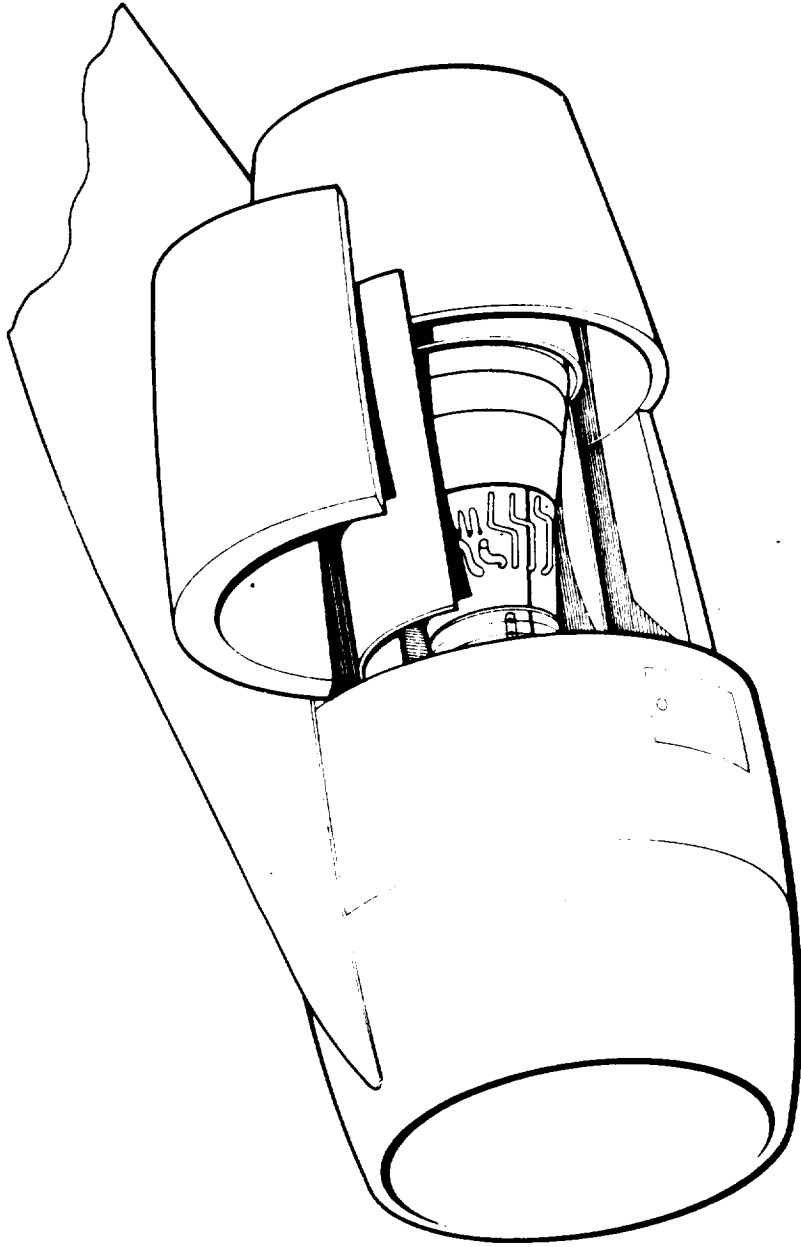
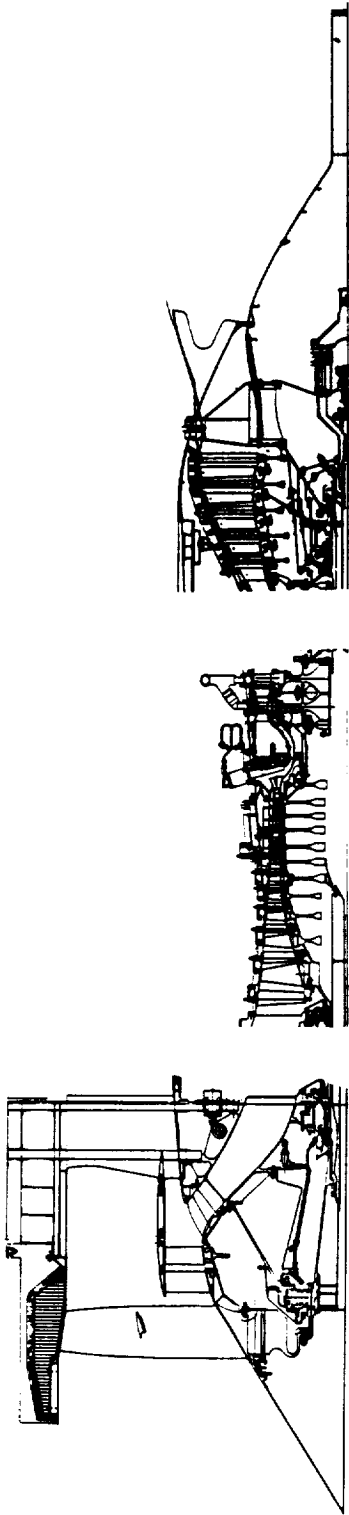


Figure 3. FPS On-Wing Access Provisions.



Fan & Inlet G/B
Module

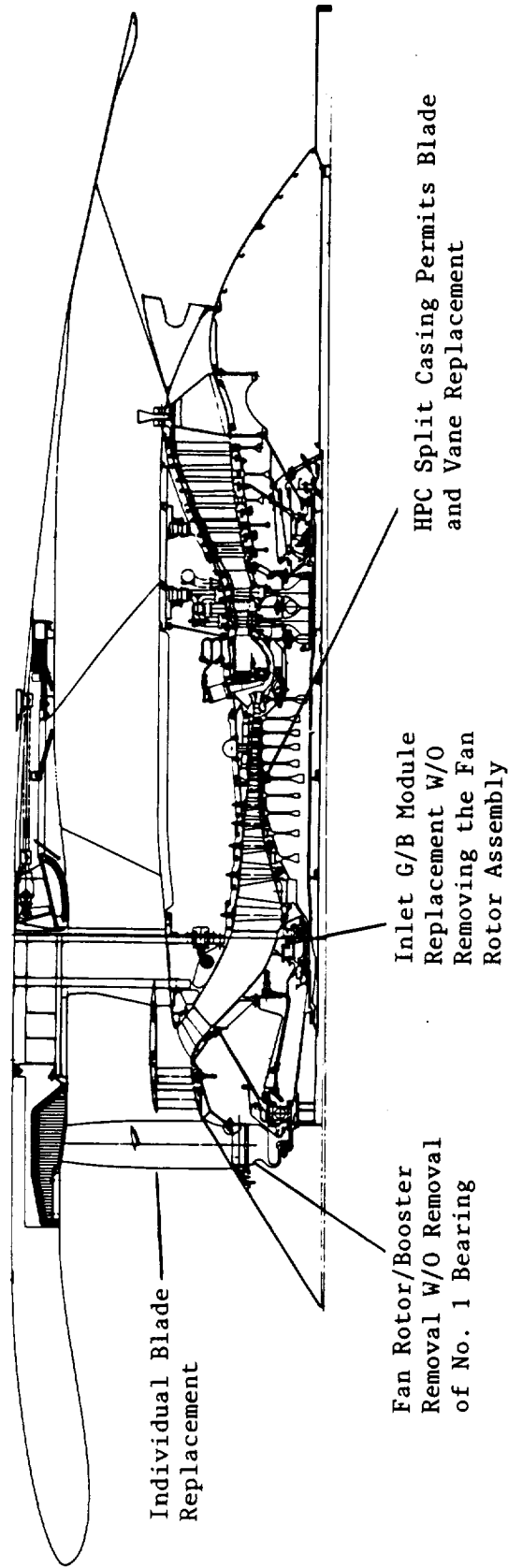
Core Module

LPT Module



Accessory Gearbox
Module

Figure 4. Energy Efficient Engine Modules.



- Borescope & Radiographic Inspection Capability
- Soap Sampling, Chip Detectors, and Filter Bypass Compatibility on the Lube System
- Fan Module Can be Removed Without Removing Any Other Modules

Figure 5. FPS Maintainability Features.

parts costs were considered. The E³ FPS maintenance cost for materials and labor is \$90.64 per engine flight hour in 1980 dollars for a fully developed, mature engine flown on an average 2-hour domestic flight.

Reliability also has a direct impact on maintainability. The FPS has been made as simple as practical to minimize the total complement of parts. Table IV compares the number of parts with the CF6-50C and lists features which will enhance reliability.

Table IV. E³ FPS Reliability Features.

	Parts Required		FPS Design Features For Improved Reliability
	FPS	CF6-50C	
Blades	1536	1673	Combustor - Single design has very low stress levels because mechanical loads carried in shell. HPT & LPT - No bolt holes through disks Fan & Booster - Built-in FOD separation
Vanes	1750	1750	
Frames	2	4	
Sumps	2	4	
Main Shaft Bearings	5	7	

It is believed that the FPS design will produce an engine superior in reliability and maintainability to that of current commercial engines.

3.3 DURABILITY

The FPS was designed for very high life and the inherent weight penalty was consciously accepted. The engine was designed for a total useful life of 36,000 hours or 36,000 mission cycles, whichever occurs first, with normal repair and maintenance. The mission cycle is shown in Figure 6.

Some features which contribute to long life are:

- Rugged, low aspect ratio blading in the fan, booster, and compressor. Part-span shrouds on fan blades.

Code: (Time in Min.)

(Time in Sec.)

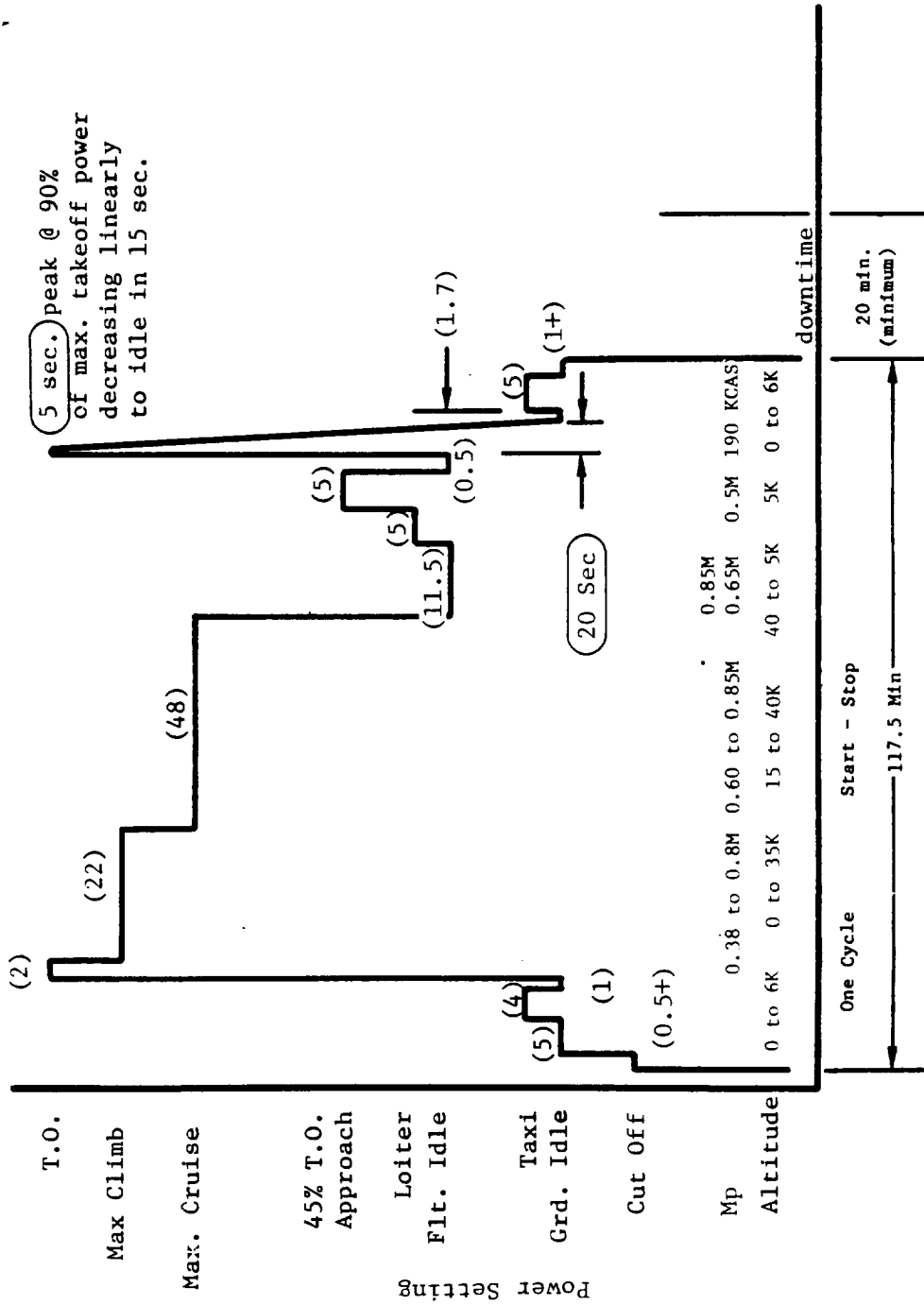


Figure 6. E3 Typical Flight Cycle.

- Long life, high-boss compressor variable stator bushings.
- Dirt and foreign object separation characteristics of the untrapped booster.
- Rugged, single joint in compressor spool.
- Shingle combustor.
- Clean, cool turbine rotor cooling air taken from center of combustor diffuser.
- No holes through turbine blade disks.

Design lives of high temperature components are given in Table V.

Table V. FPS Life.

Life, Hours (or Mission Cycles)	<u>Service Life</u>	<u>Total Life With Repair</u>
Combustor	9,000	18,000
HPT Rotating Structure	18,000	36,000
HPT Blading	9,000	18,000
Remainder of Engine		36,000

3.4 GROWTH

Planned thrust growth was a part of the FPS design. Growth requirements influenced the decision to use the quarter stage fan booster. A 20% increase in thrust can be realized within the current flowpath design.

Thrust growth levels of +5%, +10%, and +20% are summarized in Tables VI and VII. Table VI presents a summary of the major cycle parameters for the maximum climb and sea level takeoff conditions. A +5% "throttle push" point is shown as a reference for sfc and HPT inlet temperature changes without

Table VI. E³ Growth Capability.

Maximum Climb - 10,668 m (35,000 ft)/0.80 M

Parameters				
Net Thrust	FPS	+5%	+10%	+20%
Uninstalled sfc (Std Day) kg/N/hr (lbm/lbf/hr)	0.0541 (0.530)	0.0547 (0.535)	0.0555 (0.543)	0.0561 (0.549)
Overall Pressure Ratio	38.4	42.8	43.2	45.0
Bypass Ratio	6.7	6.0	6.0	5.4
Fan Bypass Pressure Ratio	1.68	1.72	1.72	1.75
Fan Hub Pressure Ratio	1.70	1.92	1.89	2.05

Takeoff - SLS/30°C (86°F)

Net Thrust, kN (lb)	173.5 (39,000)	182.20 (40,950)	190.85 (42,900)	208.20 (46,800)
HPT Rotor Inlet Temp, °C (°F)	1,365 (2,489)	1,375 (2,506)	1,416 (2,580)	1,465 (2,669)

benefit of a fan hub quarter-stage change. Table VII identifies the components which require modification. Note that all the thrust-growth points show a cooling-flow modification to maintain turbine blade life.

Table VII. Growth Component Changes⁽¹⁾

Component Change Required	+5%	+10%	+20%
New Fan Blade			X
New Booster Blading	X	X	X
High-Flowed Compressor			X
Larger HPT Nozzle Area			X
Increased Cooling Flows	X	X	X
Larger LPT Flow Function	X	X	X
New Mixer - Same Total Area			X
Smaller Exhaust Nozzle			X

(1) Engine Flowpath Unchanged.

The +20% growth engine requires a new fan blade with higher flow, tip speed, and pressure ratio; a high-flow compressor that will require some reblading and a new stator schedule; and some turbine aerodynamic changes. The interim growth steps will overspeed the same fan blade to attain the required engine airflow. The higher fan speed will permit a significant increase in hub boost (about 23%). These changes to the front of the engine, of course, require changes in the turbine stator vanes and in the mixer area split. The HPT flow function will increase 3%, with the LPT flow function

increasing 13%. The mixer total area will remain unchanged in order to maintain the same nacelle size. The exhaust nozzle area will decrease by 2%.

All disks shown on the FPS cross sections are designed for the 20% growth engine. The test engine rotating structure was designed for 20% growth, and this work provided the cross sections used in the FPS drawings.

3.5 PERFORMANCE RETENTION

The FPS was specifically design to substantially reduce in-service performance deterioration. The program goal was that the FPS deterioration be no more than half that experienced by current high bypass ratio engines.

The following features in the FPS reduce deterioration:

Features Incorporated to Reduce Long Term Aeromechanical Degradation

- Untrapped Quarter Stage Booster - Centrifuges foreign objects and dirt out of the core stream, resulting in reduced compressor airfoil erosion and cleaner airfoils.
- Low Aspect Ratio (Large Chord and Airfoil Thickness) Fan Blading - Reduced damage due to foreign objects.
- Low Aspect Ratio Booster and Compressor Blading - Smaller scale but same effect as on fan blading.
- Lower Fan Tip Speed - Reduced damage due to foreign objects.

Features Incorporated to Retain Optimum Clearances, Minimize Leakage Increases, and Reduce both Short and Long Term Aeromechanical Degradation

- Active Clearance Control - In the aft half of compressor, the HPT, and LPT. Opens clearances during thermal transients and maneuver deflections to prevent rubs.
- Material Selections - Matches response rates for stators and rotors to reduce rubs due to thermal transients.
- Mount Design - Mount points at 45° from each side of top dead center on fan frame to minimize casing ovalization and bending due to thrust loads.
- Short, Strong, Stiff Structure - Minimizes deflections.

- Short, Stiff Core Rotor with Aft Differential Bearing - Minimizes rotor bending and rotor-to-stator movement.
- Abradable Seal Materials - Minimizes stackup and transient seal rub penalties.
- High Boss, Long Life Variable Stator Vane Bushings - Reduces wear.

Deterioration characteristics of the FPS are compared to current engines in Figure 7. A large portion of the reduction in overall deterioration will come from significantly lower early deterioration.

The projected breakdown of FPS deterioration compared to a CF6-50C is given in Table VIII. Although it is an imprecise quantification, the FPS projected deterioration is assessed at half that of the CF6-50C.

3.6 ACOUSTICS

The FAA FAR 36 regulation for certification of new airplanes is more stringent than for current airplanes. The FPS was designed to conform with these regulations.

The following acoustic features are a part of the FPS design:

- Full length inlet with acoustic wall treatment.
- Long fan duct nacelle with acoustic wall treatment.
- High bypass ratio.
- Mixed core and fan stream (lower peak velocity) exhaust.
- Moderate fan tip speed.
- Integral fan outlet guide vane (OGV) and fan frame with a large gap between the vanes and fan blades.
- Low pressure turbine designed to reduce noise.

Bulk absorber materials were selected for wall acoustic treatment because the suppression characteristics were superior to conventional resonator designs. These bulk absorber materials (Kevlar and, where higher temperatures are required, Astroquartz) are used under 30%-open perforated sheet. Figure 8 shows where the acoustic treatment is used.

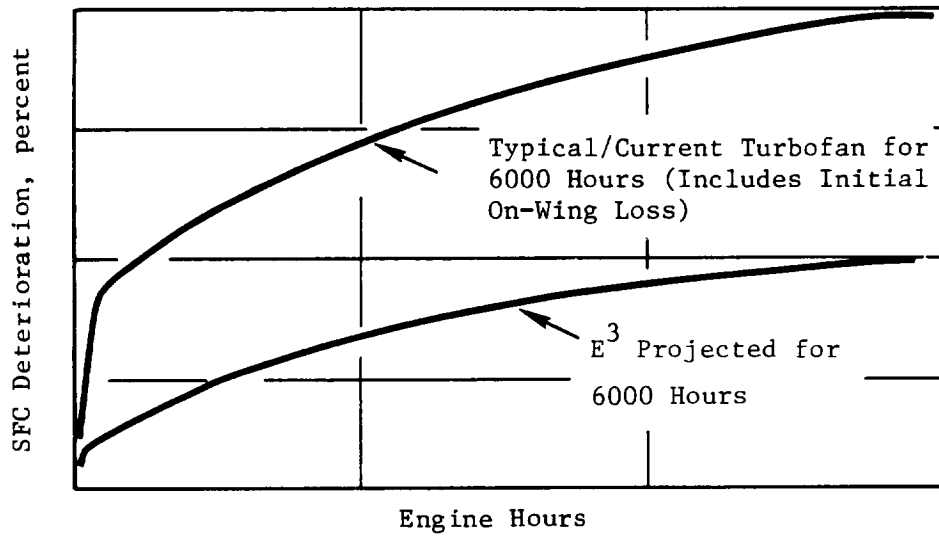


Figure 7. Performance Degradation Characteristics.

Table VIII. Estimated In-Service Performance Losses.

Causes	Estimated Losses - %		Delta % Reduction
	CF6-50C	FPS (Estimate)	
Clearances			
Fan	3	1	
HPC	13	3	
HPT	29	9	
LPT	<u>4</u>	<u>2</u>	
Subtotal	49	15	34
Leakages			
HPC	10	4	
HPT	6	5	
LPT	<u>3</u>	<u>2</u>	
Subtotal	19	11	8
Erosion			
Fan	7	4	
HPC	8	3	
HPT	2	1	
LPT	<u>5</u>	<u>4</u>	
Subtotal	22	12	10
Miscellaneous	10	10	0
Total	100	48	52

● **Advanced Bulk Absorber Treatment**

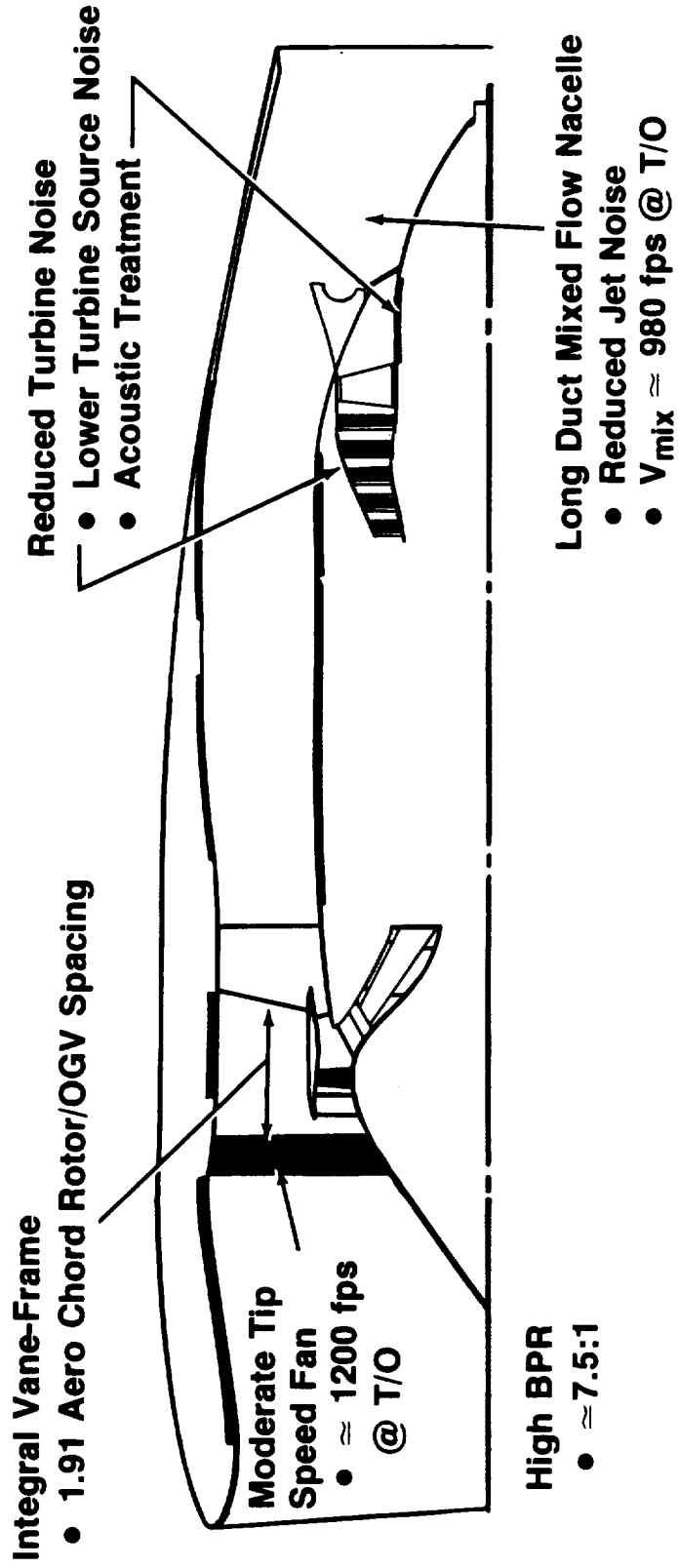


Figure 8. E^3 Low Noise Design Features.

Figure 9 compares conventional fan blade, OGV and frame strut design with those components for the E³ design.

The 5-stage low pressure turbine uses an increased gap between the Stage 4 vane and the Stage 4 blade and a high number of Stage 4 blades to reduce turbine noise. The vane/blade ratio was selected such that the noise generated by the passing frequency would not propagate out of the turbine at approach conditions.

Since the initial FPS acoustic design was selected, data on noise generation, radiation and suppression were obtained during acoustic testing of the ICLS engine. The ICLS used a nonflight nacelle which incorporated all FPS acoustic features. Tests were run with the treatment material unsuppressed and also suppressed (taped) to determine the treatment effectiveness. Based on these tests, the FPS noise level margins are shown in Table IX. The reason for the lower overall noise margin of the Boeing twin is attributed to the fact that the airframe noise level is higher to start with. The acoustics goal was met.

Since the requirement established for the FPS noise margin was 3 EPNdB, it can be seen that the acoustics goal was met with a comfortable margin.

3.7 SYSTEM COMPATIBILITY

Evaluation of the compatibility of the FPS fan and compressor includes determining the requirements for stall surge margin, deterioration sensitivity, and distortion tolerance. In addition, it includes a stability analysis consisting of a surge-line estimation and performance/stability trades.

Figures 10 and 11 illustrate the makeup of the required surge margin for the fan and compressor at the sea level takeoff thrust condition. For the fan, distortion is the largest single contributor to the stall margin requirement. For the compressor, the thermal effects on clearance produce the largest single contributor to the margin requirement.

Stability requirements have been established for the FPS fan and compressor. These are presented for a range of flight conditions in Table X. Test results from fan rig tests are also included. As shown, the fan exceeded all stability requirements. The final (10C) E³ compressor was

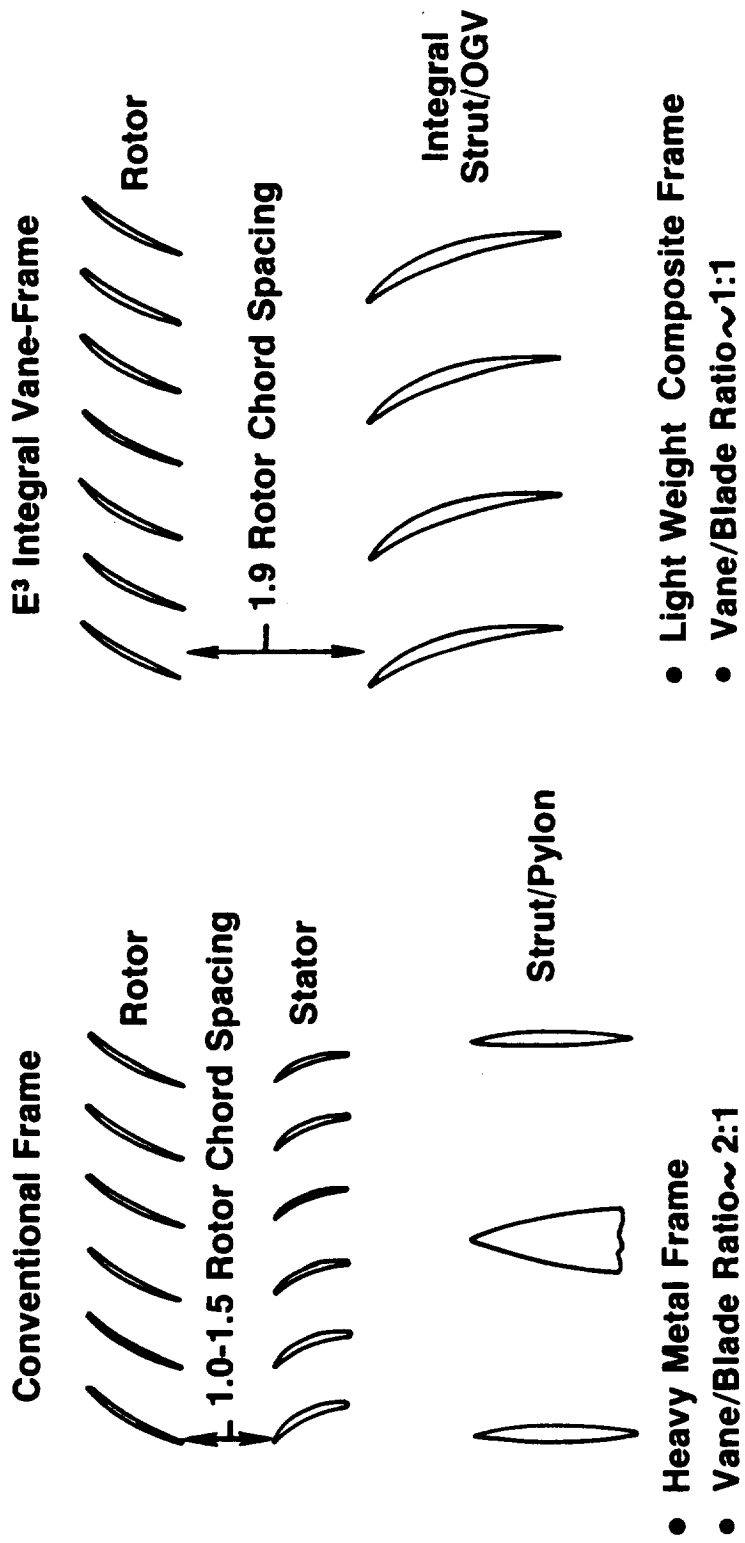


Figure 9. Fan Frame Acoustic Design.

Table IX. E³ Noise Margin from FAR 36

	Noise Margin EPNdB		
	Takeoff	Sideline	Approach
Boeing Domestic Twin Jet	2.9	6.6	1.7
Lockheed Domestic Tri Jet	5.6	7.7	4.1
Lockheed International Quad Jet	5.1	8.1	5.3
Douglas Tri Jet	4.4	6.5	3.8

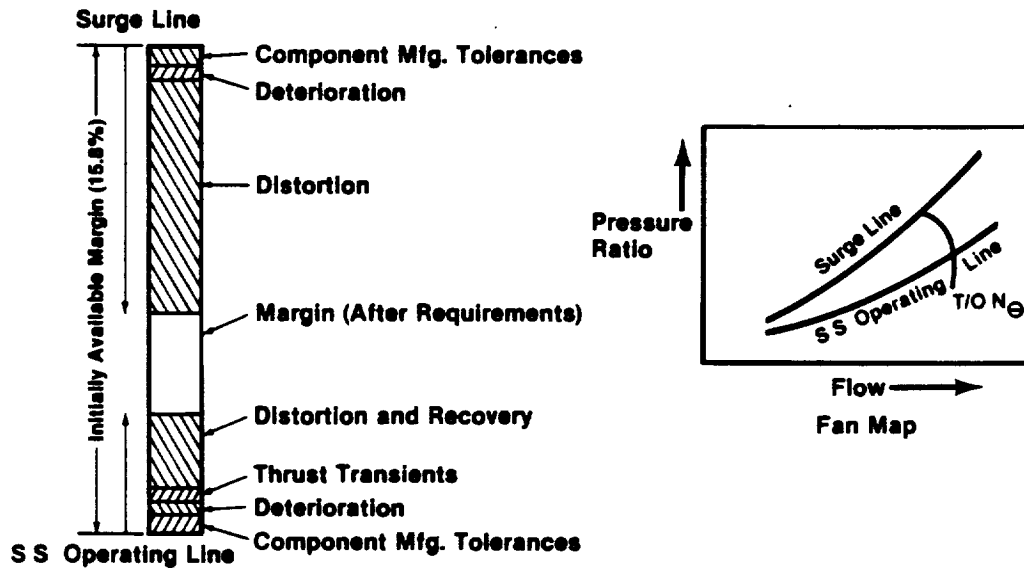


Figure 10. Sample Stability Stack Crosswind - Fan at Takeoff Thrust.

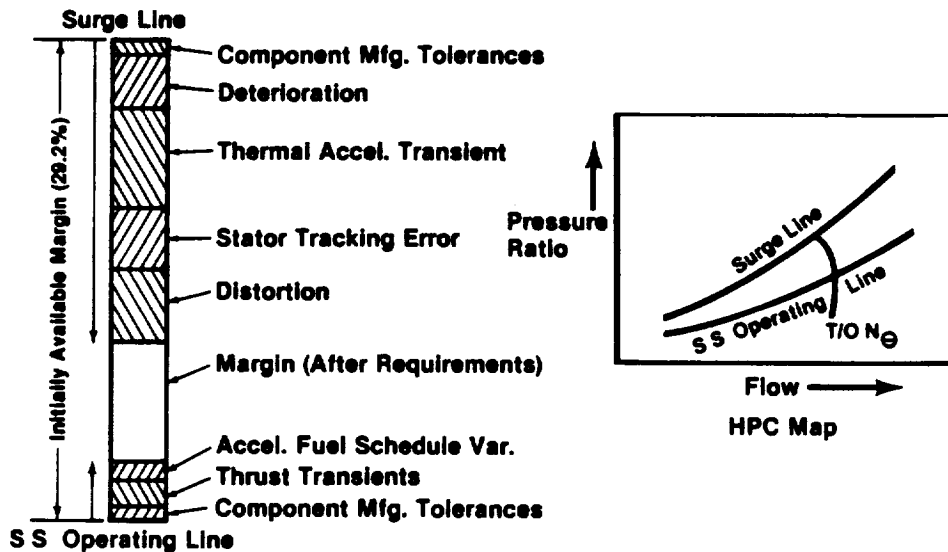


Figure 11. Sample Stability Stack Crosswind - Compressor at Takeoff Thrust.

tested only in the core and ICLS vehicles. No stalls were incurred so there are no data on stall margin. Rig tests are planned for the compressor, which will determine the stall line. The 10C compressor is expected to have sufficient stall margin to meet the stability requirements in Table X. The FPS, therefore, is projected to achieve its stability requirements.

Table X. E³ FPS Stability Assessment.

Mo/ALT	0/0	0/0	.25/0	0/8K	0/5330	.25/5330	.8/35K	.8/35K
Power Setting	G/I	T/O	T/O	T/O	T/O	T/O	MXCL	MXCR
<u>Fan</u>								
Available	4.2	16.1	18.1	15.1	16.2	18.1	13.5	14.8
Required	3.6	12.1	12.3	12.0	12.1	12.3	5.0	5.1
Remaining	+ 0.6	+ 4.0	+ 5.8	+ 3.1	+ 4.1	+ 5.8	+ 8.5	+ 9.7
<u>Compressor</u>								
Available	No stall data. 10C compressor to be rig tested in 1984							
Required*	19.0	16.9	16.9	16.8	16.9	16.9	13.3	13.4
Remaining	Positive margins expected							

*Active Clearance Control (ACC) Is Assumed.

4.0 CYCLE AND ENGINE PERFORMANCE

4.1 CYCLE HISTORY AND SELECTION CRITERIA

The E³ FPS preliminary design cycle is based on the results of a number of NASA programs involving component and cycle technology studies. As shown in Figure 12, the development of the E³ cycle began in 1974 with the study known as Study of Turbofan Engine Designed for Low Energy Consumption (STEDLEC), Reference 4. This extensive cycle and technology study of turbofan engines considered separate- and mixed-flow exhaust systems, boosted and nonboosted single-stage HP turbines, and direct-drive and geared fan configurations. All engines were studied as installed on advanced transport aircraft for evaluation against the NASA performance and economic goals.

This was followed by the Unconventional STEDLEC (USTEDLEC) program, Reference 5, which continued the turbofan studies along with turboprop engines and regenerative cycles. This study narrowed the candidates to four engine types with separate- and mixed-flow-exhaust versions of direct-drive and geared fan configurations. Concurrently, the Preliminary Design Study of Advanced Multi-stage Axial Flow Core Compressors (AMAC) defined an advanced, 10-stage, 23:1 pressure ratio compressor (Reference 6). This compressor was to be used with a two-stage HPT in a nonboosted, direct-drive, turbofan engine.

The E³ Preliminary Design and Integration (PD&I) programs studies (Reference 7) evaluated four engine types using advanced components, cycles, and material technologies against the NASA goals on operating economics, fuel efficiency, and environmental factors. Mission studies were conducted by airframe contractors based on advanced transport aircraft designs. The final cycle from this study was selected as the cycle for the E³ Component Development and Integration Program (CD&I), reported in Reference 1.

4.2 INITIAL CYCLE SELECTION PROCESS

The initial cycle selection process involved two phases. The first phase developed a family of engines which provided performance for a range of values of the significant cycle parameters. These were fan pressure ratio, bypass ratio, cycle pressure, HPT inlet temperature, and exhaust system type. These

engines were evaluated in the second phase, by airframe subcontractors, on a variety of missions which incorporated advanced concepts in transport aircraft designs. The aircraft designs included twin-jet, trijet, and quadjet configurations. The mission studies were evaluated against the NASA goals on economics (DOC), specific fuel consumption (sfc), fuel burned (W_f), emissions, and acoustics. The engines were scaled to meet specific thrust requirements.

The thrust size for the E³ FPS design was selected at 162.36 kN (36,500 lbf) by General Electric based on these mission studies and corporate evaluation of market requirements for the 1990's.

4.3 FINAL CYCLE REFINEMENT

As shown in Figure 12, the cycle went through a refinement process during the course of the E³ program. The refinements concentrated on off-design maps and start region performance rather than design point performance. The final FPS cycle incorporates component performance improvements based on rig, core, and ICLS testing. These include better component efficiency levels, lower cooling flows, and the speed/flow characteristics of the compressor. In addition, it reflects lower cooling flows required as a result of substitution of improved materials.

The final engine cycle was rematched to best utilize these changes. The cycle was matched differently than the original FPS to favor the thrust lapse rate desired for a twin engine transport. The same thrust at maximum climb was retained. Because of the better components and rematching, turbine inlet temperature at maximum climb dropped by 38° C (70° F). A slight increase in turbine inlet temperature, 22° C (39° F), was incorporated at takeoff. The better components and rematching increased takeoff thrust from 162.4 kN (36,500 lbf) to 173.5 kN (39,000 lbf). Hardware size for the final engine has not changed. Fan tip diameter is still 211 cm (83 in), and core inlet corrected flow is 54.4 kg/sec (120 lbfm/sec) at the maximum climb matching point.

Within the E³ program the component rigs, and the core and ICLS test vehicles, represent the state of development of a "first engine to test." FPS component performance is higher than that of the test vehicles by an amount

expected to occur in the full development of an engine. The FPS component performance levels are listed in Table XI. Final cooling flow rates are also included. More detailed information will be presented in the discussions of each component.

4.4 CYCLE DEFINITION

The E³ cycle parameters are shown in Table XII for the three key rating points: maximum climb, maximum cruise, and sea level takeoff. The climb and cruise points are shown for 10.67 km (35,000 ft), Mach 0.8 flight conditions. All points are defined for dry air, zero bleed and power extraction, and 100% inlet-ram recovery. The cycle design point (for component matching) is the maximum climb flight condition. The cycle parameters for maximum cruise and takeoff thrust ratings then result from the component map characteristics.

The engine thrust is constant (flat-rated) up to the flat-rating temperature, subject to a maximum HPT rotor inlet temperature. These flat rating temperatures are:

- Standard day +15° C (+27° F) for the takeoff rating.
- Standard day +10° C (+18° F) for the climb and cruise ratings.

The HPT rotor inlet temperatures shown in Table XII for each rating are at the flat-rating temperature condition. The uninstalled sfc values in Table XII are for a standard day ambient temperature. The uninstalled maximum cruise sfc is adjusted for isolated nacelle drag to determine the installed sfc goal of the E³ program.

The cycle data in Table XII are calculated from the General Electric cycle deck computer program system used on all engine programs. These are large scale computer programs that contain mathematical models of the engine components including maps, cooling and parasitic flows, pressure losses, Reynolds number effects, and exhaust system characteristics. Steady-state performance is calculated with momentum balance, energy, and flow continuity maintained from station to station in the engine. The deck also contains models of the 1962 U.S. Standard Atmosphere and thermodynamics using real gas effects including dissociation.

Table XI. FPS Component Performance - Maximum Cruise Conditions.

Fan Bypass Efficiency	89.4%
Fan Hub Efficiency	90.6%
Compressor Efficiency	86.1%
Combustor Efficiency	99.9%
Combustor Pressure Drop	5.0%
High Pressure Turbine Efficiency	92.7%
Low Pressure Turbine Efficiency	92.5%
Fan Duct (Duct Mixer) Pressure Drop	1.4%
Core Duct (Duct Mixer) Pressure Drop	1.7%
Nozzle Duct Pressure Loss	0.21%
Mixer Effectiveness	83.8%
Nozzle Coefficient	0.996
CPD Nonchargeable Cooling ⁽¹⁾ , %W ₂₅	7.46%
CPD Chargeable Cooling ⁽²⁾ , % W ₂₅	5.33%
7th Stage Cooling and Purge, % W ₂₅	1.95%
5th Stage Cooling and Purge, % W ₂₅	1.4%
<p>(1) Reintroduced to main flow upstream of HPT Vane 1 Throat.</p> <p>(2) Reintroduced to main flow downstream of HPT Vane 1 Throat.</p>	

Table XII. FPS Cycle Definition.

Parameter	Max Climb ⁽¹⁾	Max. Cruise	Takeoff
Uninstalled sfc (Std. Day), kg/N/hr (lbm/lbf/hr)	0.0541 (0.530)	0.0540 (0.529)	0.0305 (0.299)
Overall Pressure Ratio	38.4	36.5	32.4
Bypass Ratio	6.7	6.8	7.0
Fan Bypass Pressure Ratio	1.68	1.64	1.56
Fan Hub Pressure Ratio	1.70	1.66	1.58
Compressor Pressure Ratio	23.1	22.4	20.8
HPT Rotor Inlet Temperature, °C (°F) ⁽²⁾	1,244 (2,270)	1,212 (2,214)	1,365 (2,489)

(1) Cycle Match Point.

(2) Temperature at the flat-rating temperature.

4.5 REFERENCE ENGINE COMPARISON

The General Electric E³ specific fuel consumption goal is a 12% improvement over the CF6-50C engine at maximum cruise thrust at 10.67 km (35,000 ft), Mach 0.8, on a standard day, with zero bleed and power extraction and 100% inlet-ram recovery. The FPS sfc is currently 16.6% better than a CF6-50C at these conditions (installed in an isolated nacelle). Of this, 1.2% is due to installation effects.

Since the E³ has a relatively smaller core than the CF6-50C, bleed air for the aircraft cabin has a higher penalty. However, the FPS uses a fuel heater/regenerator system to cool aircraft bleed. The CF6-50C uses fan air to cool aircraft bleed. The fuel heater regenerator system recovers waste heat from the bleed air and more than balances the bleed penalty for the smaller core. If customer bleed, power extraction, and the benefit due to recovering energy from bleed air with the fuel heater/regenerator system are considered, the installed sfc improvement becomes 16.9%.

4.6 STARTING

The ability to easily start the FPS was a concern early in the E³ program. A very high compressor pressure ratio on a single rotor and the use of only the pilot zone of a double annular combustor had the potential to hinder easy starting. Because of this concern the component designs addressed far off-design operation and, during the program, testing and analysis addressed starting. The original design provided for bleeding 30% of compressor flow from the seventh stage to aid engine starting. As insurance, the core and ICLS test engines had provisions for mounting two of the largest starters currently available.

The E³ core and ICLS test engines started easily, quickly, and reliably. Start bleed and the second starter were never used. Start bleed has now been eliminated from FPS, as has the start range turbine cooling system which would have been needed if start bleed had been required. The ICLS demonstrated the ability to start in only 44 seconds. At one point in the testing program, the start fuel flows were intentionally enriched to try to precipitate compressor stall, but no stall occurred.

5.0 COMPONENT AND SYSTEM DESIGN AND PERFORMANCE

Every component except the fan frame, nacelle, and reverser has been detail designed, rig tested, and engine tested. The designs were for the test vehicles rather than a flight engine. However, the designs conformed to the weight, cost, and life requirements of the FPS. The design, fabrication, and testing of the E³ core and ICLS test engines provided a much more solid basis for an assessment of the FPS engine than is usual for preliminary design engines. Further studies and analyses using E³ or its derivatives will have the stature of being based on established, but still advanced technology, rather than a preliminary design "paper" engine.

In the following sections each component is described and the test experience related.

5.1 FAN

The FPS fan configuration was selected from a preliminary design study of alternate designs. The design selected exhibited the lowest mission fuel-burn and operating cost. The FPS fan uses shrouded fan blades, plus a quarter-stage booster under an untrapped island. The fan outlet guide vanes are integral with the fan frame and spaced 1.9 chord lengths aft of the fan blade for acoustic purposes. The E³ fan cross section is presented in Figure 13 and a photograph of the actual ICLS fan hardware is shown in Figure 14.

The fan plus quarter-stage booster design was chosen over a single-stage design with a higher tip speed and a more highly loaded hub because of its higher core-stream efficiency capability and a better growth potential for future engine development. The fan bypass stream also has a higher efficiency potential by reason of the lower fan speed.

The low aspect-ratio fan blade is expected to meet bird-ingestion design criteria. The quarter-stage configuration is expected to substantially reduce erosion and other FOD to the core compressor. Engine test experience shows that debris ingested in the hub region tends to be centrifuged to the outer span of the booster blades and pass into the fan bypass duct. Figure 15 shows two examples of calculated particle trajectories for 25 μm and 100 μm duct

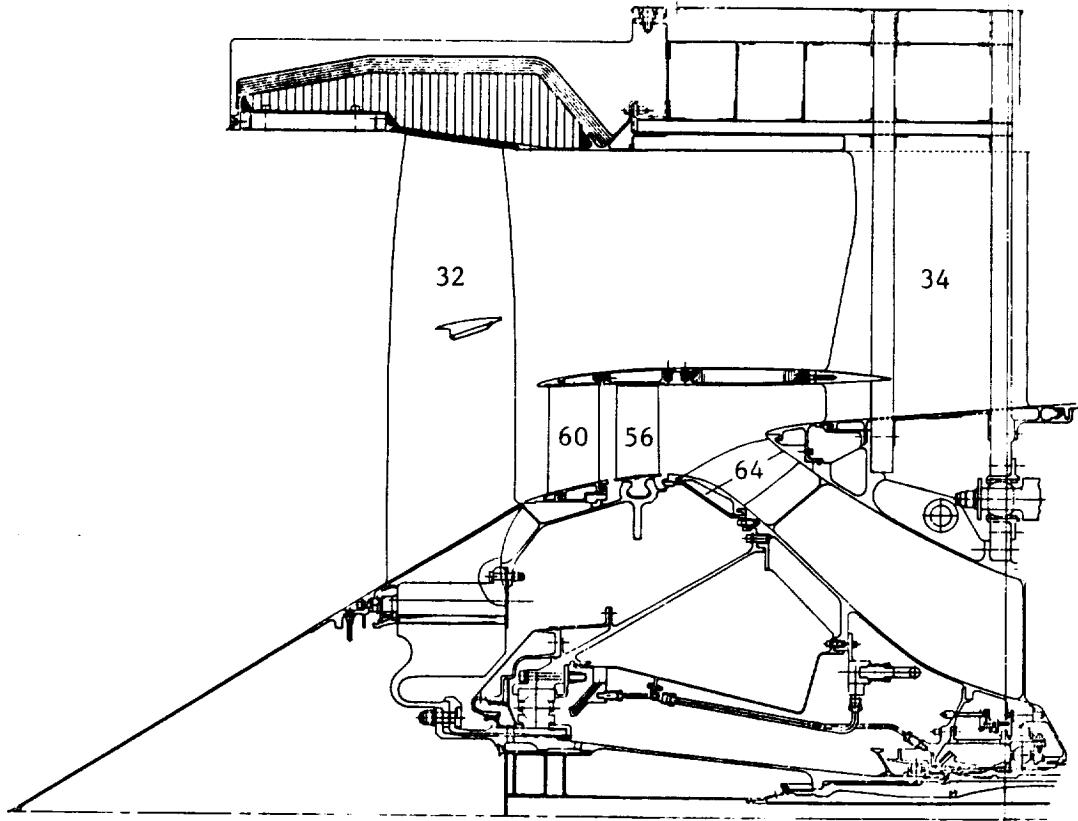


Figure 13. E³ Fan Cross Section.

ORIGINAL PAGE
OF POOR QUALITY

ORIGINAL PAGE
BLACK AND WHITE PHOTOGRAPH

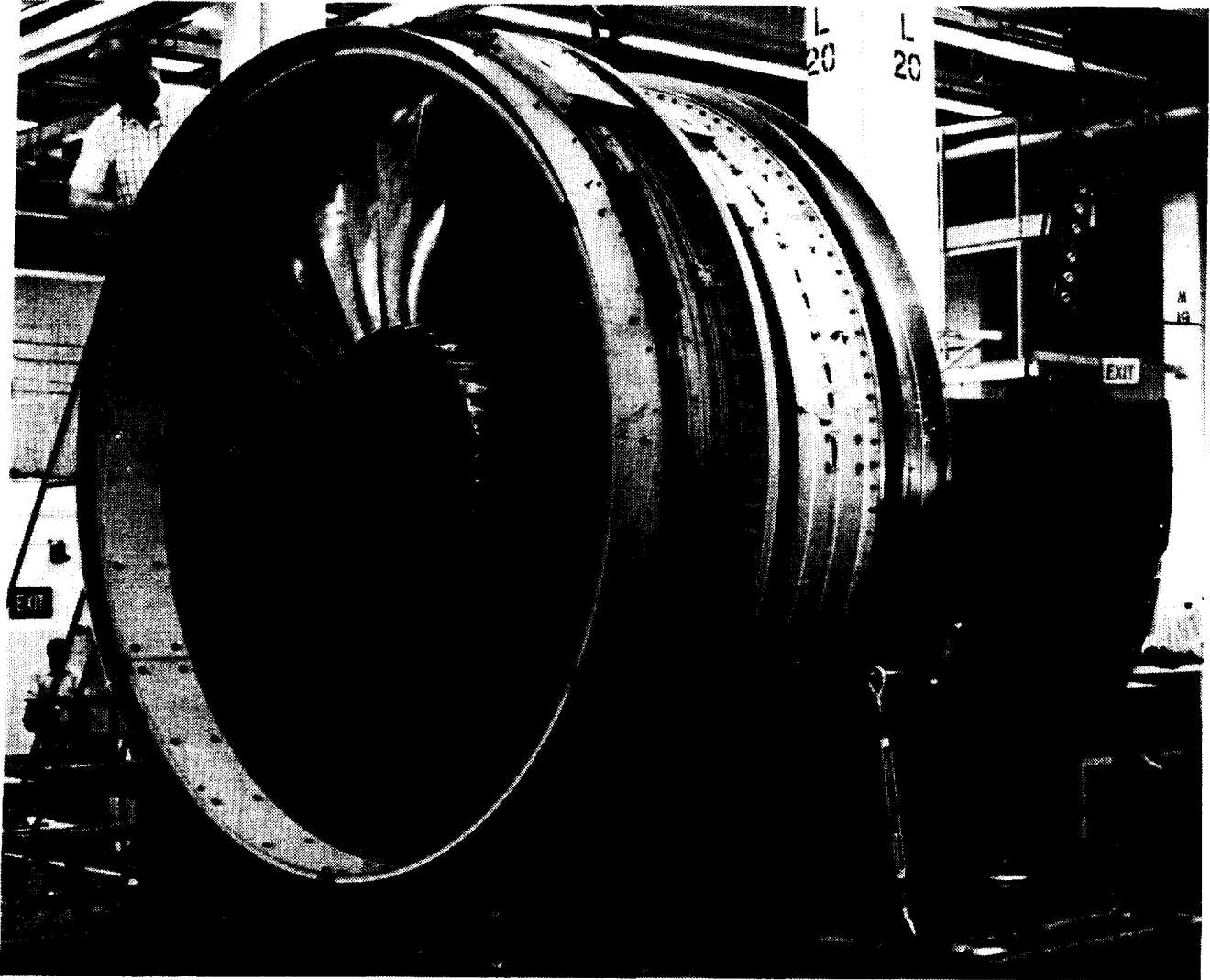
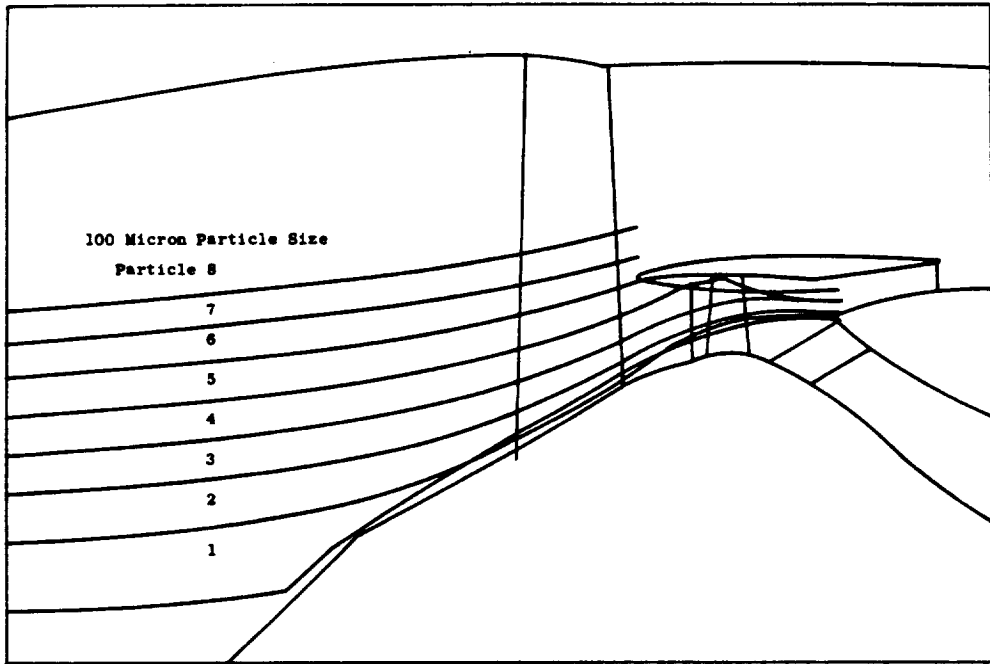


Figure 14. E³ Fan Component.



E^3 Sea Level Takeoff

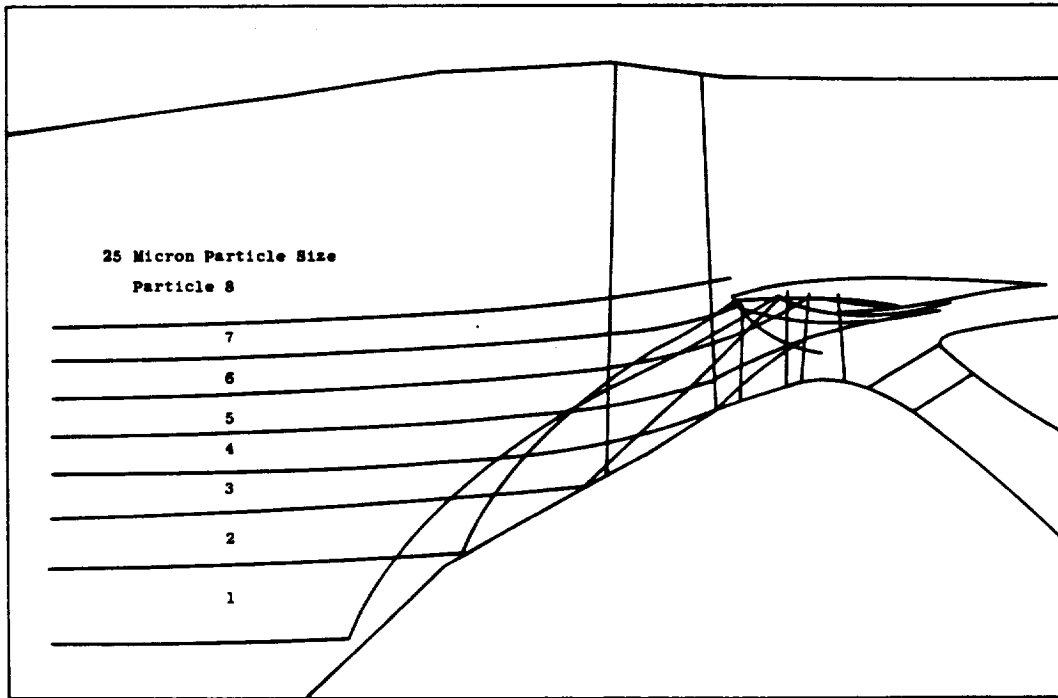


Figure 15. Particle Trajectories.

particles. In all, eight particles sizes ranging from 10 μm to 1000 μm were analytically evaluated when ingested at different radial locations of the inlet. Figure 16 shows the particle size distribution of AC Coarse, AC Fine, and MIL-E-5007C contaminants. The analytical results indicate that from one-half to two-thirds of these contaminants that enter the fan inlet within the core air capture area would be separated from the core air. The results of these analyses show that the untrapped quarter-stage configuration will result in cleaner air entering the core, a condition known to decrease core flowpath erosion and improve performance retention.

5.1.1 Aerodynamic Design

The fan has an inlet radius ratio of 0.342 and, at the aerodynamic design point, has a specific flow rate of 208.9 kg/s-M^2 (42.8 lbm/s-ft^2). The design-corrected tip speed is 411.5 m/s (1350 ft/s) producing a bypass flow total-pressure ratio of 1.65 and core flow total-pressure ratio of 1.67. The quarter-stage island splits the total fan flow so that approximately 22% of the total flow is supercharged by the quarter-stage rotor. Downstream of the booster rotor, the flow is further split with 42% of the booster flow reentering the bypass stream and the remaining flow directed through the transition duct into the core.

In the final cycle refinement, the cycle was rematched so that the fan aerodynamic design point no longer coincides with the cycle match point. Fan conditions at the aerodynamic design point and the final cycle match point are as follows:

<u>Parameter</u>	<u>Aero Design Point</u>	<u>Cycle Match Point</u>
Corrected Flow, kg/s (lbm/s)	643.3 (1419)	646.0 (1425)
Bypass Stream Pressure Ratio	1.65	1.68
Core Stream Pressure Ratio	1.67	1.70

The aerodynamic design of the fan rotor is of interest because the airfoil sections are transonic in the outer region and subsonic near the hub.

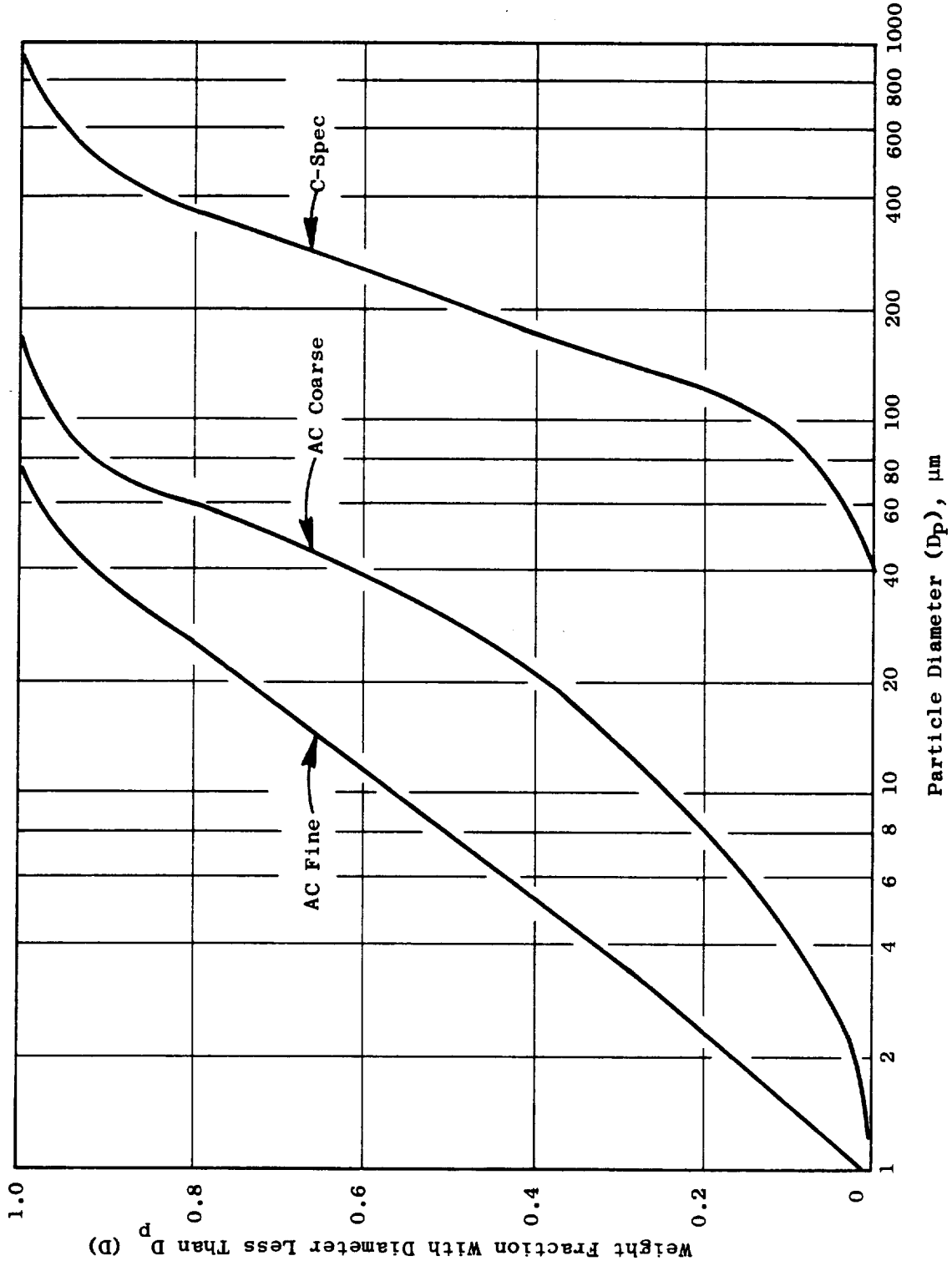


Figure 16. Typical Tests and Particle Size Distribution.

The fan rotor blade airfoil shapes were specifically tailored for each streamline section using General Electric's Streamsurface Blade Section computer program. In general, the airfoils were shaped in an attempt to minimize shock losses since the inlet Mach numbers are supersonic for all streamlines above the quarter-stage island, reaching 1.4 at the tip. Below the island streamline location, the Mach numbers range from 1.02 at 78% flow value to 0.70 at the hub streamline. The airfoils on the hub streamline were patterned after other advanced fan hub airfoil shapes that have shown excellent performance. The designs of the rotor blade sections were performed along 12 axisymmetric streamsurfaces with the surfaces viewed along a radial blade axis using the Streamsurface Blade Section program. The considerations which guide and influence the design of high transonic Mach number cascades, such as the E³ fan rotor, are presented and discussed in References 1, 2, and 3.

The inner outlet guide vane blade row, shown in Figure 17, removes the swirl received from the booster rotor and directs the flow into the core duct. To do this efficiently, the 64 vanes are swept aft and leaned with the pressure side facing the fan axis of rotation. The aerodynamic design procedure consisted of cutting the airfoil along streamlines and viewing the sections along the blade axis. The blade axis is a curved line in space, swept aft 60° from a radial line and leaned circumferentially in an amount that varies from 0° (no lean) at the OD to 20° at the ID. The stacking axis for viewing the cascade projection and for defining manufacturing sections is a straight line between the intersection of the blade axis with the OD flowpath and the intersection of the blade axis with the ID flowpath. The flow and airfoil meanline angles that are observed in this projection are referred to as cascade angles.

The sweep angle (60°) of the stacking axis was selected to be compatible with the shape of the flowpath in the region entering the core duct. The degree of lean was chosen primarily to control and minimize the level of Mach number in the hub region as the flow enters the core duct. At the entrance to the stator, the downward radial force on the flow imposed by the 20° of lean increases the static pressure and thereby reduces the inlet Mach number. This eventually leads to a lower hub diffusion rate. The lean angle drops off sharply to 0° at the OD in order to avoid an undesirable acute angle between the vane suction surface and the outer flowpath. Even though there is no lean

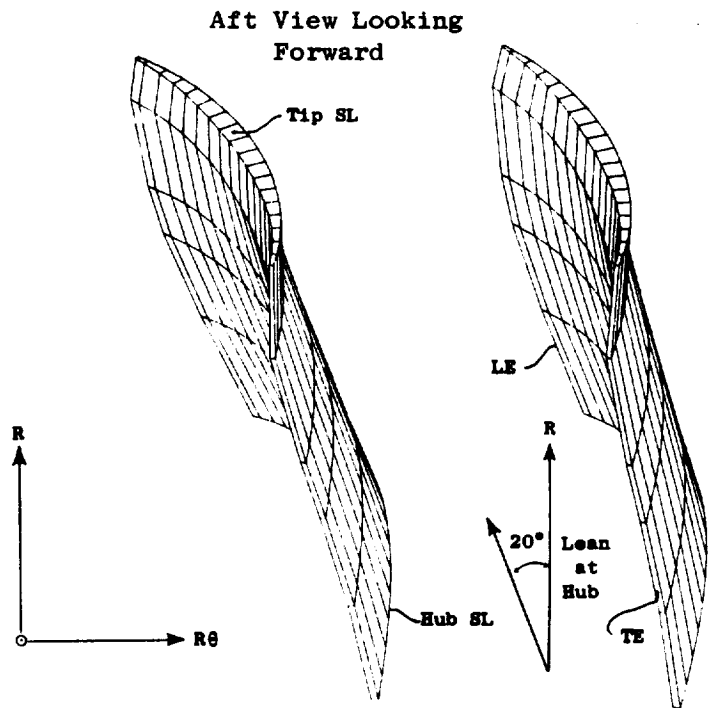
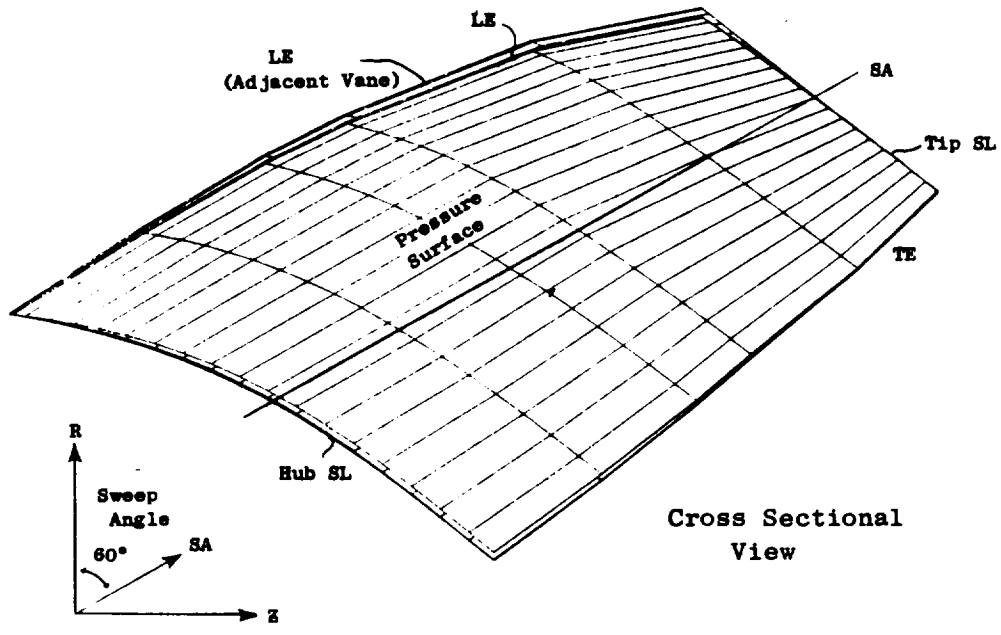


Figure 17. Inner Outlet Guide Vane.

at the tip, the radial gradient of lean tends to increase the Mach numbers slightly at the tip streamline. The reduced Mach numbers and aerodynamic loadings in the hub, where the flow is the most sensitive because of the flow-path shape, make the total lean effect favorable.

5.1.2 Mechanical Design

An important part of selecting the fan configuration was the decision to use part span shrouds. The tradeoffs involved tip speed, number of blades, solid or hollow blades, single fan stage versus fan plus booster stages, and shrouded versus unshrouded blading. Recent advances in techniques for designing lower loss part span shrouds led to the selection of 32 solid titanium blades with 50% span shrouds. This provided the lowest fuel burned without imperiling the long life capability of the fan.

The integral fan frame-outlet guide vane is a graphite composite structure with an aluminum hub. Other fan materials are: composite spinner, aluminum booster Stage 1 vane and OGV, titanium booster blade, titanium and graphite composite booster island, and aluminum liner for the containment case.

5.1.3 Performance

FPS fan performance is based on 82 hours of fan component rig testing and 65 hours of ICLS engine testing. Engine hardware was tested in the General Electric fan facility at Lynn, Massachusetts. Traverse and fixed probes were used to obtain performance and stall data for varying bypass ratios. No hardware changes resulted from the fan rig testing and the same hardware was tested again in the ICLS test vehicle.

The history of fan efficiency test results is given in Table XIII.

5.2 COMPRESSOR

The FPS compressor (Figure 18) represents a bold step in technology in that it achieves a high pressure ratio (23:1) in only 10 stages. The IGV plus stators 1 through 4 are variable. An active clearance control system improves cruise performance and reduces deterioration. The term "active" in ACC relates

Table XIII. Fan Performance.

	Maximum Climb	Maximum Cruise	Takeoff
Original FPS Requirement⁽¹⁾			
Fan Bypass Efficiency	0.879	0.887	0.900
Fan Hub and Booster Efficiency	0.885	0.892	0.897
Rig Test Results⁽¹⁾			
Fan Bypass Efficiency	0.886	0.892	0.893
Fan Hub and Booster Efficiency	0.892	0.895	0.898
ICLS Test Results⁽¹⁾			
Fan Bypass Efficiency	0.879	0.885	0.886
Fan Hub and Booster Efficiency	0.895	0.898	0.901
Final FPS Requirement⁽²⁾			
Fan Bypass Efficiency	0.888	0.894	0.891
Fan Hub and Booster Efficiency	0.905	0.906	0.909
<p>Notes: Bypass Efficiency is based on momentum averaged exit conditions to include significant profile effects in the bypass duct.</p> <p>Hub and Booster Efficiency is based on mass average exit conditions.</p> <p>(1) Consistent with original cycle match.</p> <p>(2) Revised cycle match.</p>			

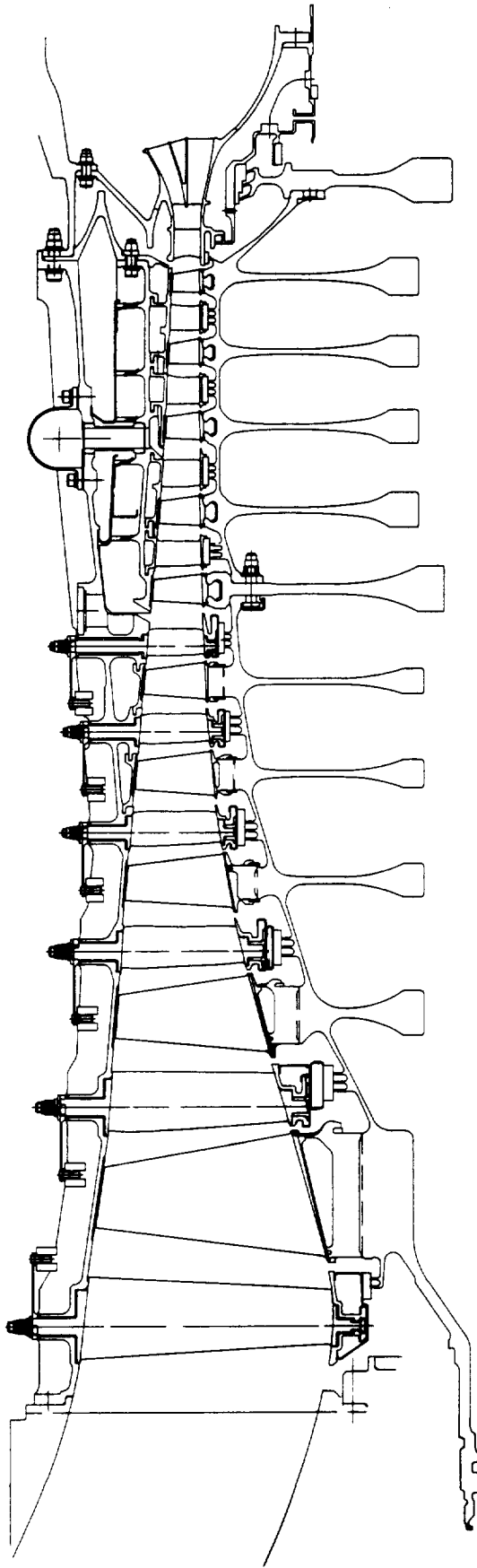


Figure 18. E3 Compressor Cross-Section.

to the actuation of the clearance control system by the engine digital electronic control.

5.2.1 Aerodynamic Design

The core compressor is an advanced technology, 10-stage unit designed to produce an operating line total pressure ratio of 23 at a design corrected tip speed of 456 m/s (1,495 ft/s). Because of the high speed, pressure ratio, and aerodynamic loading, it is one of the most technically challenging designs that General Electric has built. The basic configuration was selected during the GE/NASA Advanced Multistage Axial Flow Core Compressor (AMAC) preliminary design studies (Reference 6) conducted in 1975-1976 to identify an optimum compressor configuration for use in a low energy consumption, subsonic, commercial turbofan engine.

During the AMAC contract, parametric studies were conducted to determine the influence of the major compressor design features on efficiency, weight, cost, aircraft direct operating cost, and fuel usage. The design parameters examined were aspect ratio, solidity, inlet specific flow, exit Mach number, reaction ratio, inlet radius ratio, exit radius ratio, and number of stages. Compressor speed was set to allow each configuration studied to meet an objective level of stall margin. The studies were conducted for two engine configurations: (1) an engine having a core compressor total pressure ratio of 14 with booster stages on the low pressure spool, and (2) an unboosted engine having a core compressor total pressure ratio of 23. The study determined that the best compressor efficiency was obtained by using medium values of average aspect ratio, solidity, and reaction ratio, and by using low values of inlet radius ratio, inlet specific flow, and exit Mach number. Reducing the number of stages by using higher speeds reduced the compressor length and cost but not necessarily the engine weight. Efficiency was not severely penalized by using fewer stages, provided the blading Mach numbers did not become excessive. High rear radius ratios were beneficial when used to hold rotor tip Mach numbers of the front stages below the level at which high shock losses would be present. The optimum rear radius ratio tended to increase as the number of stages was reduced and the speed increased.

At the conclusion of the AMAC study, a 10-stage, 23:1 pressure ratio compressor was recommended for further development. This design incorporated those features mentioned above as contributing to high efficiency. The choice of 10 stages was made because this appeared to offer the best overall combination of desirable features such as compactness, low cost, high efficiency, low engine operating cost, and low fuel usage.

The decision to use the very high (23:1) pressure ratio core compressor in an unboosted engine configuration was made because it gave the lowest fuel consumption, which resulted primarily from the use of an efficient two-stage HPT. This advantage outweighed the relatively small DOC penalty compared to a boosted engine with a lower core pressure ratio and a less efficient single stage HPT. The DOC studies used 7.9¢ to 13.2¢/liter (30¢ to 50¢/gallon) fuel prices.

The technical challenge inherent in such a high pressure ratio for the core compressor was not overlooked. In fact, it is still the highest pressure ratio design that General Electric has ever undertaken; the pressure rise is approximately 30% greater than that of any production single-spool aircraft engine compressor. Both variable stators and starting bleed were provided to aid in achieving adequate low speed stall margin. The challenge of developing stator and bleed schedules that avoid potential starting and idle-to-takeoff acceleration problems was considered to be substantial. Another challenge was to minimize the efficiency penalty that might result from blade shapes compromised for off-design operation. Therefore, detailed performance analyses were made for off-design conditions during the final design process in order to establish design incidence angles and work input distributions that allow high efficiency near design speed and adequate stall margin at part speed.

Refinements to the core compressor design continued during the E³ preliminary design study. The more significant refinements somewhat increased the inlet specific flow and the exit Mach number and reduced the speed, average aspect ratio, and average solidity. These changes were made mainly to reduce cost through the use of fewer and longer chord airfoils and to increase blade erosion resistance and general ruggedness. Despite the lower speed, an increase in stall margin potential was predicted, with only a small efficiency penalty.

Many of the advanced features incorporated into the detailed design of the E³ core compressor were developed during a parallel supporting research program - the NASA-sponsored Core Compressor Exit Stage Study. This program utilized a low speed, four-stage model of the blading used in the middle and rear E³ compressor stages to develop improved airfoil shapes and vector diagrams. A baseline stage and several modified stages were tested, and worthwhile improvements in efficiency and stall margin were demonstrated by design refinements that improved the flow in the end-wall regions.

Core compressor aerodynamic cycle match requirements were established primarily for the maximum-climb-thrust power setting at a flight condition of Mach 0.8 at 10.67 km (35,000 ft) altitude on a +10° C (+18° F) day. This operating condition places the core compressor at maximum corrected airflow and total pressure ratio. The performance requirements for this operating condition are listed in Table XIV. The operating line pressure ratio listed is for zero customer bleed air and zero power extraction. The performance goals in Table XIV are for the fully developed FPS. The compressor efficiency for the core and ICLS engines was 0.5 point lower than the FPS goal.

The basic vector design tool employed was General Electric's Circumferential Average Flow Determination (CAFD) computer program. This program computed the vector diagrams and fluid properties along numerous stream surfaces for a specified flowpath geometry, stage work input distribution, and estimated loss distribution. The resulting axisymmetric, steady-state, circumferential average flow solution included all effects of the full radial equilibrium equation and internal blade row calculations for some stages.

Vector diagrams along blade and vane leading and trailing edges were then used with airfoil section design procedures and cascade analysis computer programs to determine the final blade shapes.

The output data from the CAFD computer program were the vector diagrams at the intersection of the streamlines and the calculation stations. These vector diagrams were used in the design of the E³ blades and vanes as described in the next paragraph. In addition, the vector diagrams were used to calculate blade and vane diffusion factors as an indication of the aerodynamic loading.

Table XIV. FPS Compressor Aerodynamic Cycle Match.

Parameter	Maximum Climb
Corrected Speed, % Design	98.4
Corrected Airflow, kg/s (lbm/s)	54.4 (120.0)
Total Pressure Ratio	23.0
Adiabatic Efficiency	0.860
Polytropic Efficiency	0.906
Inlet Temperature, K (° R)	304.8 (548.6)
Inlet Pressure, N/m ² (lb/in ²)	60,469 (8.77)

The aerodynamic design of the airfoils for the E³ core compressor included the design of transonic and subsonic rotor blades, subsonic stator vanes, and inlet guide vane (IGV). Fundamentally, the approach utilized for all blade and vane designs was one of tailoring stream surface blade shapes to produce specific airfoil surface velocity distributions. The first four rotors were transonic blade rows and were designed utilizing techniques employed for advanced fan stages. The remaining six stages of rotor blades and all stages of stator vanes were designed to operate in a subsonic flow environment.

Casing ports for customer bleed and compressor active clearance control (ACC), used subsequently for LPT cooling and purge, are provided at Stator 5 exit. Other casing ports for HPT cooling air are located at the Stage 7 exit. The IGV and the first four stator vane rows are variable.

The original aerodynamic design of the core compressor was completed in the second quarter of 1979. Three component tests were conducted: the front six variable stator stages were tested in the first quarter of 1980, the full 10-stage compressor was tested for the first time during the first quarter of 1981, and a second version of the full 10-stage compressor was tested early in 1982. Various design refinements, made as a result of the data obtained during this experimental evaluation, were incorporated into the final compressor version utilized in the core and ICLS test engines.

5.2.2 Mechanical Design

Unique features contributing to the design objectives of producing a lightweight, rugged, efficient rotor are shown on Figure 19. The use of low aspect ratio airfoils produces a high tolerance to foreign object damage (FOD) and stall-induced damage. Utilization of fan discharge air to cool the rotor bore helps to optimize rotor-stator clearances, thus contributing to performance. Both the forward and the aft portions of the rotor are built up by inertia welding and joined by a single bolt joint, yielding a short, stiff structure (Figure 20).

The compressor stator cross section is shown in Figure 21. Unique features of the design are denoted. Although the rotor blades are made from

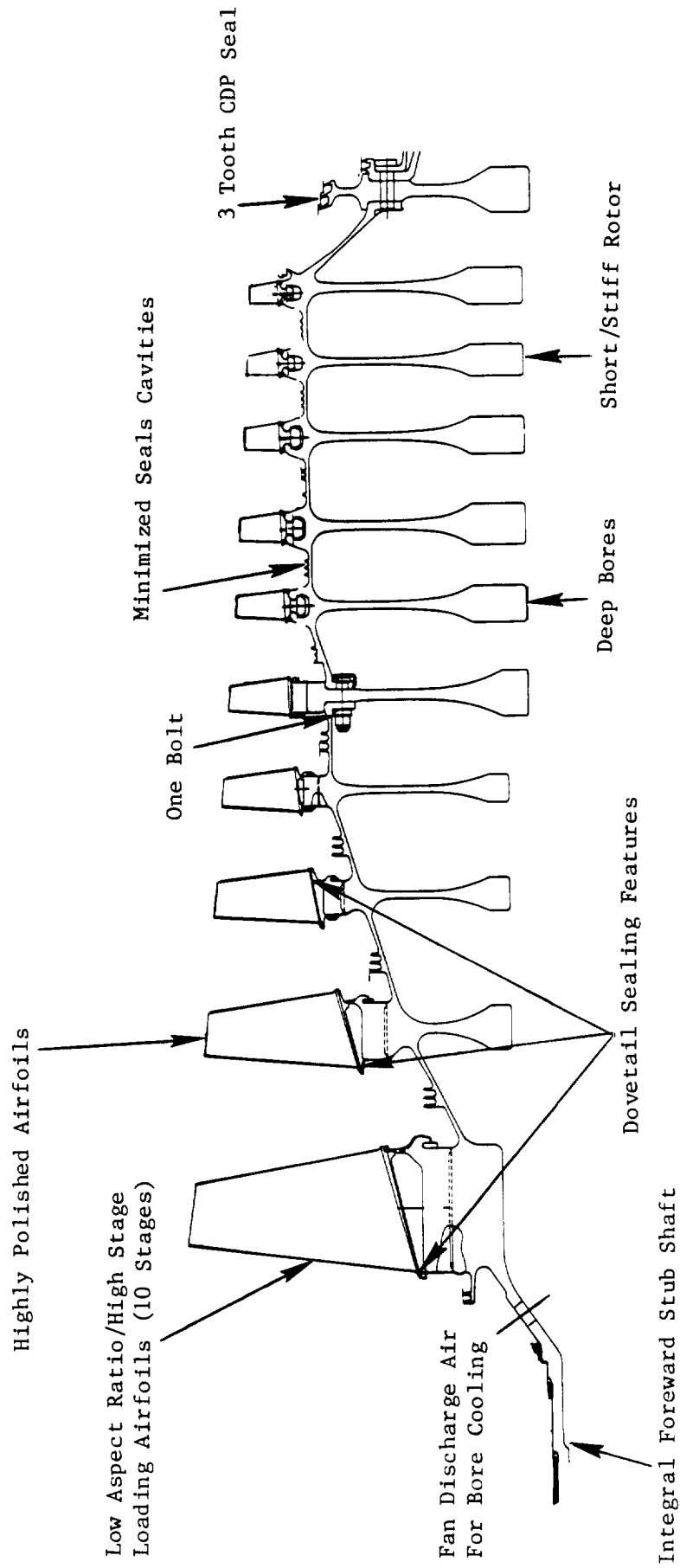


Figure 19. High Pressure Compressor Rotor Design Features.

ORIGINAL PAGE IS
OF POOR QUALITY

ORIGINAL PAGE
BLACK AND WHITE PHOTOGRAPH

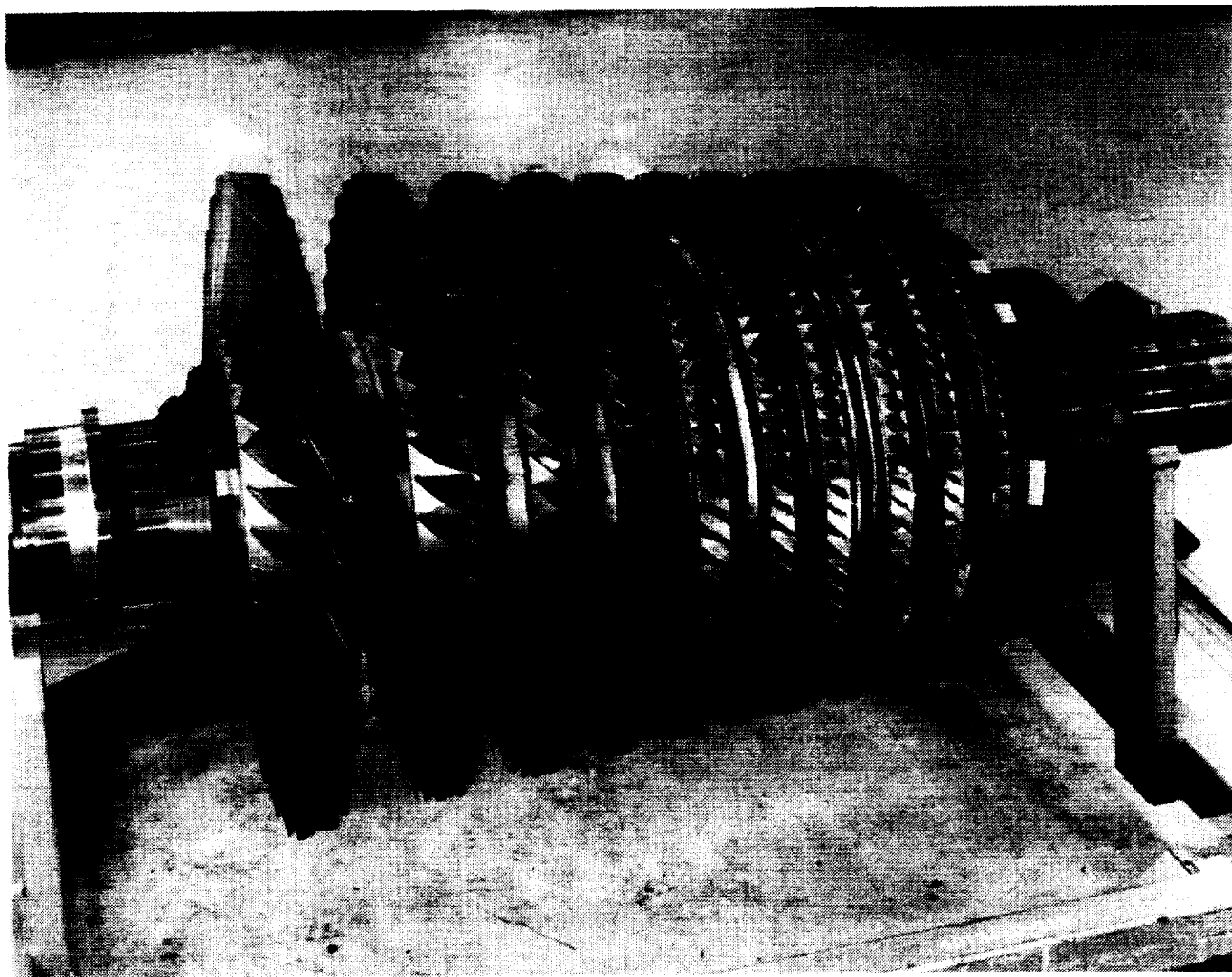


Figure 20. Compressor Rotor Hardware.

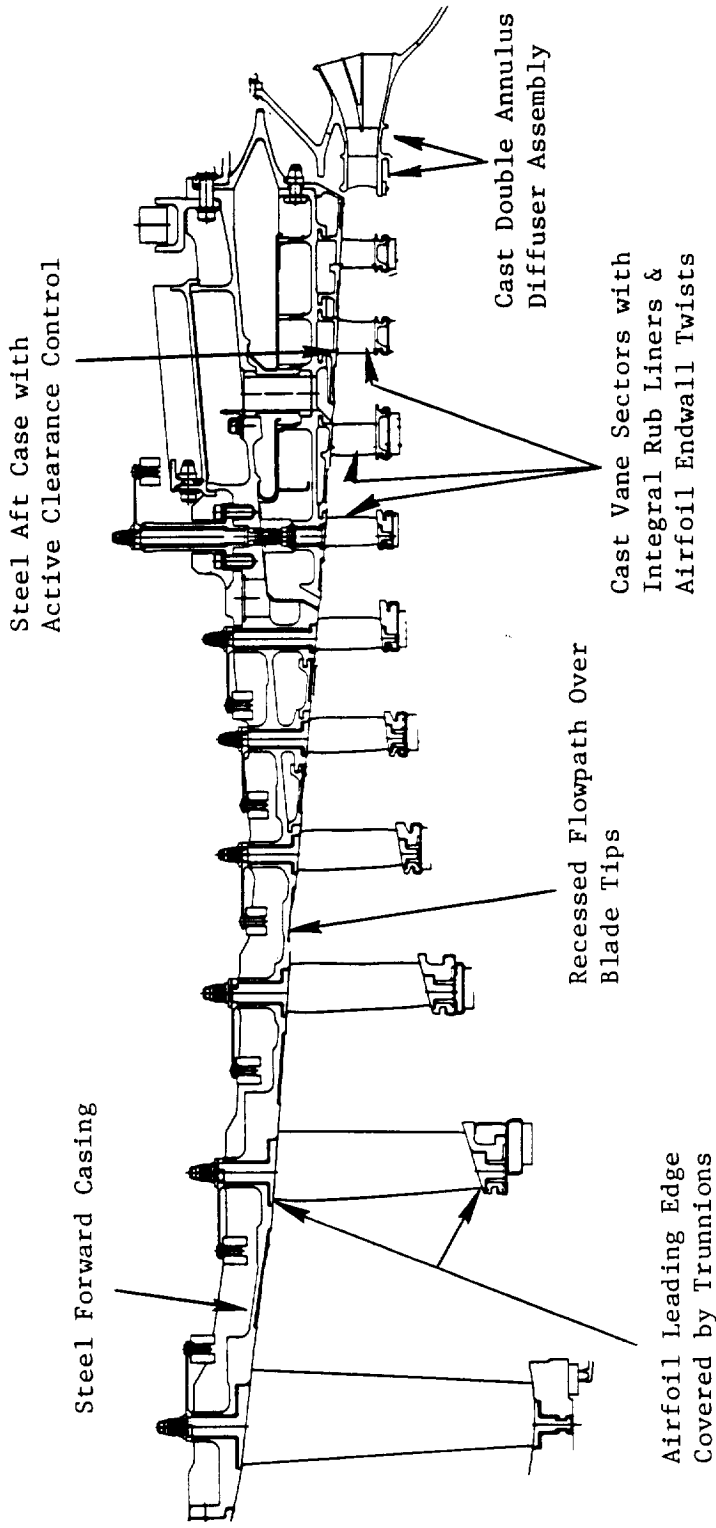


Figure 21. Compressor Stator Design Features.

titanium, titanium fire prevention is assured by the use of nontitanium casings and vanes. To improve compressor cruise performance, the aft case is designed to provide active control of rotor-stator clearances. This is accomplished by isolating the casing structure from the hot flowpath gases and then bathing the structural rings with cooler Rotor 5 discharge air to shrink the casing closer to the rotor blade tips. This cooling air is collected in the annulus over Rotor 10, then is ported through the forward case and piped aft where it is used to cool the LPT and rotor cavity. The air flow is controlled by a fuel-activated valve. The variable vanes are actuated by a torsion bar system which permits nonlinear schedules, low hysteresis, and accurate stator positioning.

The compressor discharge diffuser is a unique cast structure featuring a flowpath that is split into two annular passages and supported by hollow struts. A portion of the air exhausting at the splitter island is ducted inboard through the hollow struts to provide cooling for the HPT. The geometry of the diffuser is so complex that it required an advancement in the state of casting technology in order to be produced. In the early designs, it was planned that the outlet guide vane (OGV) ring would be cast integrally with the diffuser. However, the successful welding of the OGV ring to the diffuser for the core engine has proved this to be a more workable approach.

Blading for rotor Stages 1 through 5 is fabricated from titanium while the blading for Stages 6 through 10 is of Inco 718 material. The forward rotor drum and Stage 6 disk are titanium. The material for the aft drum is powder René 95. The IGV and stators 1 through 4 are A286 stainless steel; stators 5 through 9 are Inco 718. The casing is M152 steel.

5.2.3 Performance

The knowledge of FPS compressor performance derives from 357 hours of compressor rig testing, 44 hours of core engine testing, and 64 hours of ICLS engine testing. A 6-stage rig and two builds of 10-stage rig were tested in the General Electric Lynn compressor test facility. These rigs used engine hardware. Each step of the compressor rig testing identified good and poor qualities which determined design changes for the subsequent step. A final design was tested in the core and ICLS engines. This compressor design

exceeded its efficiency goal by 0.5%. Also, the engine compressor met its flow and pressure ratio at 1.9% lower speed than originally intended, a desirable condition.

The compressor efficiencies are given in Table XV.

5.3 COMBUSTOR

The combustor cross section is shown in Figure 22, and hardware is shown in Figure 23. The most unique feature of the combustor is the double annular arrangement. This achieves very low emissions while retaining very short engine length.

The E³ emissions goals are the EPA-proposed 1981 standards as they stood when the E³ program started in 1978. These standards have since been relaxed; however, the E³ program has retained the original standards as a program goal.

The following materials are used in the combustor:

Casing	Inco 718
Diffuser	Inco 718
Fuel Nozzle Body	Stainless Steel
Dome	Hastelloy X
Shingles	X-40

Thermal barrier coating is used on the dome and shingle liners.

5.3.1 Aerodynamic Design

The combustor is a short-length, double-annular design. The double-annular feature is used to provide low emissions over a wide range of power levels. Only the outer pilot zone is used at low power levels, and it is tuned for low fuel-air ratios. At higher power levels, both zones are used. The inner main zone is tuned for higher fuel-air ratios.

The combustor uses dual-cone nozzles for fuel injection. Compressor discharge airflow is directed to the combustor by a split duct prediffuser. Forty-eight percent of the air flows through the outer passage of the prediffuser toward the pilot stage dome, and the remaining 52% is directed toward

Table XV. Compressor Performance.

	MAX CLIMB	MAX CRUISE	TAKEOFF
Original FPS Required Efficiency ⁽¹⁾	0.857	0.861	0.871
10B Rig Test Efficiency ⁽¹⁾	0.847	0.849	0.855
Core and ICLS Test Efficiency ⁽¹⁾	0.854	0.856	0.858
Final FPS Required Efficiency ⁽²⁾	0.860	0.861	0.863

(1) Consistent with original cycle match.

(2) Consistent with final cycle match.

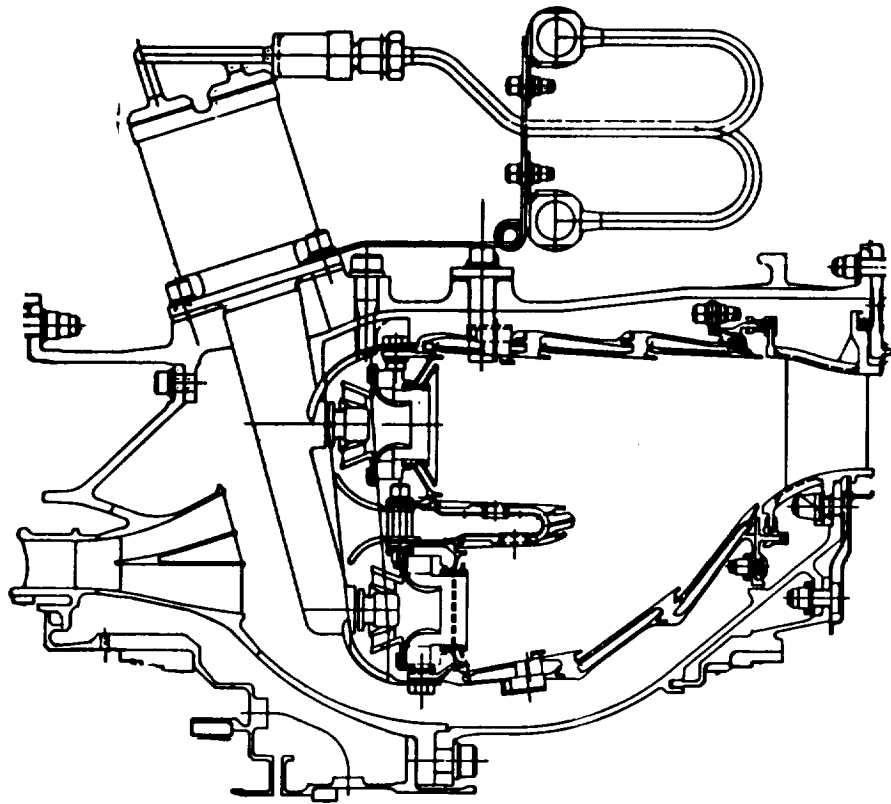


Figure 22. E³ Combustor Cross-Section.

ORIGINAL PAGE
BLACK AND WHITE PHOTOGRAPH

ORIGINAL PAGE IS
OF POOR QUALITY

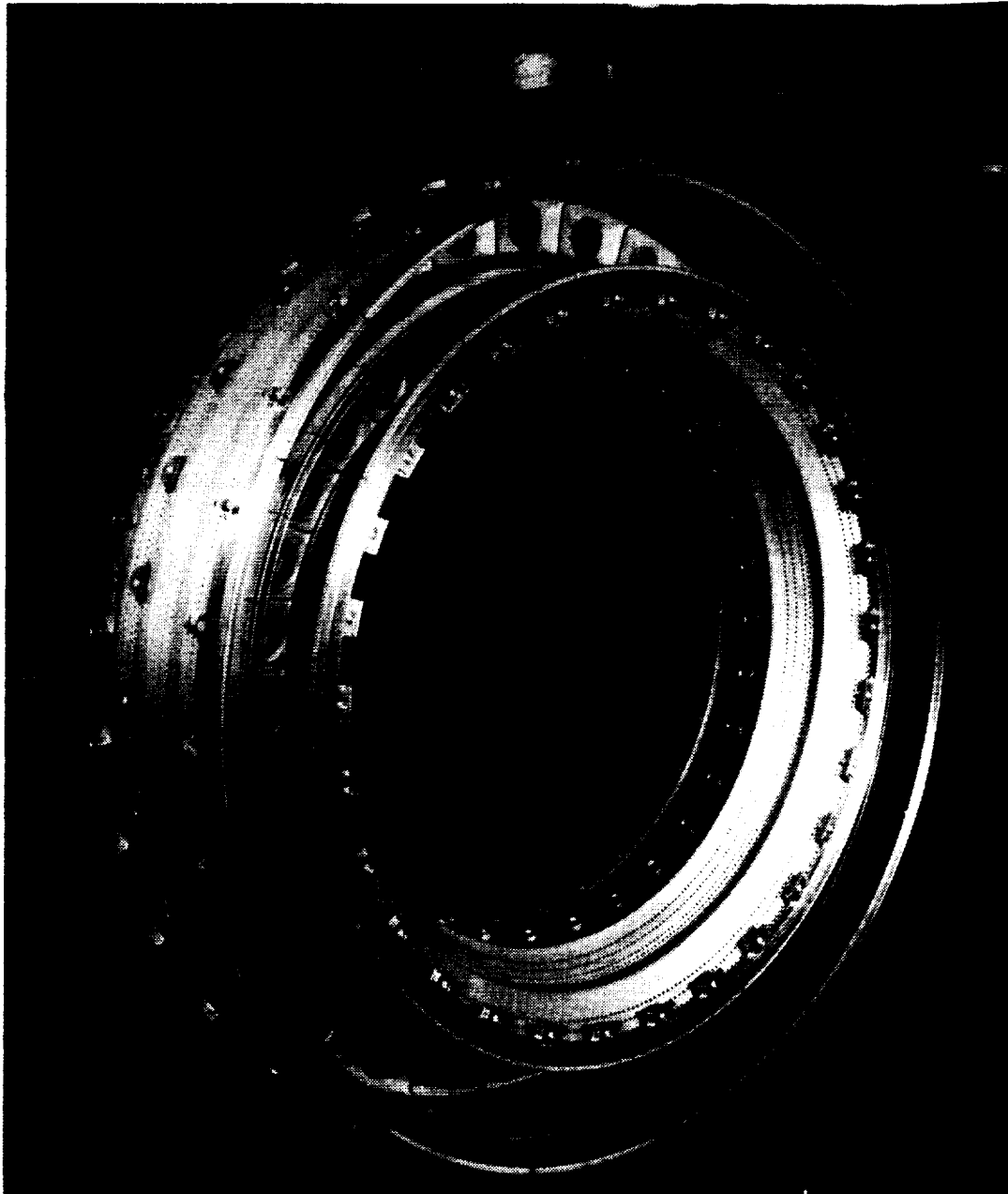


Figure 23. Combustor Liner/Dome Assembly - Aft Looking Forward.

the main stage dome by the inner passage of the prediffuser. The dome cups of the pilot stage and the main stage are each comprised of axial primary and counterrotating radial secondary airflow swirlers. The liners are of double wall construction and use impingement plus spent-film cooling on the segmented (shingle) section adjacent to the hot gas stream.

Fuel injection for each E³ combustor dome is provided by duplex-type fuel pressure atomizing nozzle tips mounted on a single stem. These fuel nozzles are described in more detail in the Mechanical Design section which follows. Each of the two tips has a low-fuel-flow primary system for good atomization at low power operating conditions and a high-fuel-flow secondary system to achieve the required fuel flow levels at high power. Fuel flow is supplied to the fuel nozzles by an annular manifold system. Fuel nozzle inlet check valves keep the manifold full and pressurized during shutdown to prevent fuel leakage into the combustor and to reduce start times. Fuel flow to the duplex nozzle tips is controlled by each of two scheduling valves (one for each tip) located in the housing above the stem. The fuel nozzle stem is encased in a heat shield to insulate the fuel from hot compressor gas temperatures. Each fuel-carrying tube within the stem is surrounded by a clearance gap to provide additional insulation.

5.3.2 Mechanical Design

A centerbody structure separates the outer diameter pilot zone from the inner main zone of the combustor. The double annular dome design consists of 60 identical swirl cups. Fuel is injected into the combustor through 30 dual-tip fuel nozzle assemblies. Each nozzle features independent fuel metering. The combustor utilizes a double-wall shingled liner design to provide long life. The combustor assembly is supported at the forward end by 30 support pins positioned radially to transmit all loads from the liners to the outer combustor casing. The combustor-to-stator interface is sealed with fishmouth seals which accommodate axial and radial thermal expansion and assembly clearance stackups between the components.

The outer casing supports the combustor assembly, fuel nozzles, fuel delivery system, and ignition system. Ports are provided in the casing for borescope inspection, compressor bleed, and instrumentation leadout.

The liner assembly consists of three axial rows of shingles in the pilot and main zones which are installed in outer/liner support liners. Each row of shingles forms an annular impingement cavity with the support liner. The impingement and dilution holes are laser drilled into the support liners which are machined from forgings. An assembled inner shingle liner is shown in Figure 23.

5.3.3 Performance

FPS combustor performance is based on 320 hours of rig testing and 109 hours of core and ICLS engine testing. Annular sector and full annular rig tests were conducted at Evendale, Ohio. Combustor pressure drop is set by the minimum required for the HPT vane cooling air circuit. Goal pressure drop will be achieved in the FPS. The combustor efficiency, established from balanced cycle analysis of core testing, was higher than the goal. This may have been due to an underassessment of efficiency of prior combustors rather than an improvement in combustor efficiency. Start ignition, staging from single- to double-annular combustion, and operational stability were all as desired during engine testing and would be so in the FPS. No smoke was visible during engine testing. The engine test combustor did not incorporate all emissions features so it was not expected to meet the NO_x emissions goals. Earlier rig testing with all features established that FPS goal emissions would be achieved. A summary of combustor performance goals, achievements and projections is presented in Table XVI.

The emissions projections in Table XVI are for 4% ground idle and for the use of only the pilot dome during landing approach. Two further points should be made. First, emissions can be reduced by increasing idle thrust to 6%. This would be undesirable because of higher fuel usage and the heavy braking required during aircraft taxi operations. Second, while the practice of cutting back to pilot dome only during approach is feasible, it is also undesirable from a flight safety consideration. The effects of idle thrust and of single- versus double-annular combustion during approach are shown in Table XVII. These FPS values are those actually achieved during full-scale combustor component tests.

Table XVI. Combustor Performance.

Parameter	FPS Requirement	Core & ICLS Test Results (Projected to FPS)	FPS Projection
Pressure Loss	5.0% at Max Power	5.0%	5.0%
Efficiency	99.6% at Max Power	99.95%	99.90%
Starting	-----	Started easily	Acceptable starts
Staging	-----	Successful at 10% thrust	Successful
Stability	-----	No audible noise or resonance	Stable
Emissions			
• SAE Smoke Number	≤ 20 SAE at High Power	Core - Measured < 10 SAE ICLS - No visible smoke	< 10 SAE
• Carbon Monoxide	3.0 lbs./1,000 lbs. Fn · Hr. · Cycle	2.82%	2.82%
• Hydrocarbons	0.4 lbs./1,000 lbs. Fn · Hr. · Cycle	0.20%	0.20%
• Oxides of Nitrogen	3.0 lbs./1,000 lbs. Fn · Hr. · Cycle	4.23% (Did not incorporate NO _x Feature)	3.0 (Based on rig test)

Table XVII. FPS Emissions.

Emissions In lbs./1,000 lbs. Fn · Hr. · Cycle					
		4% Fn Ground Idle		6% Ground Idle	
	FPS Requirement	Pilot Zone Only On Approach	Pilot and Main Zones On Approach	Pilot Zone Only On Approach	Pilot and Main Zones On Approach
CO	3.00	2.82	3.45	2.58	3.14
HC	0.40	0.20	0.26	0.19	0.24
NO _x	3.00	2.98	2.66	2.80	2.51

5.4 HIGH PRESSURE TURBINE

The E³ high pressure turbine (HPT) provides an advancement in turbine aerodynamic, cooling, and mechanical design technology over current production engines such as the CF6-50C. Moderate stage aerodynamic loading, efficient use of cooling air, low wheel space windage, and advances in flowpath contouring, vector design, and airfoil design all result in improved efficiency. The high wheel speed of the HPT, plus extended life requirements, dictated a very "clean" structural design.

Active clearance control is used to reduce blade tip clearances during cruise and to open clearances during flight conditions where rubs are likely to occur. Clearances are closed by impinging fan air on the HPT case. During the takeoff and early climb segments of the flight, the impingement air is shut off so that clearances will be large enough to accommodate thermal excursions and engine deflections. During cruise, impingement air is turned on to contract the casing, reducing clearances.

An active clearance control heating circuit warms the HPT casing quickly during the initial warmup of the engine. This circuit ducts hot compressor discharge air into the HPT active clearance control manifold to expand the casing, thus opening clearances. It is used only during low power warmup. This circuit prevents blade tips from rubbing when a cold engine is accelerated to full power.

The HPT cross section is shown in Figure 24. Photographs are shown in Figures 25 through 27.

5.4.1 Aerodynamic Design

In order to meet the cycle requirements and goals of this program, a two-stage turbine of moderate loading was selected. The aerodynamic design point was chosen to be the maximum climb condition at Mach 0.8 and 10.67 km (35,000 ft), +10° C (+18° F) standard day. This point was determined to be the most stringent, based on a comparison of ICLS and FPS requirements. The significant turbine operating point data are summarized in Table XVIII.

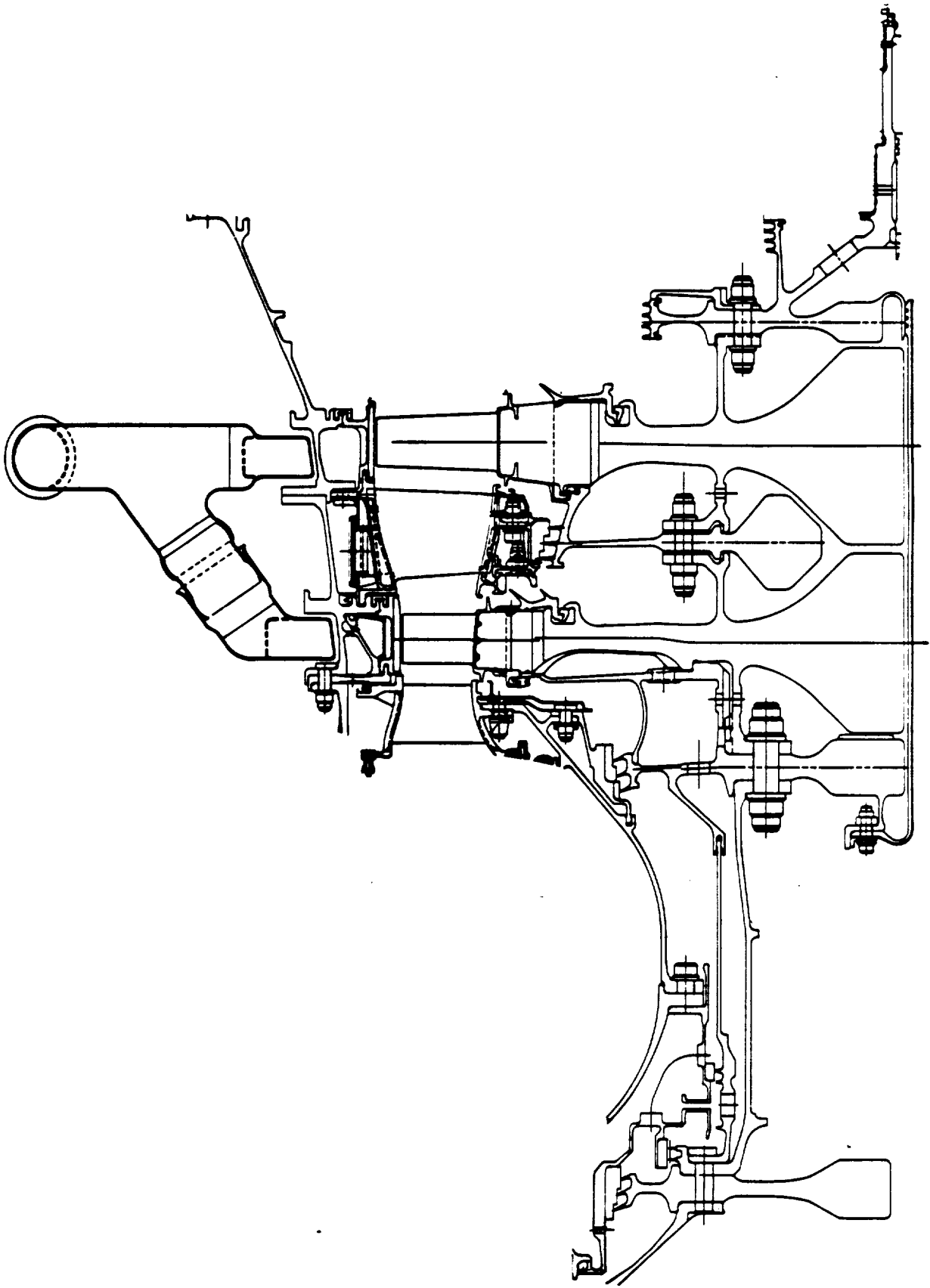


Figure 24. E³ High Pressure Turbine Cross Section.

ORIGINAL PAGE
OF POOR QUALITY

ORIGINAL PAGE
BLACK AND WHITE PHOTOGRAPH



Figure 25. Stage 1 High Pressure Turbine Nozzle Assembly.

ORIGINAL PAGE
BLACK AND WHITE PHOTOGRAPH

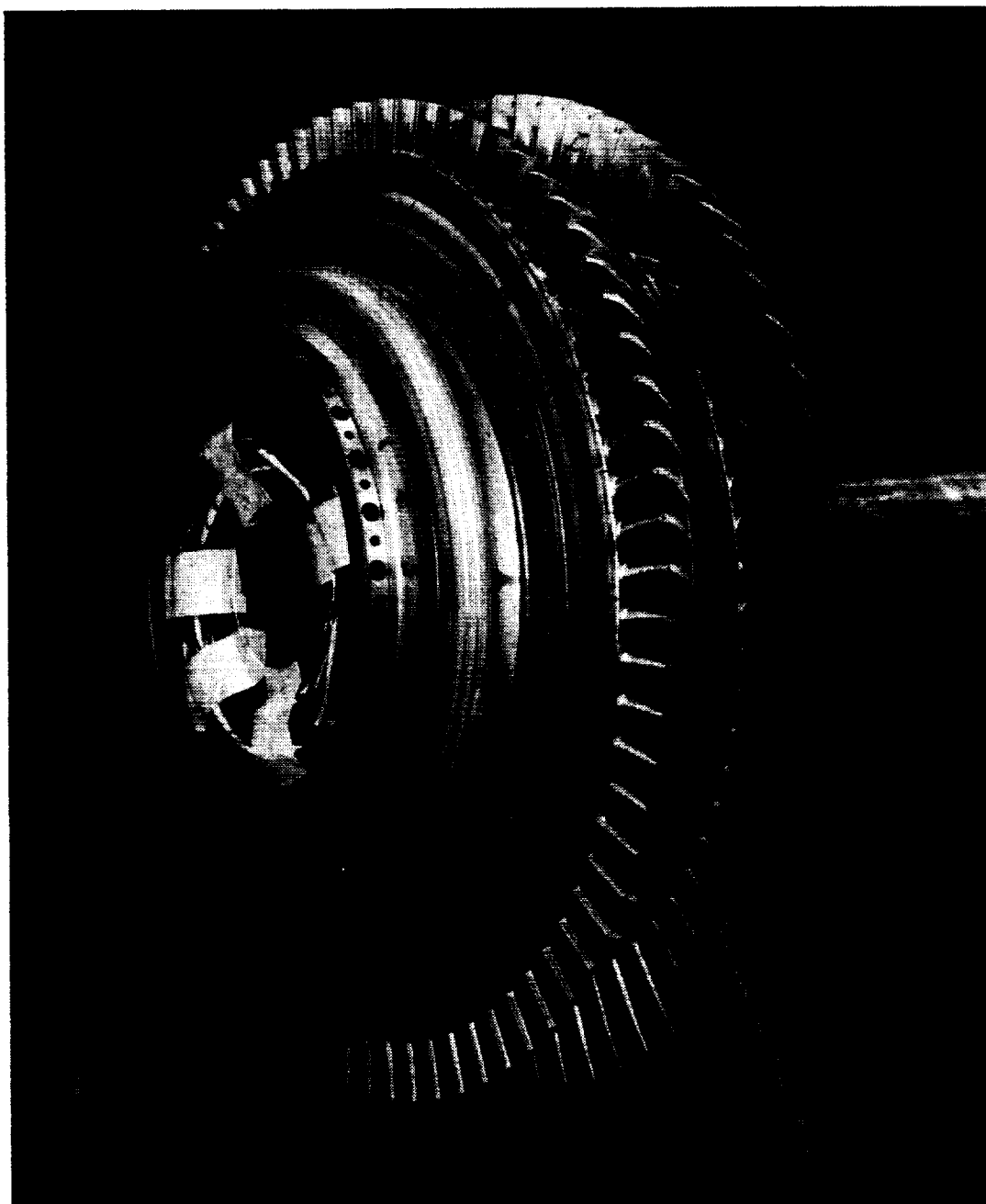


Figure 26. High Pressure Turbine Rotor Assembly.

ORIGINAL PAGE
BLACK AND WHITE PHOTOGRAPH

ORIGINAL PAGE IS
OF POOR QUALITY

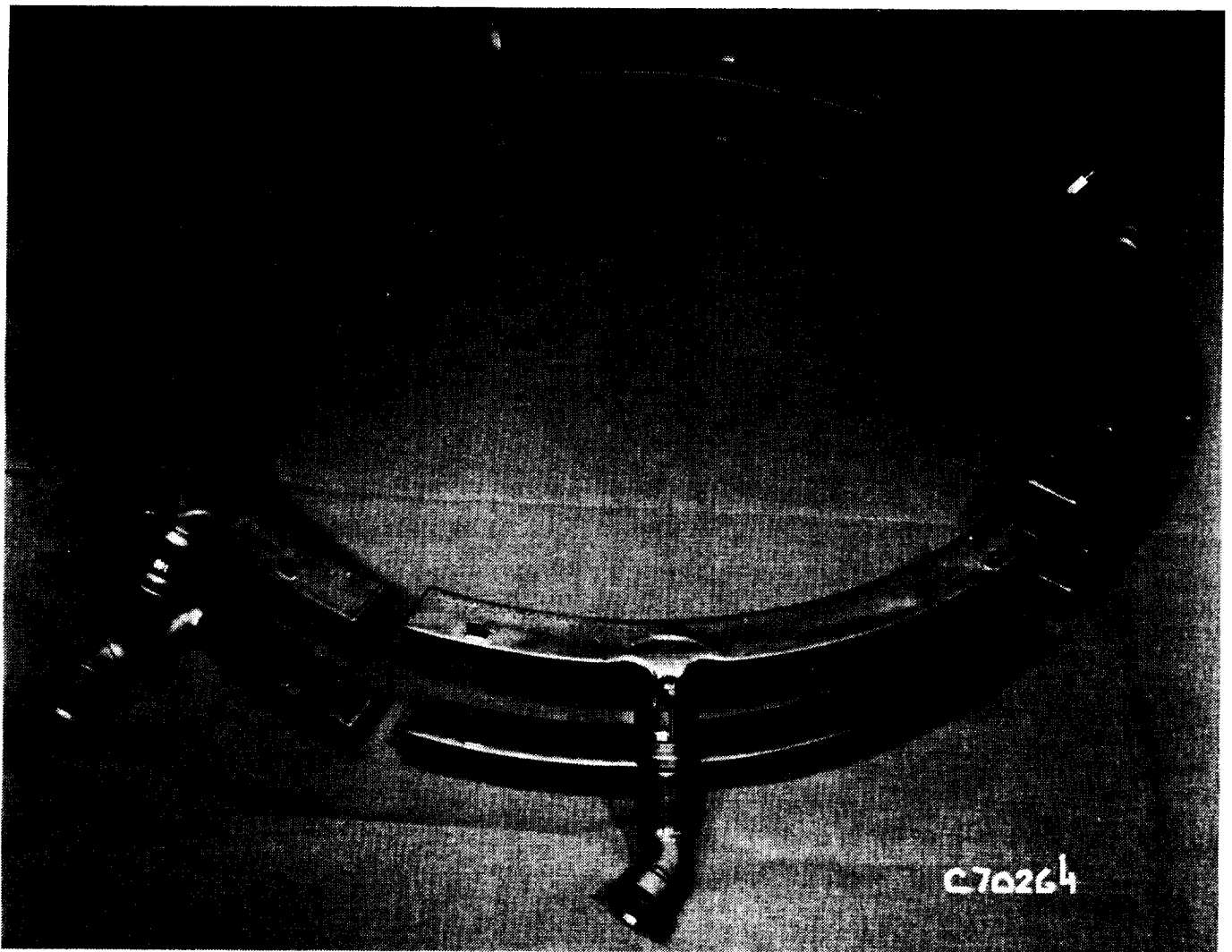


Figure 27. High Pressure Turbine Active Clearance Control Manifolds.

Table XVIII. HPT Aerothermodynamic Cycle Match Point.

Parameter	Units	Maximum Climb
Inlet Temperature, T_{41}	K (° R)	1,517 (2,730)
Energy, $\Delta h/T$	J/kg·K (Btu/lbm/° R)	355.5 (0.0849)
Speed, N/\sqrt{T}	rad/sec· \sqrt{K} (rpm/ $\sqrt{° R}$)	33.47 (238.3)
Corrected Flow, $W\sqrt{T/P}$	$g\sqrt{K}/\text{sec}\cdot\text{Pa}$ (lbm $\sqrt{° R}/\text{sec}\cdot\text{psi}$)	0.8643 (17.64)

With minimum cruise specific fuel consumption (sfc) and flight fuel burn as the primary evaluation criteria, a series of systems trade studies were performed to identify the turbine configuration and flowpath dimensions for use in subsequent detailed analyses. Single-stage and two-stage turbines were considered. The two-stage turbine was selected because the high turbine loading dictated by the high pressure ratio compressor best utilizes two turbine stages to maximize efficiency.

The turbine pitchline diameter was established through trade studies which recognized blade loading, blade aspect ratio, weight, tip clearance, and transition to the LPT. The resulting diameter was thought to be close to optimum for the overall HPT/LPT system.

Further trade studies for determining optimum annulus heights were conducted by making vector calculations in which stage exit annulus heights were varied individually. The effects on efficiency of the consequent variation of tip clearance, aspect ratio, edge blockage, aerodynamic loading, and gas deflection were evaluated. Variation in flowpath wetted area and the consequent effect on cooling air consumption and loss were evaluated concurrently and were included in the turbine efficiency evaluation. The design values of annulus area were selected slightly below the aerodynamic optimum in order to minimize the high weight penalty that would be imposed for relatively small gains in efficiency.

Using the flowpath developed in the annulus height studies, further studies were conducted to identify the most appropriate stage energy distribution. The calculations were executed in a manner similar to the annulus height studies but maintaining constant blade aerodynamic loading. The results of this study indicated that an optimum distribution would exist at approximately 48% to 50% energy extraction in the first stage. However, given the requirement that the second-stage vane coolant supply pressure exceed gas total pressure, it would have been necessary to shift from compressor seventh to eighth stage cooling air extraction, with a net increase in sfc. Consequently, the stage work distribution was selected at 56.5% in the first stage, the minimum consistent with seventh stage extraction.

The through-flow analysis was executed using a method that solves the full three-dimensional, radial equilibrium equation for circumferentially averaged flow. The procedure accounts for streamline slope and curvature, the effect of radial blade force component due to airfoil sweep and dihedral, airfoil blockage, and radial gradients of flow properties. Calculations were made with radial gradients of blading losses and also with local flow addition to simulate cooling flow injection. Temperature dilution and momentum losses associated with coolant addition were accounted for. The airfoil inlet angle selection considered mixing between streamtubes, combustor temperature profile, and secondary flow effects.

Airfoil cascade analysis was accomplished by a streamtube curvature method which calculates the compressible flow along a stream surface determined from the through-flow analysis, thus accounting for variations in streamtube thickness.

5.4.2 Mechanical Design

General Electric's E³ HPT represents an advanced technology design aimed at achieving high efficiency while still meeting the component life objectives.

The HPT mechanical features are as follows:

- Inducer System - Reduces the temperature of blade cooling air.

- Impeller - Increases blade coolant air pressure in order to maintain sufficient backflow margin between cooling air pressure and hot gas-path pressure.
- Inner Tube - Separates the compressor rotor purge air from cooling air feeding the Stage 2 blades.
- Deswirler - These are rotating vanes built as an integral part of the inducer disk. The purpose of these vanes is to eliminate any potential hazard from acoustic vibration or "vortex whistle."
- Boltless Blade Retainers - This design requires no bolts through the rim of the disk for support. Elimination of these holes enhances the low cycle fatigue capability of the disk.
- No Bolts in Disks - The main structural portions of the disks contain no holes. This feature is essential in achieving a long life in disks.
- Interstage Disk - Provides better interstage seal clearance control with subsequent reduction of leakage across the interstage seal.
- Single-Wall Structures - The use of a single-wall casing structure simplifies the geometry configuration for the ACC system. Direct access is provided for the ACC cooling air to impinge on the casing, which directly controls the shroud-to-blade clearances. No holes penetrate the casing wall.
- Stage 1 Ceramic Shrouds - Ceramic shrouds require less cooling air compared to other types of shroud material. Resulting cooling air reduction increases thermodynamic efficiency.
- Stage 2 Solid Shrouds - Use of a solid shroud configuration is expected to improve component life relative to present designs.
- Active Clearance Control System - Impinges fan air on turbine casing by FADEC-scheduled demands to reduce clearance at cruise and retain large clearance for thermal transients and maneuver deflections.

The following materials are used in the HPT:

Casing	Inco 718
Stage 1 Vane Airfoils	MA754 ODS with TBC
Stage 1 Vane Bands	Mar-M-509 with TBC
Stage 1 Vane Inner Support	René 41
Stage 1 Shroud	ZrO Ceramic
Stage 2 Vane	N4 with TBC
Stage 2 Shroud	Geneseal
Stage 1 Blade	N4 with TBC

Stage 2 Blade	DS Eutectic (Noncooled)
Blade Disks	René 95
CDP Seal Disk	AF115
Interstage Disk	AF115
Aft Disk	Inco 718
Blade Retainers	AF115
Shafting	Inco 718

5.4.3 Cooling Design

The cooling flow supply circuits are shown in Figure 28. Compressor discharge air cools the Stage 1 vane and the structure above the Stage 1 blade shroud. Air is drawn from the center of the split combustor diffuser for the rotor cooling circuit. The flow reversal into the center of the diffuser separates foreign particles from the air for the rotor cooling circuit. This flow is accelerated tangentially by a radial inflow inducer nozzle prior to entering the shroud. This air purges the rotor cavities and cools the Stage 1 blades. Seventh stage compressor bleed air cools the Stage 2 vanes, cools the structure above the Stage 2 blade shroud, purges the structure under the Stage 2 vane, and purges the wheel space cavities adjacent to that structure. Air that leaks through the compressor discharge seal is used to purge the cavity between the inner combustor case and the HPT Stage 1 disk. Fifth stage bleed purges the aft wheel space cavity after passing through the LPT turbine Stage 1 vane.

Cooling air impingement and film are used to cool the Stage 1 vanes and bands. Two impingement inserts are used in the vane.

The Stage 1 blades use two cooling circuits. In the forward circuit, air traverses a three-pass (up-down-up) serpentine passage, flows through a row of holes in a radial web, impinges on the back side of the leading edge, and then flows through the airfoil wall to provide film cooling. In the aft circuit, air flows outward into a chamber. A portion of the air blows aft for convection cooling and then exits at the pressure side of the trailing edge. The remainder of the flow traverses a down-up serpentine passage and discharges into the tip cavity.

--- Vane and Shroud Cooling Air
..... Disk and Blade Cooling Air

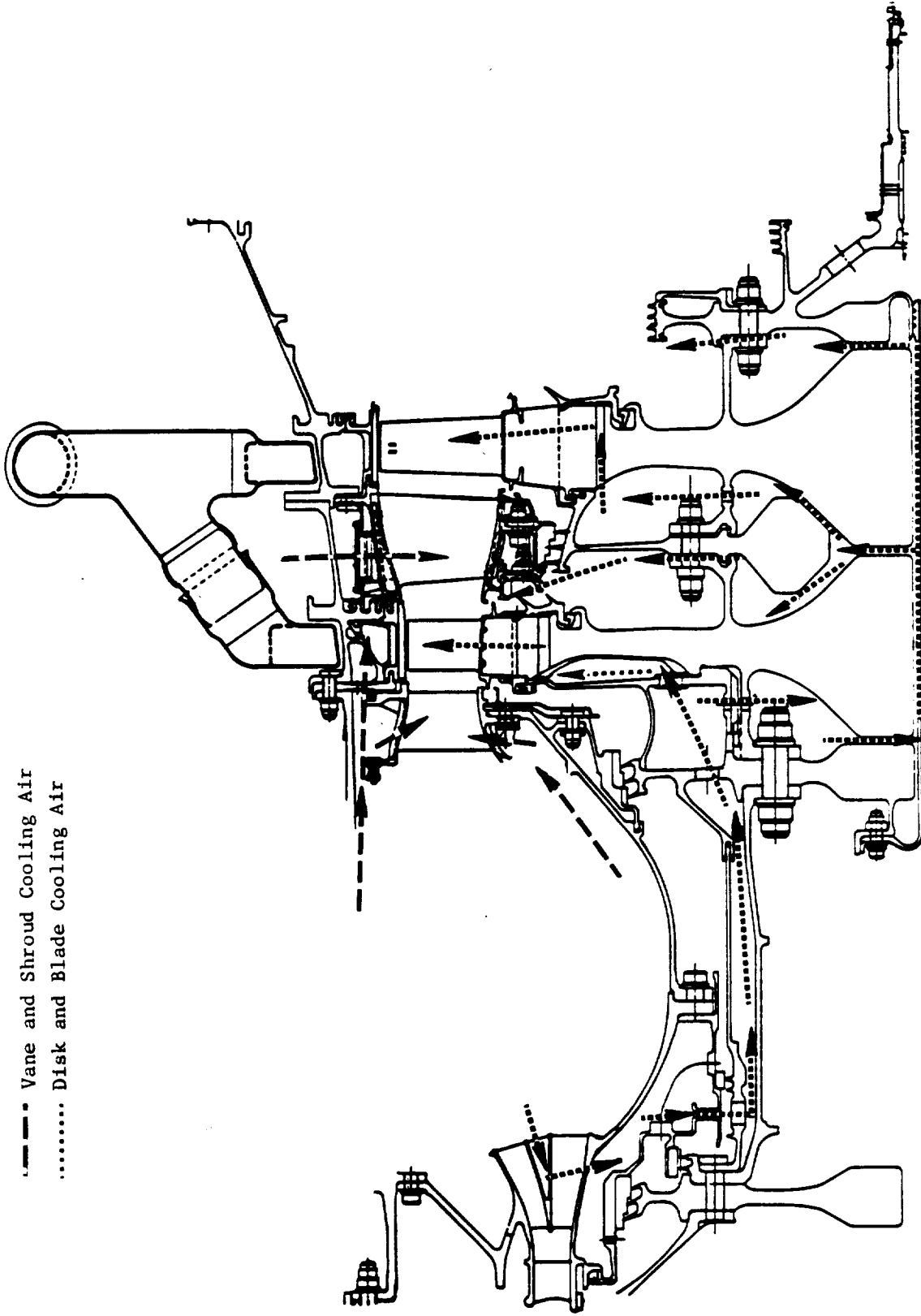


Figure 28. High Pressure Turbine Cooling Flow Supply Circuits.

The Stage 2 vane cooling air passes through holes in an insert to impinge on the vane wall, then provides cooling of internal walls by convection, and is subsequently ejected through slots on the pressure side of the vane's trailing edge. The Stage 2 blade is a high taper design using DS eutectic material and is not cooled.

Air for the HPT ACC system is extracted from the fan duct through a split scoop. The air, once inside the scoop, is slowed efficiently through a 2:1 area ratio diffuser to recover as much as possible of the fan duct dynamic head. After diffusion, the HPT ACC air is ducted to the modulation valve in the pylon. After flowing through the valve, the air is delivered to a 270° circumferential rectangular duct built into the core cowl outside the HPT. From this circumferential duct the air is routed through four pipes to the impingement manifold surrounding the HPT casing. There are four impingement-manifold segments surrounding each of the two turbine stages. The impingement manifolds have rectangular cross sections and allow the required proximity of small impingement holes to the casing clearance control rings and bolt flanges. The clearance of each stage in the HPT is accomplished by impinging the fan air on the casing, ACC rings, and bolt flanges.

The compartment outside the HPT is isolated from the rest of the engine volume between the core engine and the inner fan duct flowpath by the fire safety wall, also called the pressure bulkhead. This is necessary because the pressure of the spent impingement air is lower than the fan duct static pressure at maximum ACC flow rates. From this isolated cavity, the spent ACC air can flow inward through the struts of the rear frame to the aft centerbody and discharge out the vent stinger at a velocity such that much of the thrust is recovered.

A means of heating the casing during engine warmup was also devised. The heating system impinges 0.3% W₂₅ of compressor discharge air on the outside of the casing. This is done for 200 seconds after the engine is at stabilized idle power conditions. The purpose of heating the casing is to prevent blade tip rubs if the engine were to be accelerated to full power while the casing was relatively cool compared to the rotor.

Extensive studies have been conducted on the HPT to evaluate the characteristics and possible problem areas of the ACC system. Typical results of

a few of these studies are presented in Figures 29 through 31. The Stage 1, interstage seal, and Stage 2 clearance analyses at start, takeoff, and cruise are summarized for hot-day conditions. In this particular analysis, the casing was allowed to heat up during start, idle (8.3 minutes), and takeoff (2 minutes) before the ACC air was turned on as the engine was throttled back to maximum climb. The ACC air was left on at that rate up to 10.67 km (35,000 ft), and the engine was allowed to stabilize thermally at maximum cruise before going through a throttle chop to flight idle and reburst back up to maximum cruise. This mission includes a few of the most severe transient cycle variations that can be expected in airline service and can be used as an indication to show the deficiencies and capabilities of the ACC system.

The design approach used was to set a 0.64 cm (0.025 in.) clearance at takeoff for both the first-stage and the second-stage blade tips. This also sets the buildup clearance. The interstage seal buildup clearance will be such that a slight rub will occur at takeoff; this will ensure minimum seal clearance for all conditions.

The results of this analysis are presented in Figures 29 through 31. Table XIX summarizes the analysis and shows the expected performance requirements.

5.4.4 Performance

FPS HPT performance is based on 319 hours of cascade and rig testing and 109 hours of core and ICLS testing. Full scale but nonengine hardware was rig tested in the Evendale turbine test facility. Cooling was fully simulated where it affected the aerodynamics of the turbine, but airfoil internal geometry was not simulated. Since performance was sufficiently above goals, further diagnostic testing and evaluation of alternate designs were cancelled in order to utilize program funds elsewhere. This hardware is still available and further improvements in performance might be realized by testing it. Cooling was separately explored in a heat transfer cascade.

Based on rig and engine testing, the turbine efficiency results are presented in Table XX.

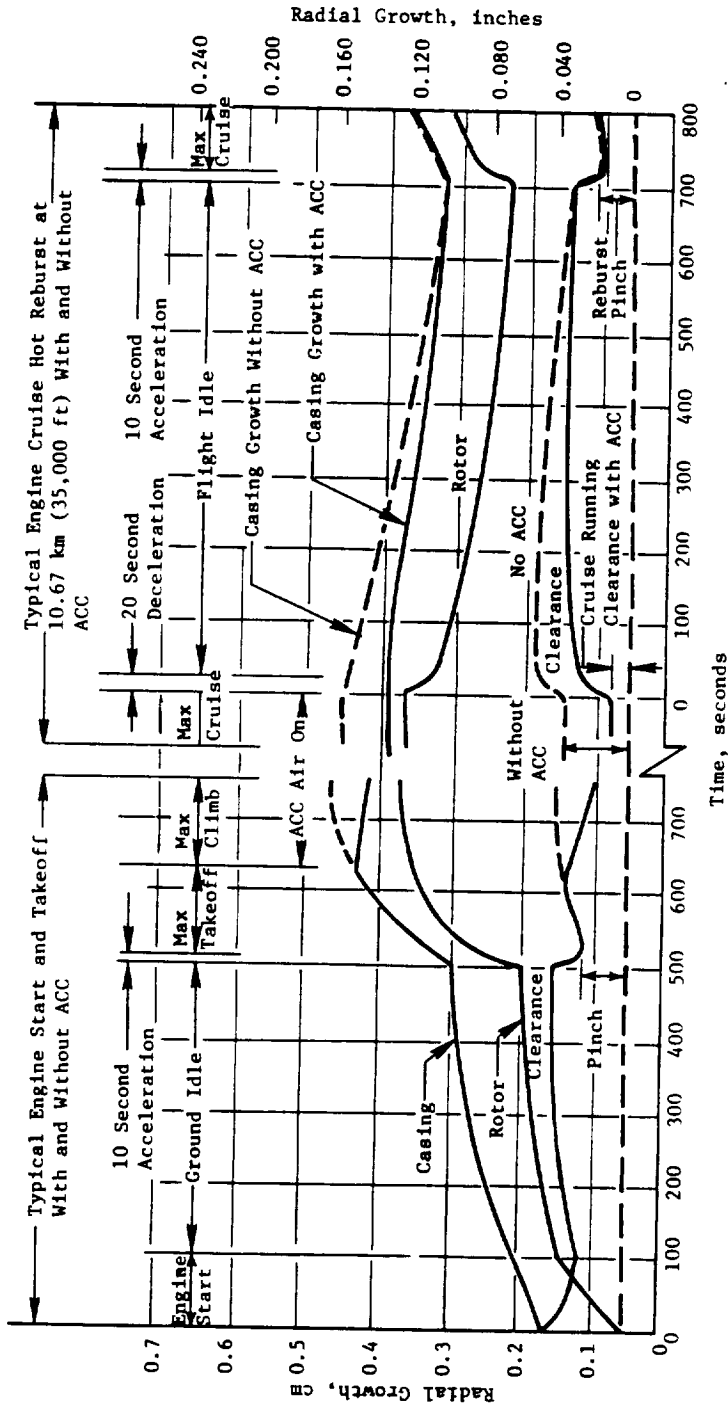


Figure 29. Stage 1 Blade-Tip Clearances.

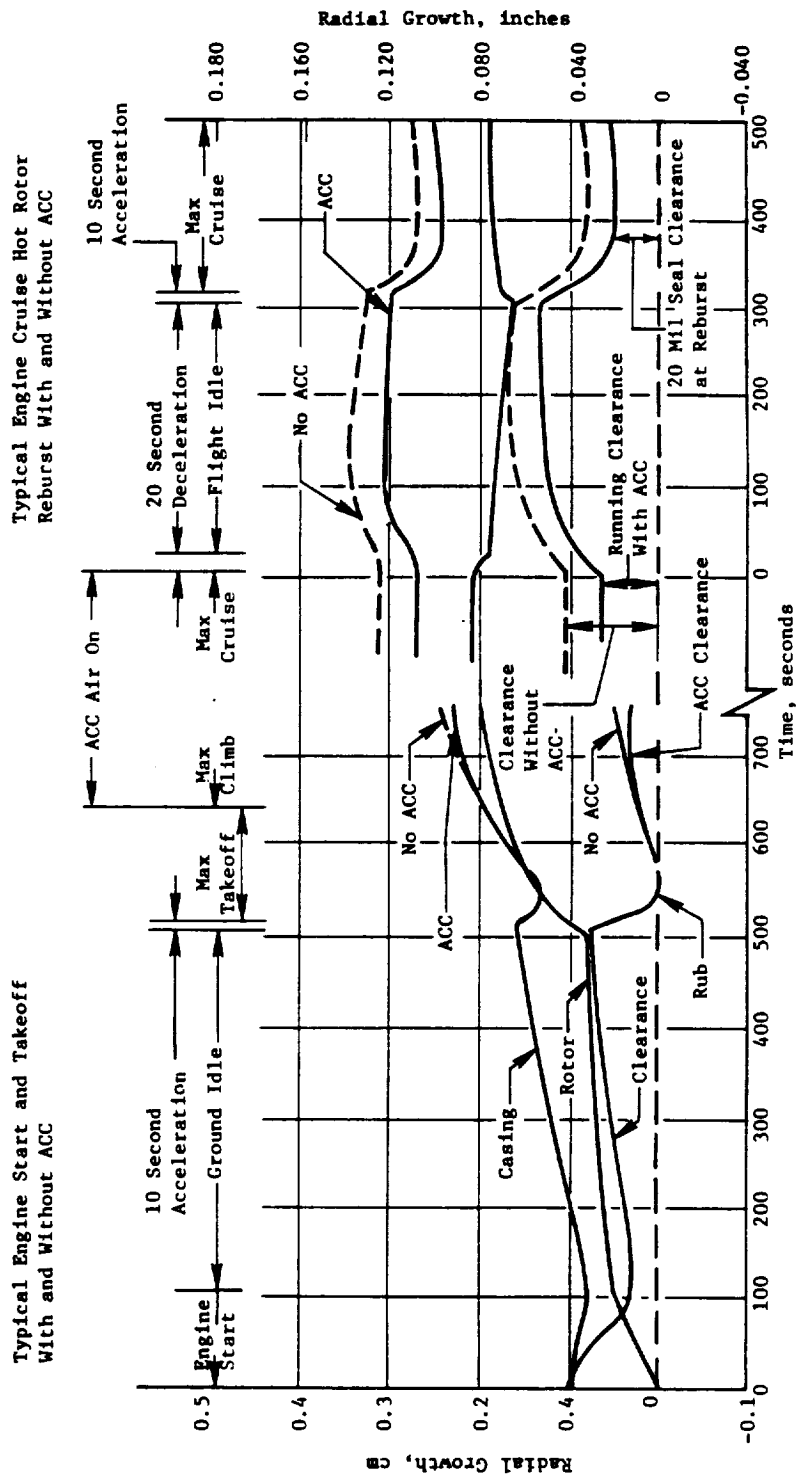


Figure 30. Interstage Seal Clearances.

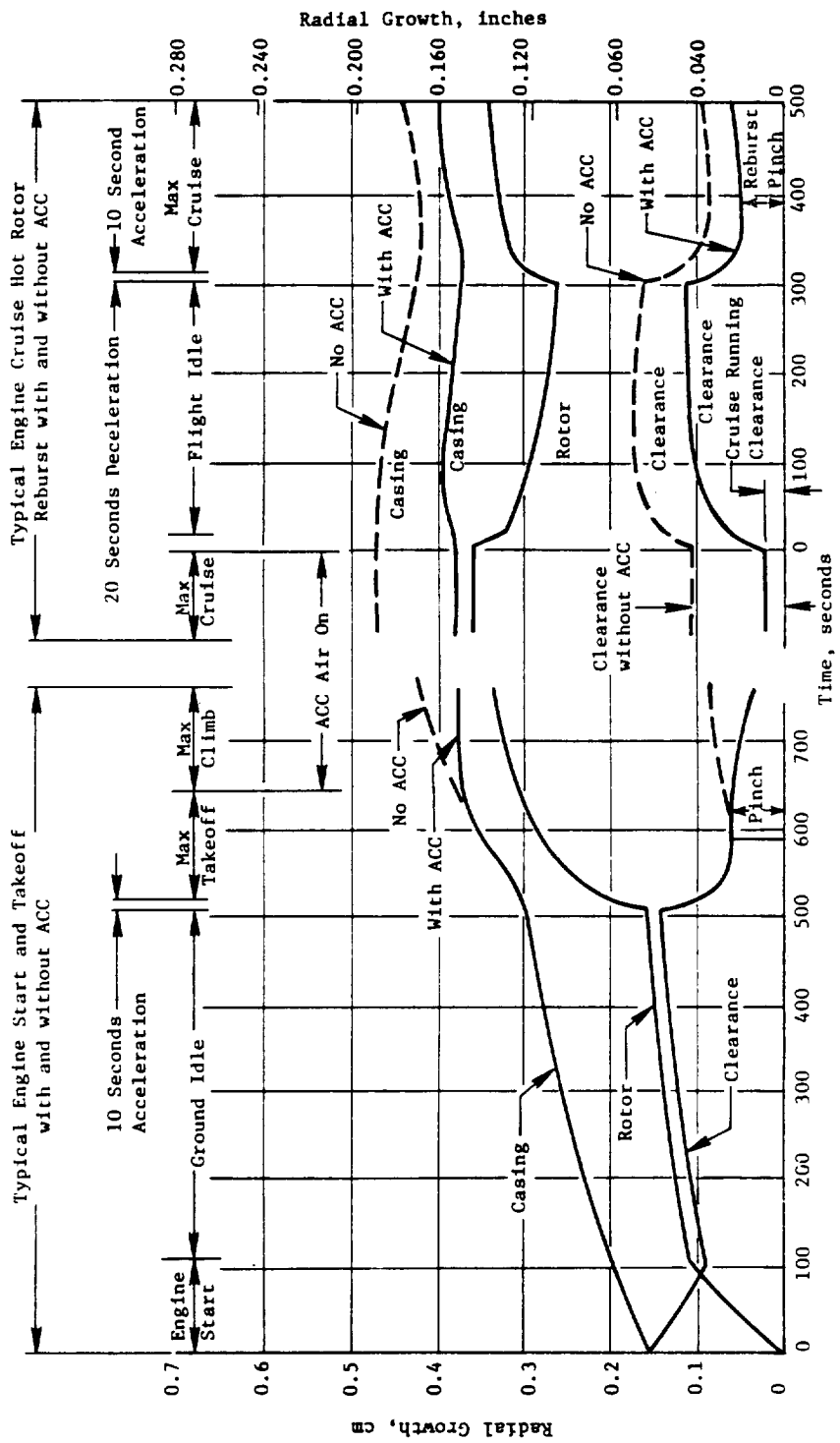


Figure 31. Stage 2 Blade-Tip Clearances.

Table XIX. Active Clearance Control System Payoff.

- Based on Air-Turbine Data and 0.041 cm (0.016 in.) Clearance
- Maximum Climb, 10.67 km (35,000 ft) Altitude

	$\Delta\eta_T$ /mm	$\Delta\eta_T$ /mil	Clearance No ACC,		Clearance With ACC,		$\Delta\eta_T$
			cm	in.	cm	in.	
Stage 1	1.732	0.044	0.094	0.037	0.053	0.021	0.924
Stage 2	0.669	0.017	0.109	0.043	0.069	0.027	0.459
Interstage Seal	0.472	0.012	0.102	0.040	0.033	0.013	0.150
$\Delta\eta_T$ Total					+1.533		
$\Delta\text{sfc}\eta_T$					-1.24%		
$\Delta\text{sfc}W_C$					+0.02%		
Net Δsfc					-1.22%		
W_C (Fan Air) - 0.15% W_{25}							

Table XX. High Pressure Turbine Performance.

	Max Climb	Max Cruise	Takeoff
Original FPS Required Efficiency ⁽¹⁾	0.924	0.924	0.920
Rig Test Efficiency ⁽¹⁾	0.925	0.925	0.926
Core & ICLS Test Efficiency ⁽¹⁾	0.925	0.925	0.926
Final FPS Required Efficiency ⁽²⁾	0.927	0.927	0.921
Original Cooling Flows, %W25			
Non-chargeable Flow (Enters Ahead of Vane 1 Throat)		9.24	
Chargeable Flow (Enters Downstream of Vane 1 Throat)		9.00	
Final Cooling Flows, %W25			
Non-chargeable Flow		7.46	
Chargeable Flow		5.33	

(1) Consistent with original cycle match.

(2) Consistent with final cycle match.

Also included in Table XX are the status cooling flow rates. The original FPS was designed using CF6-based heat transfer coefficients. Although lower coefficients were anticipated, the more conservative cooling flows were used in the cycle. Core engine test experience established that E³ turbine heat transfer coefficients are significantly lower, especially on the pressure side of the airfoils. The reduction is attributed to the more efficient aerodynamics. The final FPS cooling flow rates reflect the lower coefficients and also reflect reductions resulting from material changes and adding thermal barrier coating.

5.5. LOW PRESSURE TURBINE

The low pressure turbine configuration was selected after investigation of alternate designs, trade-off studies, payoff evaluations, and extensive preliminary design analyses aimed at achieving high aerodynamic efficiency while maintaining maximum mechanical integrity.

The LPT is a five stage, moderately loaded, low throughflow design with an outer wall slope of 25° and with acoustic treatment designed into it. The LPT is close coupled to the HPT by means of a 7.62 cm (3 in.) axial length transition duct. The flowpath has been sized to accommodate a potential growth application. The cross section is shown in Figure 32, and the rotor hardware is pictured in Figure 33.

In order to improve roundness control and radial clearances, the casing is a full 360° structure, rather than two 180° halves, with nozzle stators attached in multivane segments. The LPT rotor assembly employs high-aspect-ratio, tip-shrouded blading in disks connected by bolted flanges in low-stress attachment areas. The rotor assembly is supported by a single bearing cone.

Active clearance control is an integral part of the LPT design. The ACC uses fan bleed air routed from pylon scoops to a distribution manifold for impingement on the casing. The ACC system reduces blade tip and interstage-seal radial clearances at selected high-performance operating points.

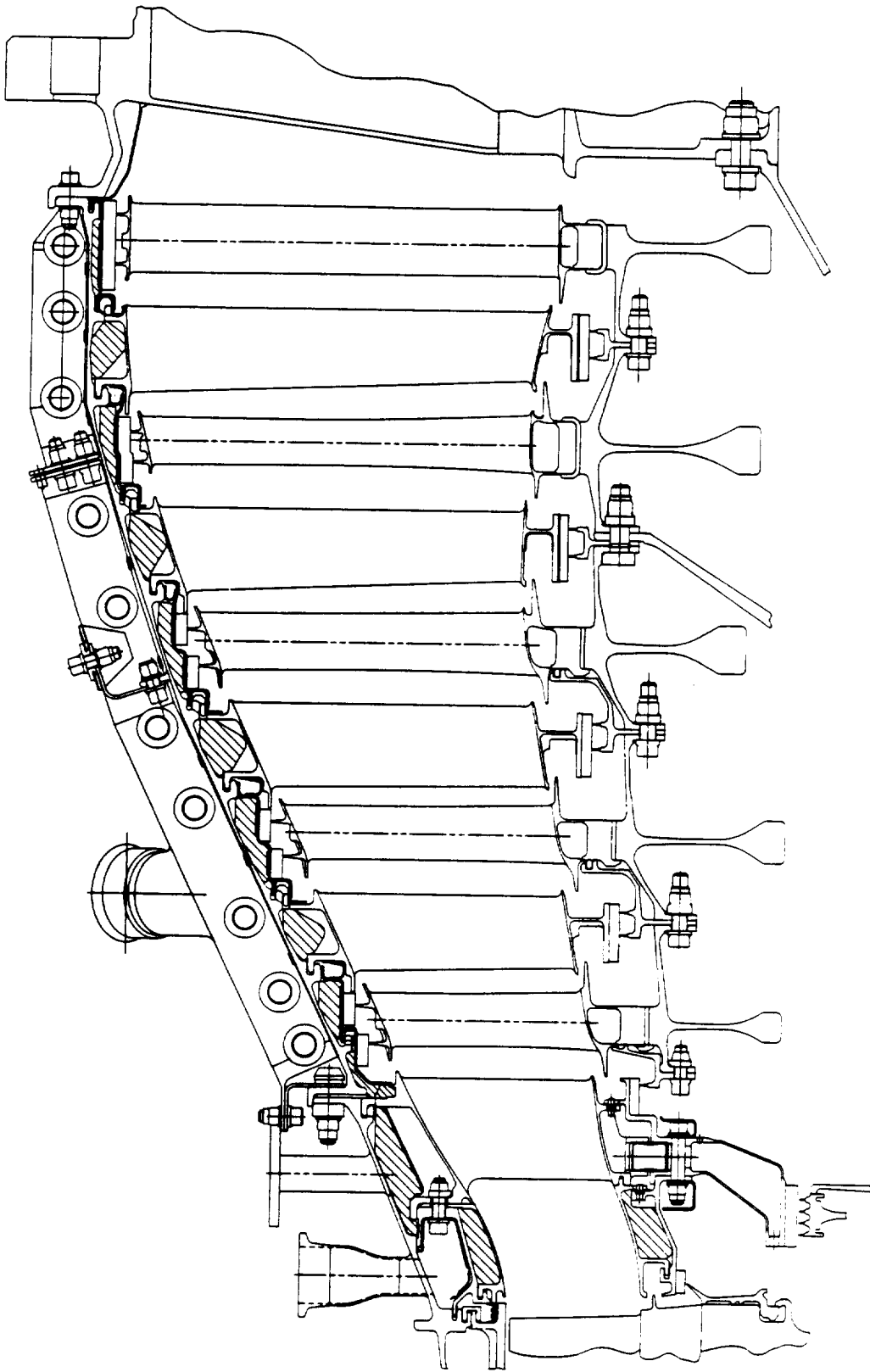


Figure 32. E³ Low Pressure Turbine Cross Section.

ORIGINAL PAGE
OF POOR QUALITY

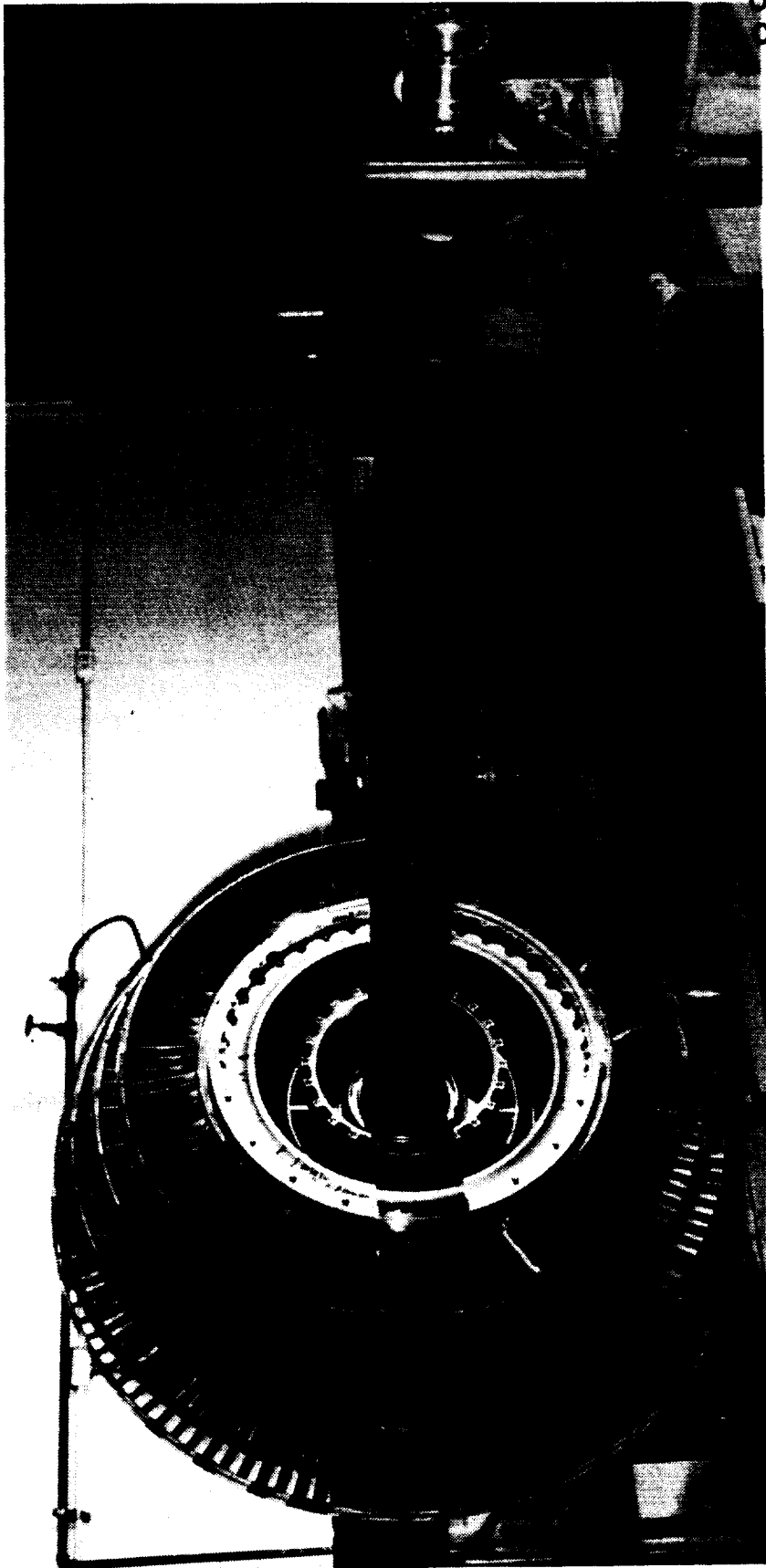


Figure 33. Low Pressure Turbine Rotor Assembly.



5.5.1 Aerodynamic Design

The LPT was designed to the M0.8/10.67 km (35,000 ft) maximum climb flight condition. Cycle match parameters for maximum climb are given in Table XXI.

The selection of a five-stage configuration was based in part on results obtained during the IR&D-funded Highly Loaded Fan Turbine (HLFT) technology development program and also on E³ system studies aimed at minimizing direct operating cost (DOC). These system studies evaluated the impact of turbine loading, weight, and cost on DOC and indicated a relative optimum at a loading level attainable in five stages. Further, significant performance gains at this loading level had been demonstrated in the HLFT program, indicating that the ICLS goal could be met with a five-stage turbine.

The five-stage flowpath and stage work split were defined through an iterative technique, whereby a candidate outer wall contour was selected (within the limitations on wall slope and exit diameter) and the inner wall contour and stage energy distribution were iterated concurrently to yield acceptable levels of loading ($gJ\Delta h/2u^2$) and flow coefficient (V_z/u) for each stage. The analysis used a stage-by-stage efficiency estimate which accounted for the effects of loading, flow coefficient, tip slope, aspect ratio, and clearance.

Turbine acoustic treatment is incorporated into the LPT flowpath. The axial gap between the Stage 4 vane and Stage 4 blade is increased to 1.4 blade chord lengths and the number of the Stage 4 blades is increased to achieve cutoff tuning. This reduces the amount of sound propagating out of the turbine. Stage 4 is used rather than Stage 5 because it is more highly loaded.

The gas path through-flow or vector diagram analysis was based on a calculation procedure that solved the full, three-dimensional, radial-equilibrium equation for axisymmetric flow, accounting for streamline slope and curvature, the effects of radial component blade force due to airfoil sweep and dihedral, and airfoil blockage and radial gradient of flow properties. Calculations were made with radial gradients of blading losses to simulate end-loss effects.

Table XXI. LP Turbine Cycle Match Point.

Parameter	Units	Maximum Climb
Inlet Temperature, T_{49}	K (° R)	1056.3 (1901.4)
Energy, $\Delta h/T$	J/kg/K (Btu/lbm/° R)	326.5 (0.07798)
Speed, N/\sqrt{T}	rad/sec \sqrt{K} (rpm/ $\sqrt{° R}$)	11.21 (79.79)
Corrected Flow, $w\sqrt{T/P}$	g \sqrt{K} /sec \cdot Pa (lbm $\sqrt{° R}$ /sec \cdot psi)	3.936 (80.27)

5.5.2 Mechanical Design

The LPT rotor is an uncooled design composed of disks with integral spacer arms and bolted joints between each stage. The main support cone extends from the sump between the HPT and LPT rotors and attaches at the LPT spool between the Stage 3 and Stage 4 disks. The LPT blading is a proven cast design with tip shrouds and multitang dovetails. Inner stage seals of the LPT spool are repairable, two-tooth designs and are attached at the bolted flange joints between the disk spacer connections. They provide good performance (low leakage) and easy replacement.

In the LPT stator assembly, the casing is a continuous, no-split-flange design with wall insulation and local impingement cooling for improved clearance control. The Stage 1 nozzle consists of conventionally cast four-vane segments attached by a hooked tang at the outer flowpath. Stages 2 through 5 nozzle vanes are cast six-vane segments attached by hook tangs to the outer case supports. Outer honeycomb seals are brazed to sheet metal backing strips that hook into the outer casing and assist in the radial retention of the Stages 2 through 5 nozzles. The inner diameters of these vanes have integral seals which consist of honeycomb brazed to the cast vane seal support. Interlocks are built into the integral seals to provide torsional stiffness and restraint without the need for separate bolted restraint pieces. A full-ring inner seal is bolted to the Stage 1 vane and consists of three sections of honeycomb brazed to a sheet metal structure.

An active clearance control system is incorporated which utilizes fan air to thermally shrink the casing at selected operating points, thus improving seal clearances.

The following materials are used in the LPT:

Casing	Inco 718
Stationary Tip Shroud Seals	Hastelloy X Honeycomb
Stationary Inner Seals	Hastelloy X Honeycomb
Stage 1 Vane	René 125
Stage 2-5 Vanes	René 77
Stage 1-5 Blades	René 77
Stage 1-5 Disks	Inco 718

Stage 1-5 Rotating Seals	Inco 718
Shaft Cone	Inco 718

5.5.3 Cooling Design

The major portion of the rotor purge air is defined by estimates of the seal clearances and the required flow to block the seals and prevent the flowpath gases from being injected into the rotor cavity. To accomplish this, 1.4% of the fifth-stage compressor bleed air is used to purge the outer and inner bands of the Stage 1 nozzle, cool the vane approximately 56° C (100° F), block the HPT rotor balance seals, and purge the LPT rotor cavity. A small portion of the rotor purge air leaks into the sump purge cavity and eventually exits through the center vent of the primary exhaust nozzle. But the majority of the flow returns to the LPT flowpath and work is recovered as the purge air expands through the remaining stages and out through the exhaust nozzle. The flow through the Stage 1, 2, and 3 rotor spacer arm flanges is defined by the required spacer arm temperatures.

The prime source of LPT cooling air is fifth-stage compressor bleed. Bleed air is used for compressor ACC and then is delivered to the turbine through six pipes equally spaced around the Stage 1 LPT nozzle cooling supply manifold. This manifold, which is integral with the casing and outer transition duct hanger, distributes the cooling air uniformly around the inside of the casing. Next, cooling air is fed into the nozzle vanes and across the flowpath to the inner nozzle support structure.

The LPT forward rotor cooling/purge air supply consists of interturbine seal leakage air and air that is injected tangentially into the rotor cavity from the wheel space cooling supply plenum. The total cooling air supply to the rotor cavity will be 0.91% W_{25} for the base engine and 1.08% for the growth engine.

No cooling air is used to purge the aft rotor cavity, thus improving engine performance. Instead of cooling air, LPT exhaust gas from the hub of the fifth stage rotor is routed through the aft rotor cavity. This reduces the transient temperature gradients in the rear frame hub, as well as between the bore and rim of the Stage 4 and 5 disks. The maximum gas temperature at the hub of the five-stage rotor is 599° C (1100° F) for a deteriorated FPS

engine, well within the maximum allowable material limits of 1250° F. In addition, between idle power and maximum takeoff power, this gas temperature changes by only 111° to 167° C (200° to 300° F); therefore, thermal gradients at high rpm are moderate.

Except for cooling of the Stage 1 vane by the purge air flowing through it, no airfoil cooling is used in the LPT.

Active clearance control in the E³ LPT is accomplished by shrinking the casing that supports the stationary seals. During steady-state cruise conditions, the casing shrinkage is accomplished by cooling the metal, taking advantage of the high coefficient of thermal expansion of Inco 718. By cooling the casing 167° C (300° F) it is possible to reduce the clearance by 0.152 cm (0.060 in.) which is more than adequate to accomplish the objective of active clearance control. The casing cooling system relies heavily on experience with the CF6-50 LPT casing impingement cooling system. In that system the low pressure, low temperature fan air is used as coolant and is impinged on the outside of the LPT casing by means of an array of manifolds. In the E³ system, fan air is extracted from the fan duct by means of a scoop. The air is routed to the impingement manifold through a control valve and a 270° core cowl manifold.

The ACC valve in the FPS is controlled by the full authority digital electronic control (FADEC). Fan speed, fuel flow, and compressor exit temperature and pressure are the FADEC inputs used to control the LPT ACC system. The FADEC defines the best clearances for a particular flight condition. The thermal history of the rotor and casing will be factored into the control so that the required cooling for the casing can be defined.

The outer casing will be kept under the design objective metal temperature of 677° C (1250° F) by impingement cooling with fan air. The ACC and the casing impingement cooling scheme are combined into one system. The cooling of the casing requires 0.1% W₂₅; this is increased to 0.3% for obtaining adequate cooling in order to achieve minimum clearances.

5.5.4 Performance

FPS LPT performance is based on 374 hours of rig testing and 65 hours of ICLS testing. The turbine rig was a 0.67 scale of the ICLS design which has slightly less flair compared to the FPS. The rig test hardware was a non-flight design. Testing of the inlet transition duct and the first two stages revealed a flow deficiency along the outer wall. The design was changed and the full 5-stage turbine was tested. LPT efficiency test results are presented in Table XXII. LPT efficiency in ICLS is based on a balanced cycle analysis. The LPT deficiency exhibited in ICLS testing was unexpected and unexplained. FPS efficiency is based on the results of LPT rig testing.

5.6 TURBINE FRAME

Figure 34 is a photograph of the turbine rear frame with the aft sump installed. Its primary functions are to maintain alignment of the rotor system within the static structure, transmit loads across the gas flowpath, provide engine structure spring elements, and help maintain airfoil tip clearances. In addition, this frame has been designed for removing residual turbine swirl and supporting the centerbody, mixer, and the No. 5 bearing housing. Also, it has provisions for three engine mounts and ground handling features. The turbine frame is used to route sump lube lines across the gas flowpath, and provides a path to vent engine active clearance control air to ambient pressure. Acoustic panels have been incorporated in the turbine frame to reduce engine noise.

The FPS frame represents a unique solution to the problem of providing extreme stiffness while accommodating severe thermal gradients. The FPS frame achieves its goals by using a variable thickness polygonal outer casing, 12 radial struts, and heated rings on the inner casing. Figures 35 and 36 show the frame design. (Outer wall details actually represent the ICLS turbine flowpath which is slightly different than FPS.) The frame material is Inco 718.

Radial struts are used in order to achieve the high required spring rate of 1,751,181 N/cm (one million pounds per inch) from the bearing to the strut plane at the casing. The radial struts are stiffer than semitangential

Table XXII. Low Pressure Turbine Performance.

	Max Climb	Max Cruise	Takeoff
Original FPS Required Efficiency ⁽¹⁾	0.917	0.917	0.921
Rig Test Efficiency with 1/4 Point Credited for FPS Flaired Flowpath ⁽²⁾	0.918	0.917	0.920
ICLS Test Efficiency ⁽¹⁾	0.895	0.894	0.895
Final FPS Required Efficiency ⁽²⁾	0.927	0.925	0.928

(1) Consistent with original cycle match.

(2) Consistent with final cycle match.

ORIGINAL DESIGN IS
OF POOR QUALITY

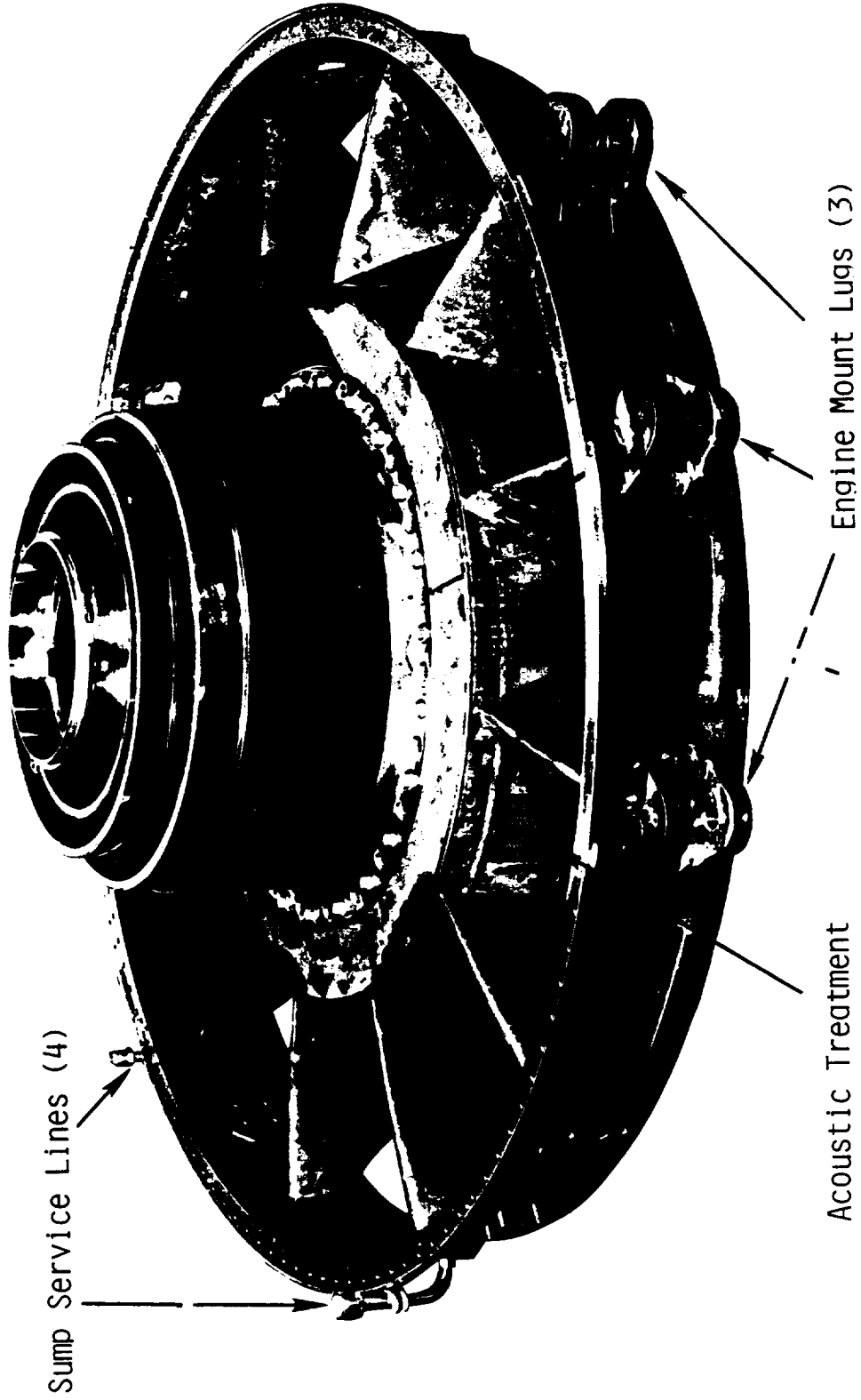


Figure 34. Turbine Frame with Aft Sump Installed.

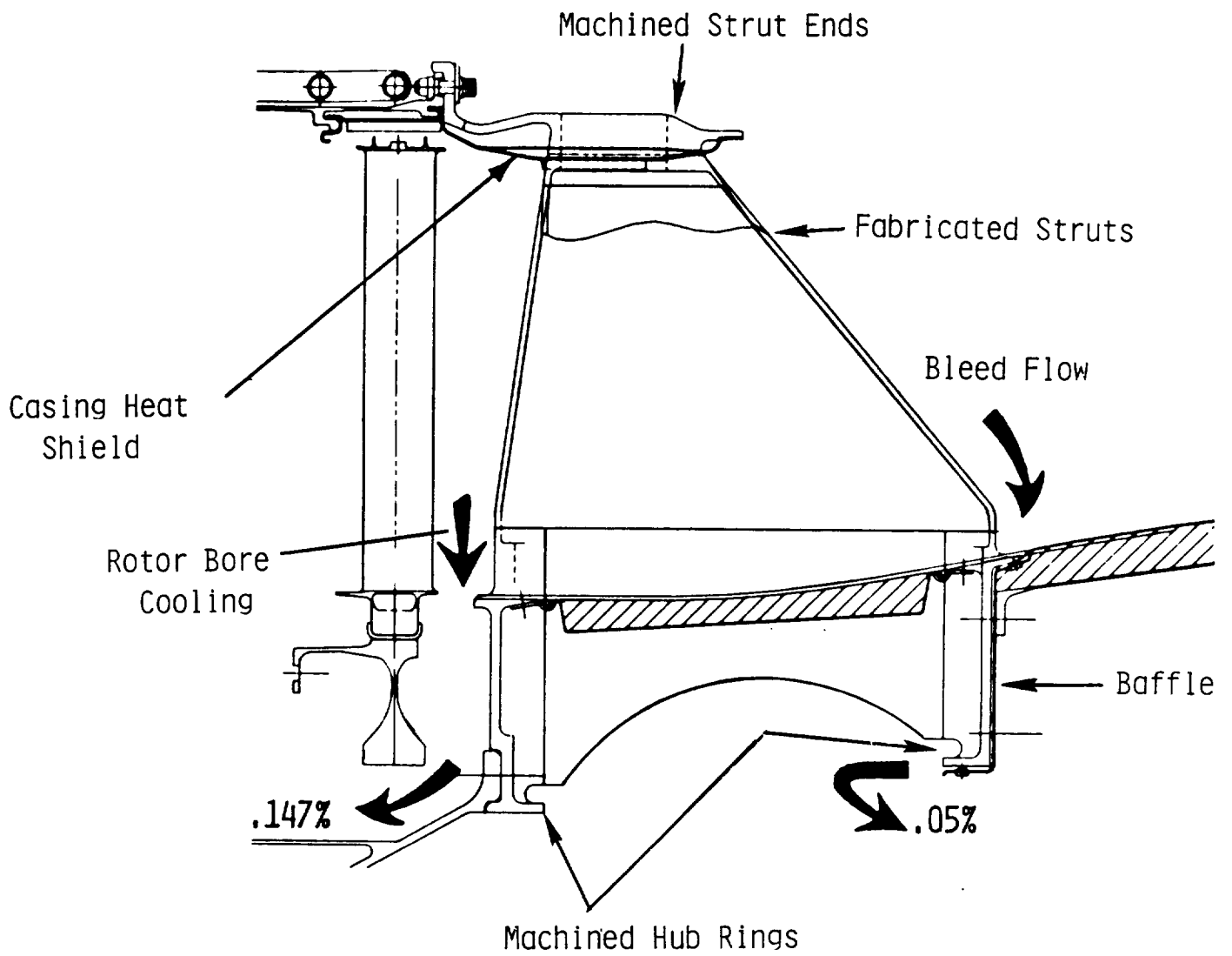


Figure 35. E³ Turbine Frame Cross Section.

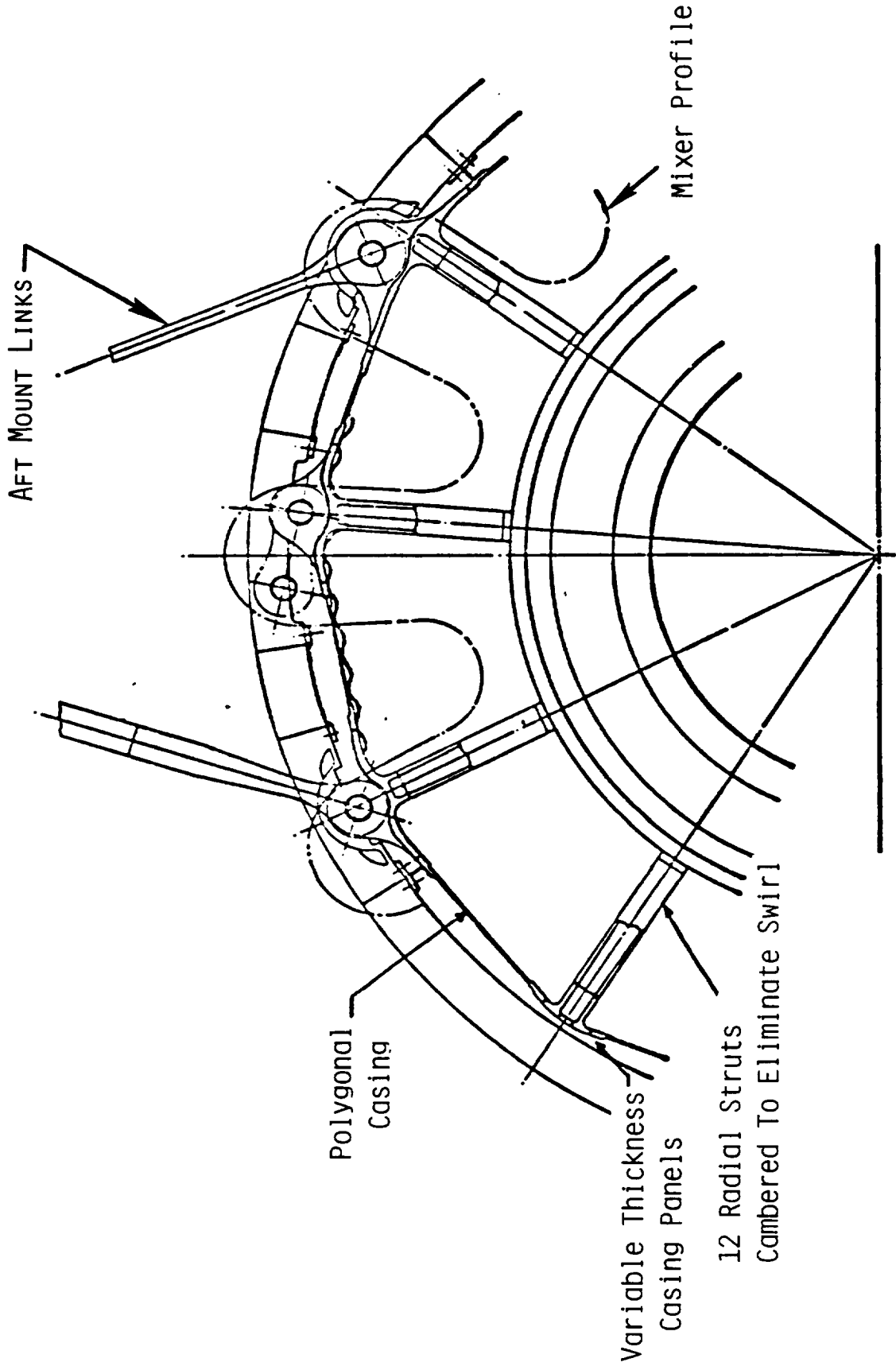


Figure 36. E³ Turbine Frame Cross Section - End View.

struts because they are shorter, which also results in a lower strut weight. In addition, the struts have been cambered to remove residual turbine swirl.

The polygonal outer casing carries point loads more effectively than a conventional cylindrical casing. That is, with radial loads reinforced by the struts, a polygonal casing loads up uniformly in tension or compression, while a cylindrical case is subject to high bending stresses at the strut ends. The polygonal case is also stiffer, due to its lower flexibility under the imposition of radial loads at the struts.

The polygonal panels are chem-milled between strut ends to reduce the stock thickness. This produces preferential strain distribution in the casing. By thinning the panel in the center, more straining takes place in the panel center than at the ends where the welds are located. These panels are made of wrought sheet material and can withstand higher stress levels than cast strut ends.

In order to reduce the maximum thermal expansion difference between the frame major components, two thermal expansion control features are incorporated into the design. One feature is a sheet metal heat shield on the outer casing as shown in Figure 35. This liner serves as a radiation shield and both decelerates the thermal response of the casing during transient operation and effects a lower steady-state casing operation temperature. The other feature concerns convectively heating the frame hub with flowpath gas (rotor bore cooling), also shown in Figure 35. The forward hub ring is heated by means of flowpath gas bled radially inward between the last stage of the low pressure turbine and the frame hub. The aft hub ring is heated by bleeding hot gas radially inward between a sheet metal baffle and the aft hub ring. Bleeding the flowpath gas radially inward is possible because the entire cavity inside the frame hub, including the aft centerbody, is vented to ambient through the center vent tube. The relatively large mass comprising the frame hub usually results in a hub thermal response which lags the other frame components and, therefore, results in larger thermal expansion differences during transient operation. Convectively heating the hub accelerates its thermal response and again reduces the thermal expansion differences which can exist during both transient and steady-state operation. The hot gas used to heat the hub has a low impact on performance since it is reinjected into the gas

stream at the center vent tube exhaust. Acoustic treatment panels are placed beneath the shear cylinder between the struts. The panels contain Astroquartz with nominal density of 25.63 kg/m^3 (1.6 pounds per cubic foot) and are 1.27 cm (1/2 inch) deep. The shear cylinder portions above these panels are perforated with 0.158 cm (1/16 inch) diameter holes in a standard staggered pattern with 30% open area.

5.7 SUMPS, DRIVES, CONFIGURATION, AND LUBE SYSTEM

5.7.1 Bearing System

The FPS engine is a simply arranged, two-sump engine. It is a five-bearing machine with three bearings, a ball and two roller bearings, supporting the low pressure (LP) system. The high pressure (HP) system is supported by a forward thrust bearing and an aft intershaft roller bearing. The intershaft bearing mounted between the LP and HP systems eliminates the need for a "hot" frame with its cooling air requirements.

5.7.2 Forward Sump

The forward sump design is shown in Figure 37. Included in this sump are both the LP and HP system thrust bearings, whose loads are reacted by the stiff front frame. The No. 2 roller bearing, which adds support to the long LP system shafting, is also located in the forward sump just ahead of the power takeoff (PTO) drive gear. The PTO gearbox is driven directly from the compressor stub shaft and drives radially outward through the bottom strut in the front frame.

The thrust bearing for the HP system is mounted in a housing which features a centering spring. The bearing is fluid damped with a multishim arrangement that is end-sealed by piston rings.

The main shaft and PTO bearings are either jet or underrace lubricated and cooled. Oil is supplied from a common manifold, with the oil for the fluid damper being supplied from its own manifold.

The forward sump sealing system consists of labyrinth seals pressurized by fan discharge air. The sump is vented through the LP fan shaft, with the vent air being exhausted out the aft center vent tube. Also included in the

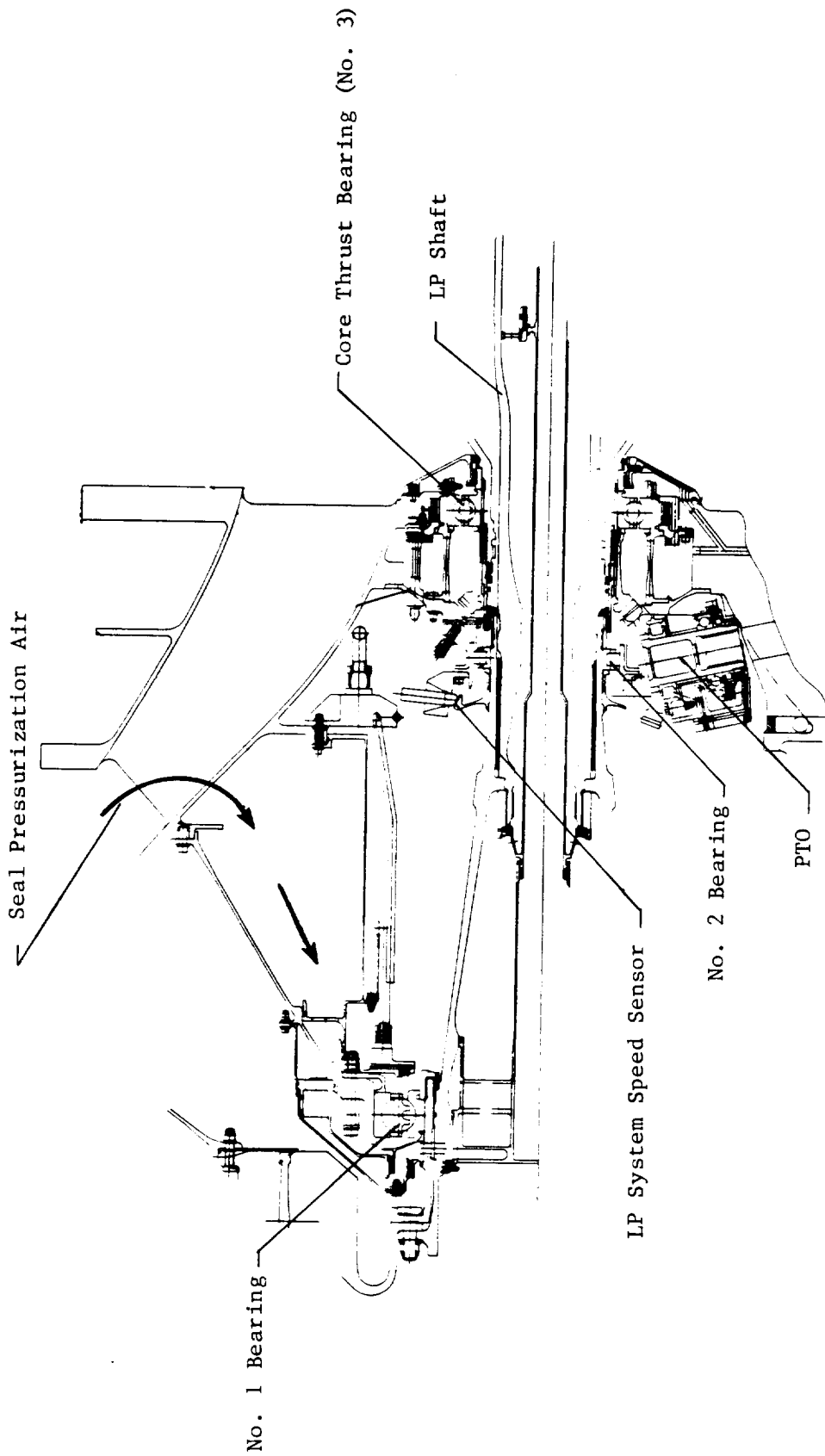


Figure 37. E3 Forward Sump Design.

forward sump is an LP rotor speed pickup. This device involves a "cogged" wheel which is mounted to the LP shaft just forward of the No. 2 bearing. This wheel is sensed by a stationary magnetic pickup mounted to the No. 2 bearing housing, thus providing a rotor speed signal.

5.7.3 Aft Sump

The aft sump configuration is shown in Figure 38. This sump includes the No. 4 and No. 5 roller bearings. The No. 4 bearing is an intershaft roller bearing with its outer race mounted in a housing having a controlled spring rate, and is attached to the LP shaft and its inner ring mounted to the aft HP stub shaft. The No. 5 bearing, supporting both the HP and LP rotor systems, is mounted to the aft turbine frame. Both the No. 4 and No. 5 bearings are underrace cooled, with cooling oil supplied by a jet mounted to the No. 5 bearing housing.

The aft sump sealing system features labyrinth seals pressurized by fan discharge air which flows from the forward sump to the aft sump through an annulus formed by the outside diameter of the vent shaft and the inside diameter of the LP shaft. Compressor rotor cooling air flows around the aft sump through sealed cavities and is directed out the aft center vent tube. The rotor cooling and the seal pressurization air cavities "blanket" the sump with cooler air, protecting it from the high turbine cavity temperatures. The aft sump is vented through an air/oil separator which is mounted on the end of the LP shaft. Aft sump vent air mixes with the vent air from the forward sump and is exhausted through the aft center vent tube.

5.7.4 Configuration

The configuration encompasses the following areas:

- Pneumatic piping for the compressor and turbine active clearance control systems and turbine cooling
- All external lube and fuel lines
- All electrical harnesses
- The pressure bulkhead.

Fan discharge air plus 5th and 7th stages of the compressor are bled to accomplish the pneumatic functions.

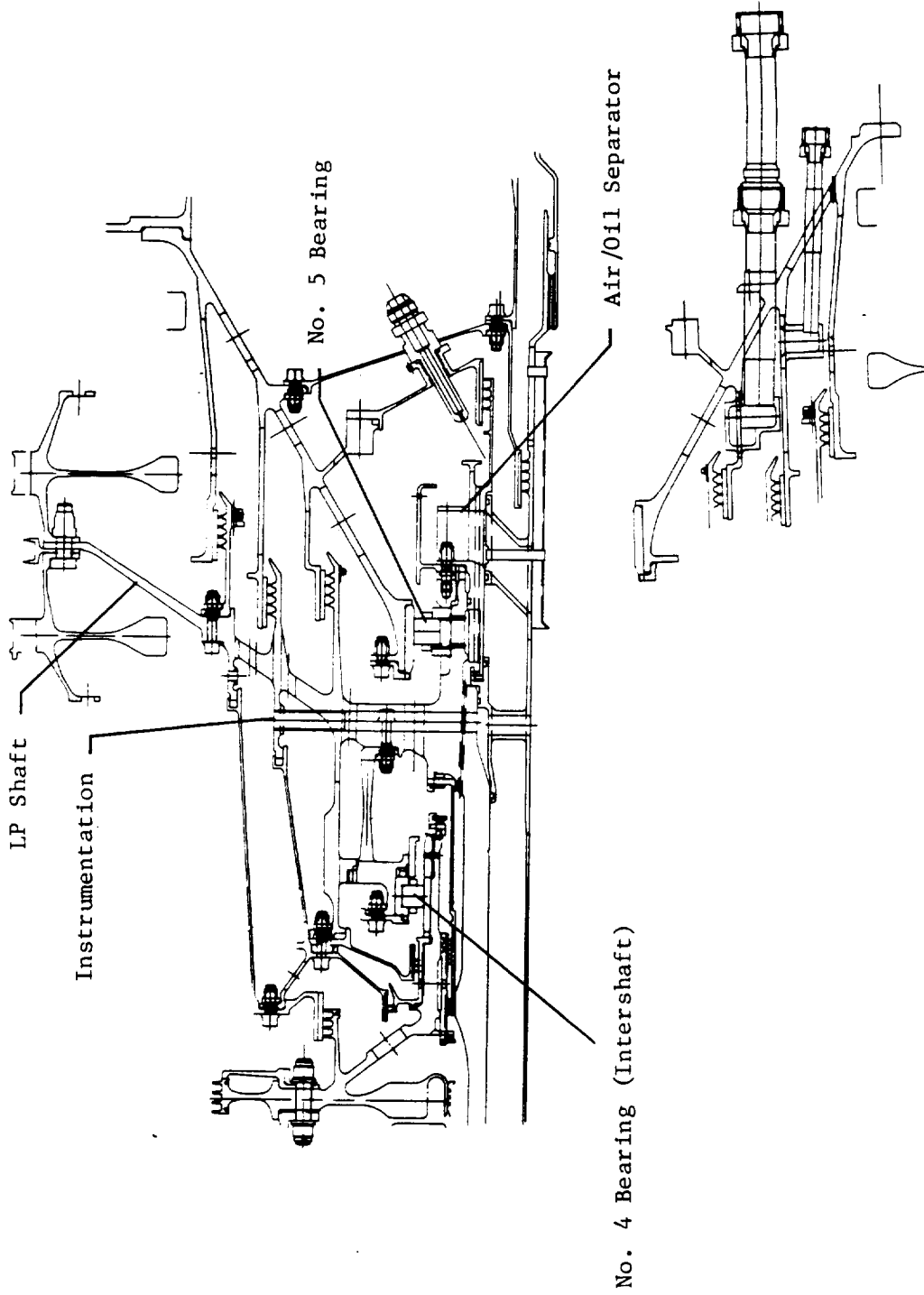


Figure 38. E³ Aft Sump Design.

Fifth stage air is used to control the clearance in the aft stages of the compressor. This is accomplished by the use of a valve which allows air to pass over the casing of these stages to reduce clearance or bypass this cooling function in varying degrees. The discharge air from this system is then utilized to cool the LPT vanes. Seventh stage air is used to cool the HPT second stage nozzles. Fan air is used to control the clearance of both the HPT and LPT.

The fuel lines supply fuel to the pilot and main burners. In addition, fuel is used to hydraulically power all of the control valves in the system.

The electrical harnesses transmit the Full Authority Digital Electronic Control (FADEC) signals to and from the various electrohydraulic servovalves and electronic feedback devices in the system.

A six-sector curved pressure bulkhead is used to create a low pressure region around the turbine outer casing to provide a "sink" for the turbine clearance control cooling air. It was designed for radial temperature gradients of 389° C (700° F) and an axial pressure gradient of 48 kPa (7 psid). The design also includes metal bellows to minimize air leakage where piping penetrations were required.

5.7.5 Lube System

The lube system is typical of other General Electric high bypass fan engines. Lubrication and cooling oil is supplied to each sump and to the gearbox by a single supply pumping element, then scavenged using separate scavenge pumping elements. Oil filters are used on both the supply and scavenge side of the lube system. The supply filters protect the sumps and gearbox from contamination, and the scavenge element has an inlet screen to protect the pumping elements from larger debris. Check valves are located in the lube supply side to prevent backflow of oil into engine sumps, which could cause flooding at engine shutdown.

The sump systems and gearbox are center vented aft to the exhaust nozzle of the engine.

5.8 EXHAUST SYSTEM

THE FPS uses a full length exhaust duct. The mixer combines the fan and core streams prior to being discharged through a single exhaust nozzle. A center vent tube extending from the tail cone, located ahead of the exhaust plane, out through the center of the nozzle, vents purge and leakage air from the aft sump and turbine frame cavities.

The major components of the ICLS exhaust system flowpath include the fan exhaust duct, the pylon, the exhaust nozzle, and the mixer/centerbody. The aerodynamic designs of these flowpaths have been developed through a combination of analytical studies and scale model performance tests to provide a high performance exhaust system compatible with a lightweight, low drag nacelle.

The fan exhaust duct has been designed for low Mach numbers to minimize duct pressure losses and, at the same time, to be compatible with a thrust reverser, a core-mounted gearbox, and the mixer flowpath. Typical Mach numbers for separate flow nacelle fan ducts range from 0.45 to 0.50, whereas the E³ fan duct ranges from 0.40 to 0.45. The fan duct flowpath has been included in all the scale model mixer performance tests, and results have verified a low pressure loss design.

The pylon cross section flowpath has been designed with two major considerations. The forward, or nose, portion of the pylon was designed to assure aerodynamic compatibility with the fan by proper selection of nose angle and axial location relative to the fan OGV's. The aft portion of the pylon from the maximum width to the trailing edge was designed to be aerodynamically compatible with the mixer and to provide low pressure loss. The pylon has been simulated in the scale model mixer development tests, and back-to-back testing with and without the pylon verifies pressure losses lower than predicted. The engine aft mount links are positioned over the turbine frame, as shown in Figure 36, to minimize drag and to eliminate any potential interaction with or impact on the mixer. These links were also tested in the scale model mixer development program and were shown to have both low drag/pressure loss and no effect on the mixer aerodynamics. The FPS has a low area ratio, converging-diverging exhaust nozzle for desired takeoff-to-cruise nozzle flow coefficient characteristics.

The E³ program contributed a major advancement in mixer technology. The FPS mixer is the product of a comprehensive analytical and test program. It uses 18 scalloped lobes with corresponding corrugations in the centerbody. The mixer design is shown in Figure 39. A center vent tube extends from the tail cone through the nozzle exhaust plane as shown in Figure 1. Mixer performance is summarized in Table XXIII. The original pressure loss goal is now seen as unrealistic; however, better mixing effectiveness is projected based in part on an increase in mixer protrusion into the flowpath. The original sfc improvement goal can be achieved with a different combination of mixer pressure loss and mixing effectiveness.

The mixer is made of Inco 718. The centerbody and links from the centerbody to the mixer are Inco 625.

5.9 NACELLE

The E³ Flight Propulsion System was designed with an integrated nacelle to permit a significant weight reduction for the total installed system. Major elements of the nacelle design include:

- Integral, composite construction of the fan frame, the outer portion of which forms the outer surfaces of the nacelle.
- Substantial use of composite materials in the inlet and aft cowling and in acoustic treatment of the inlet and the exhaust flowpath.
- Lightweight fan containment based on the use of Kevlar fibers to trap and hold engine-generated debris in the event of fan damage.
- A long-duct, mixed-flow exhaust system to enhance propulsive efficiency, achieving a higher level of engine performance with a smaller fan and low pressure turbine than would be required for a comparable separate-flow system.
- A reverser contained entirely in the outer wall of the nacelle, without need for bifurcation and cross-duct linkage, and extensive application of composite materials in the reverser to reduce the weight of the design.
- An engine mount system design chosen with particular attention to minimizing engine deflections due to mount loads to promote close control of turbomachinery clearances.

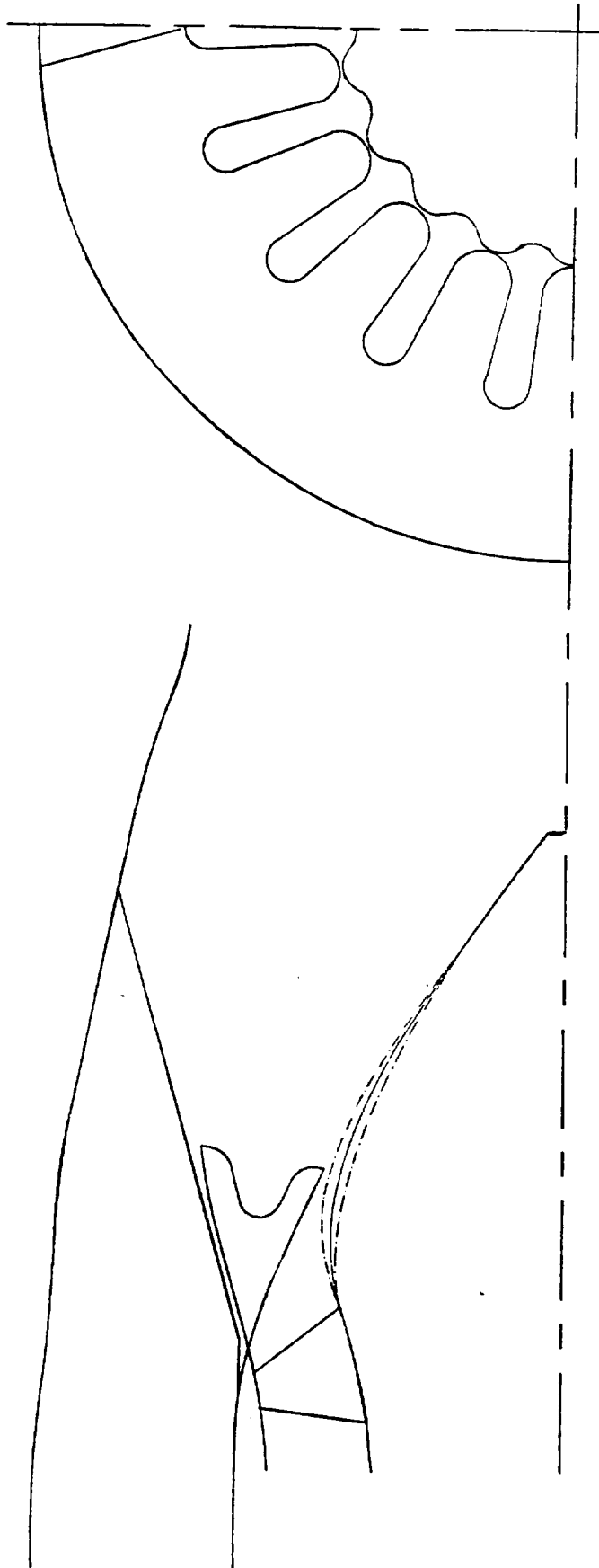


Figure 39. E³ Mixer.

Table XXIII. Mixer Performance at Maximum Cruise.

	Original Goal (Reference 1)	Best Scale Model	FPS Projection
Mixing Effectiveness, %	75	79	85
Pressure Loss, $\Delta P/P$, %	0.20	0.57	0.57
SFC Improvement, %	3.1	2.6	2.9

- Nacelle aerodynamic lines chosen for slimness and low cruise drag. To achieve as small an external-nacelle profile as possible, the accessory package is located in the core compartment.
- A reverser hinged at the pylon attachment and latched at the bottom for ease of maintenance access to the core engine and accessories. The core cowl panels are hinged to the pylon to form a separate inner door system.

The aggressive use of advanced structural design and low drag aerodynamics is estimated to contribute a 0.6% cruise drag reduction to a 15% to 20% installation weight saving relative to the current technology of the CF6-50C nacelle that was the E³ program baseline.

The general arrangement of the E³ nacelle is shown in Figure 40.

5.9.1 Fan Reverser

The fan thrust-reverser design is a fixed cascade, translating-sleeve/blocker-door configuration. The reverser is made in symmetrical circumferential halves, each half hinged to the aircraft pylon and latched to the other half along the bottom centerline, allowing ready access to the engine (Figure 41). The reverser consists of the fixed support structure including the cascade section, the outer translating sleeve, the blocker doors and linkage mechanism, and the actuation system. Since the actuation system is located outboard of the cascades, the cascade section is made in circular arc sectors with passageways (slots) between them for the blocker door links to pass through. The blocker door is a floating design with the forward section supported by a slider-link mechanism consisting of a drive link connected to a unison ring and a drag link with a fixed pivot on the aft support structure. Drive links connect each blocker door to the translating sleeve.

The unison ring is located outboard of the cascades and is supported by "T" shaped ends riding in a slot in the fixed-structure main axial beams. A forward acting load is imparted to the unison ring by a series of compression springs mounted between it and the translating sleeve. This load is sufficient to hold the blocker doors in the stowed position during forward thrust operation. The floating feature of the unison ring also serves to eliminate the effect of manufacturing and assembly tolerance accumulation in the system. The translating sleeve is driven by the actuation system and serves as

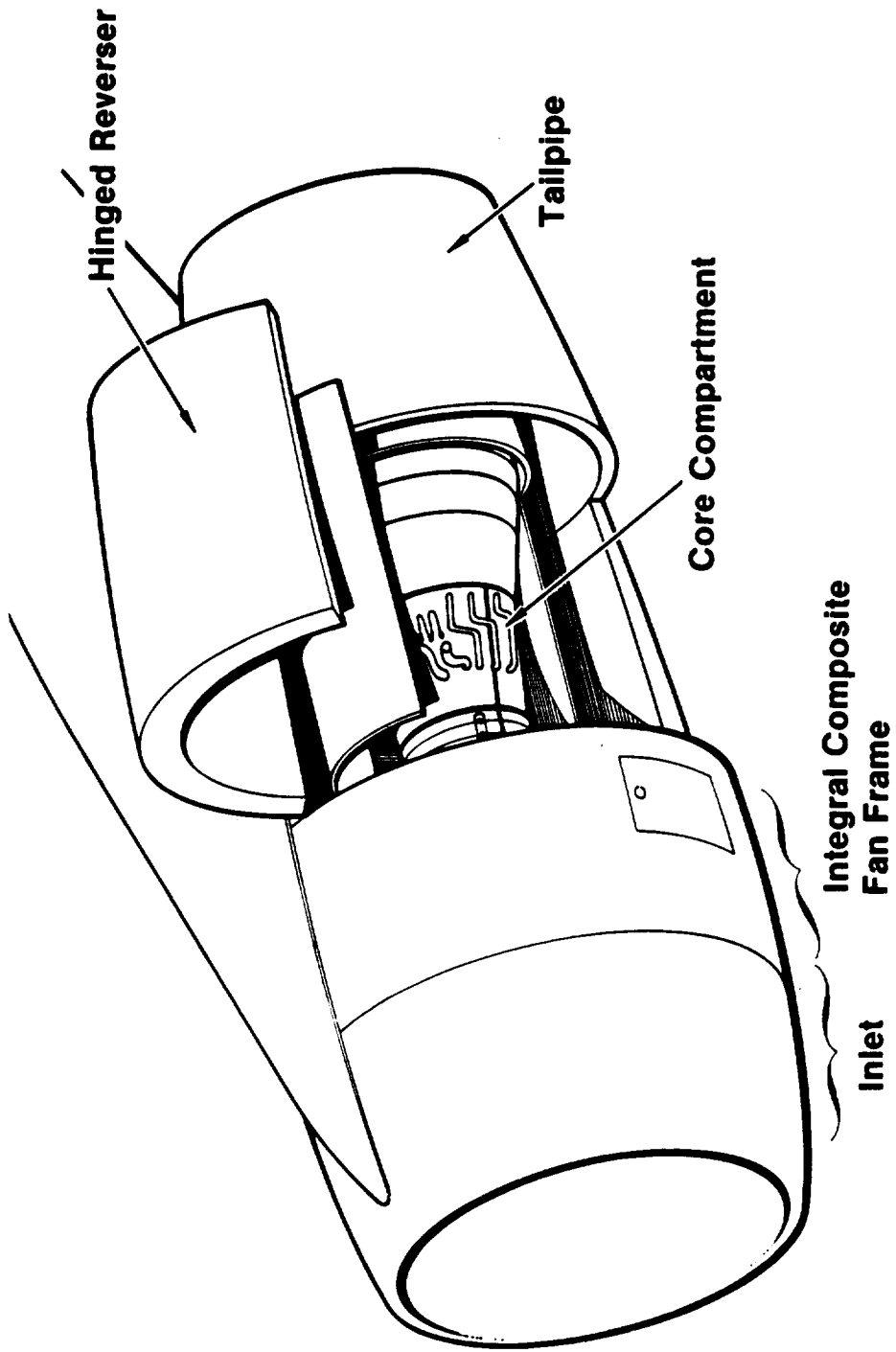


Figure 40. Nacelle General Arrangement.

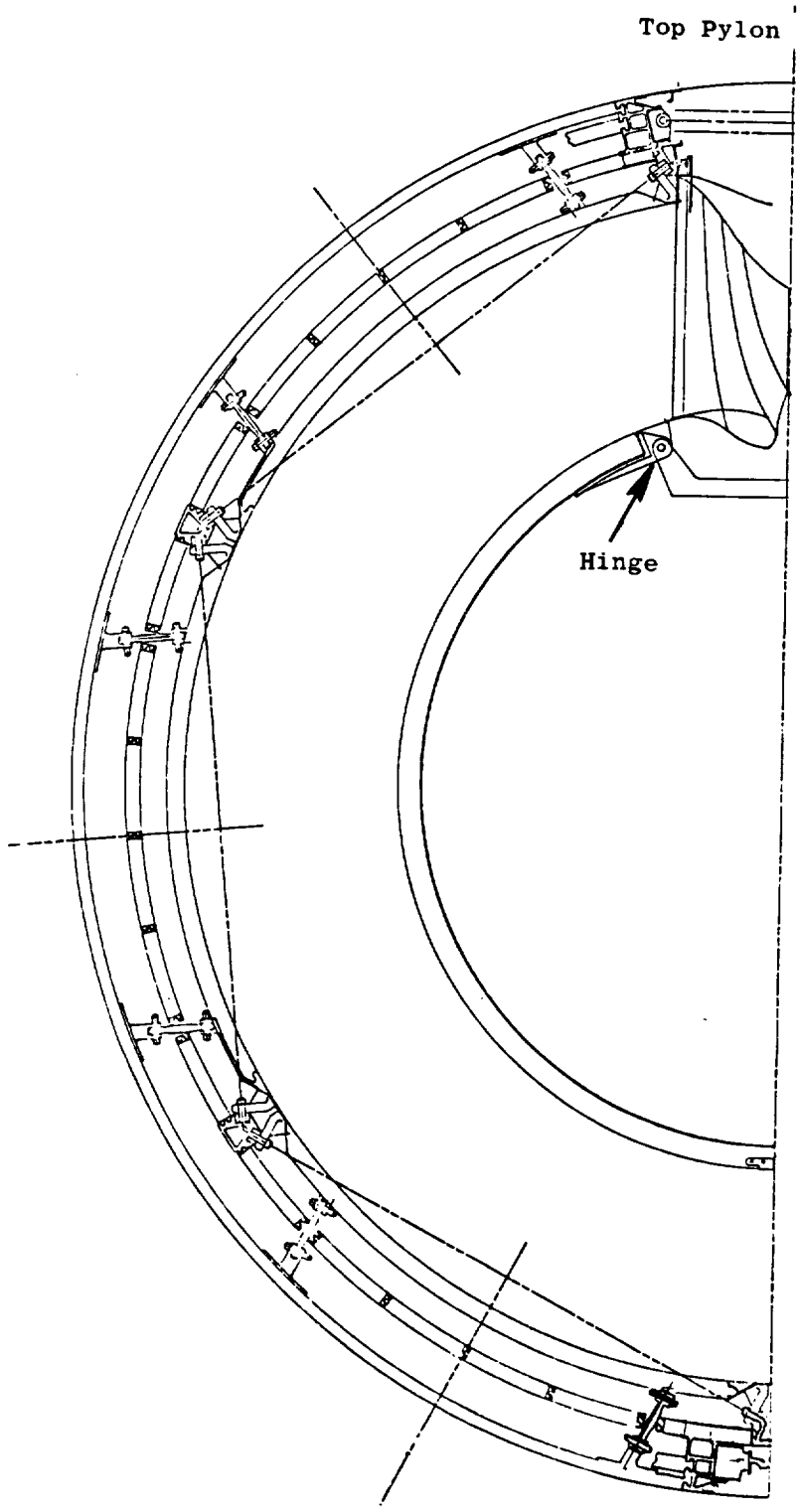


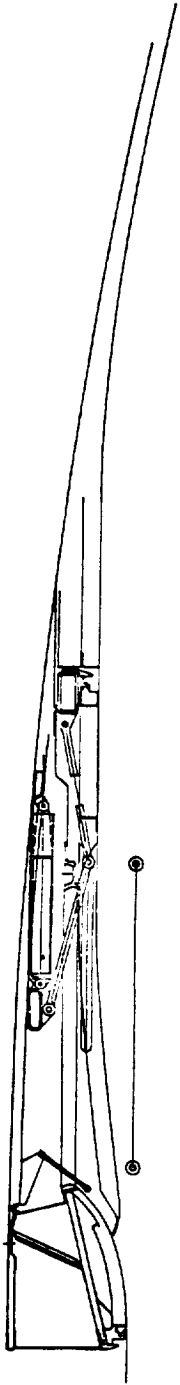
Figure 41. Front View, Reverser Cross Section.

the blocker door and unison ring driver as well as the outer nacelle flow-surface fairing. Figure 42 shows the translating sleeve, unison ring, and compression springs.

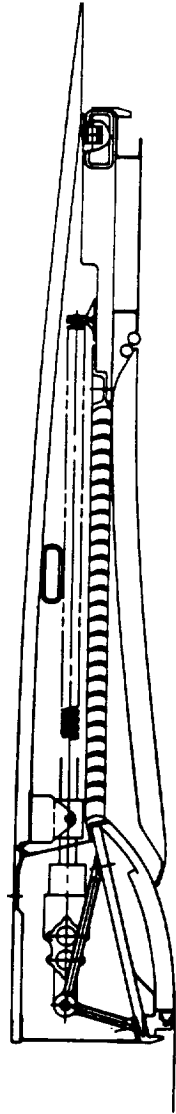
As the translating sleeve is moved aft by the actuators to uncover the cascades, the blocker doors are moved aft along with it. Because the unison ring is not being driven at this time, the unison ring spring load tends to cause the aft end of the blocker doors to stay in the stowed position. To prevent interference of the blockers with the fixed structure aft of the doors, the blocker door rollers ride along a ramp surface on the back side of the blocker, forcing the door into the fan stream sufficiently to clear the fixed structure but not enough to cause a large decrease in fan-duct flow area. At a predetermined point in the sleeve translation, a bumper on the sleeve contacts the forward face of the unison ring, causing it to move aft with the sleeve and blockers for the remainder of the actuator stroke. The aftward movement of the unison ring forces the slider-link mechanism to rotate towards the engine centerline, causing the blocker doors to rotate about the forward support rollers, blocking the fan stream and diverting it through the cascades.

Figure 42 also illustrates the reverser in the stowed and deployed positions. The aerodynamics of the reverser are based on previous General Electric experience with large turbofan reverser designs. Cascade area was mixed to provide an adequate effective area margin, fully deployed, relative to the discharge flow requirements of the fan bypass. The desired fan operating line for reverse thrust is lower in pressure ratio at corrected airflow than the normal forward-thrust-mode fan operating line at static conditions. This was done in order to provide additional stall margin if required and to provide a reduction in core engine and turbine temperature at fan speed relative to forward mode operation.

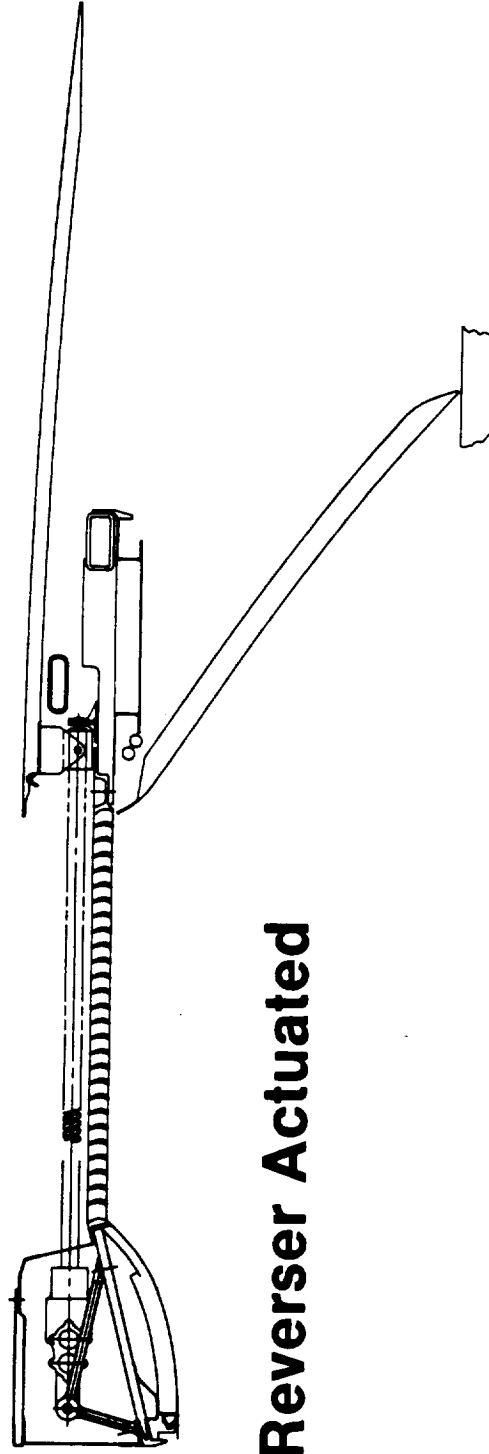
Overall thrust effectiveness of the fan reverser is improved by core thrust spoiling of the mixed exhaust system. In the reverser mode, the absence of bypass flow in the tailpipe causes a reduction in low pressure turbine back pressure and allows the core speed to be reduced relative to



Reverser Translating Sleeve and Blocker Door.



Reverser Stowed



Reverser Actuated

Figure 42. E³ FPS Thrust Reverser Actuation.

forward mode operation. This "rotor matching" effect causes a significant reduction in core stream thrust potential which is reduced still further by the aerodynamic spoiling effect of dump diffusion out of the mixer core chutes into the tailpipe. These effects, evaluated in a cycle computer model, are based on previous scale model exhaust mixer tests.

The overall system reverse thrust effectiveness is shown in Figure 43 compared to a CF6-50C with and without the turbine reverser. The E³ effectiveness compares closely to the effectiveness achieved with the CF6-50C with turbine reverser and exceeds the -50C level without turbine reverser.

5.9.2 Mount System

The engine mount system is designed to minimize engine backbone bending and circular distortions that result from the engine vertical, side, and thrust loads. Circular distortions in the engine (compressor) casing are generated by the vertical and thrust (axial) load reaction at the forward mount location (fan frame).

The engine mount system uses seven links as shown in Figure 44. The four front mount links connect to mount brackets attached to the aft side of the frame. Two links carry vertical and side loads, while the other pair of links carry the thrust load. The aft three-link system attaches to the turbine rear frame. The short lateral link provides roll and side load restraint, while the pair of links carry vertical loads. All links are mounted in uniballs.

Analytical studies have shown that the major component of the circular distortion of the engine casings due to the thrust load reactions at the forward mount can be minimized by reacting the thrust load at two points separated by 90°. The FPS engine thrust mounts are located, one on each side, at 45° from the top vertical. Figure 45 shows the location of the forward mount brackets on the aft side of the fan frame.

All forward links are located under the core compressor cowling aft of the fan frame. The aft lateral link is located within the pylon. The aft vertical links are streamlined and extended through the fan stream from the pylon to the turbine rear frame.

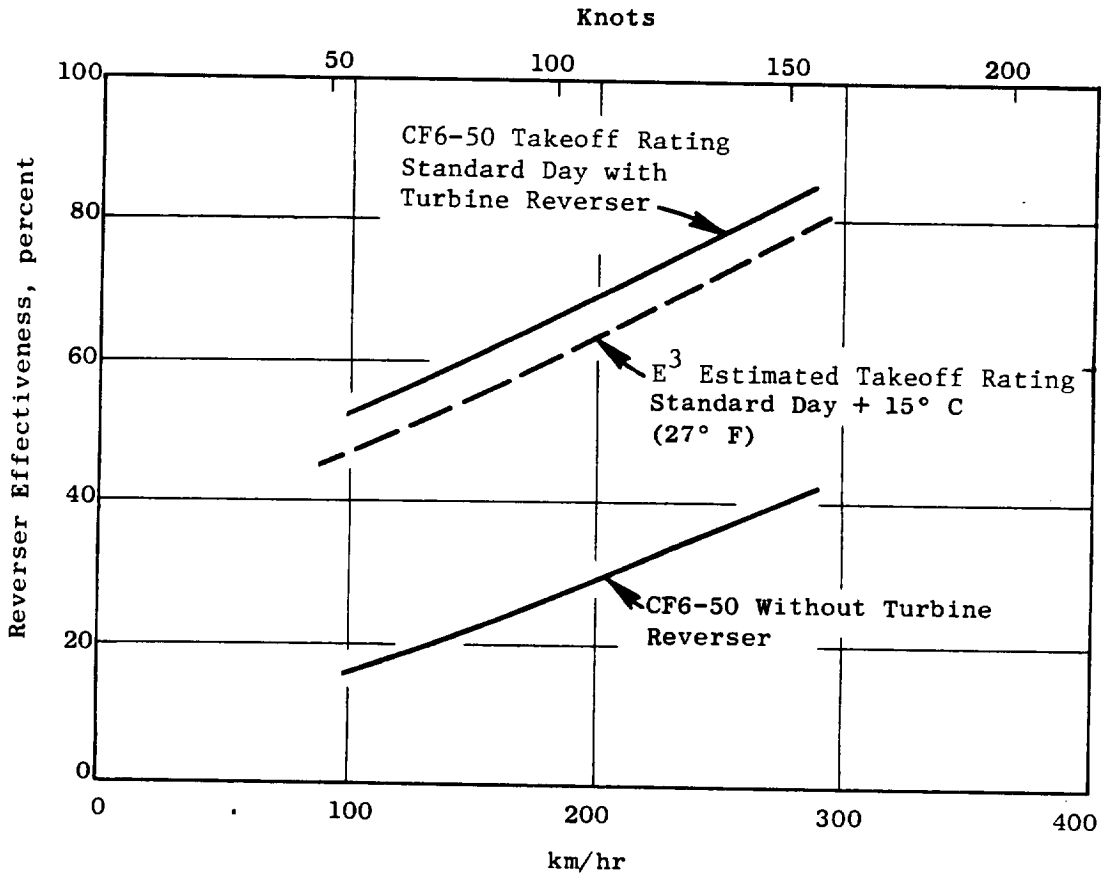


Figure 43. Overall Engine Reverse Thrust Comparison.

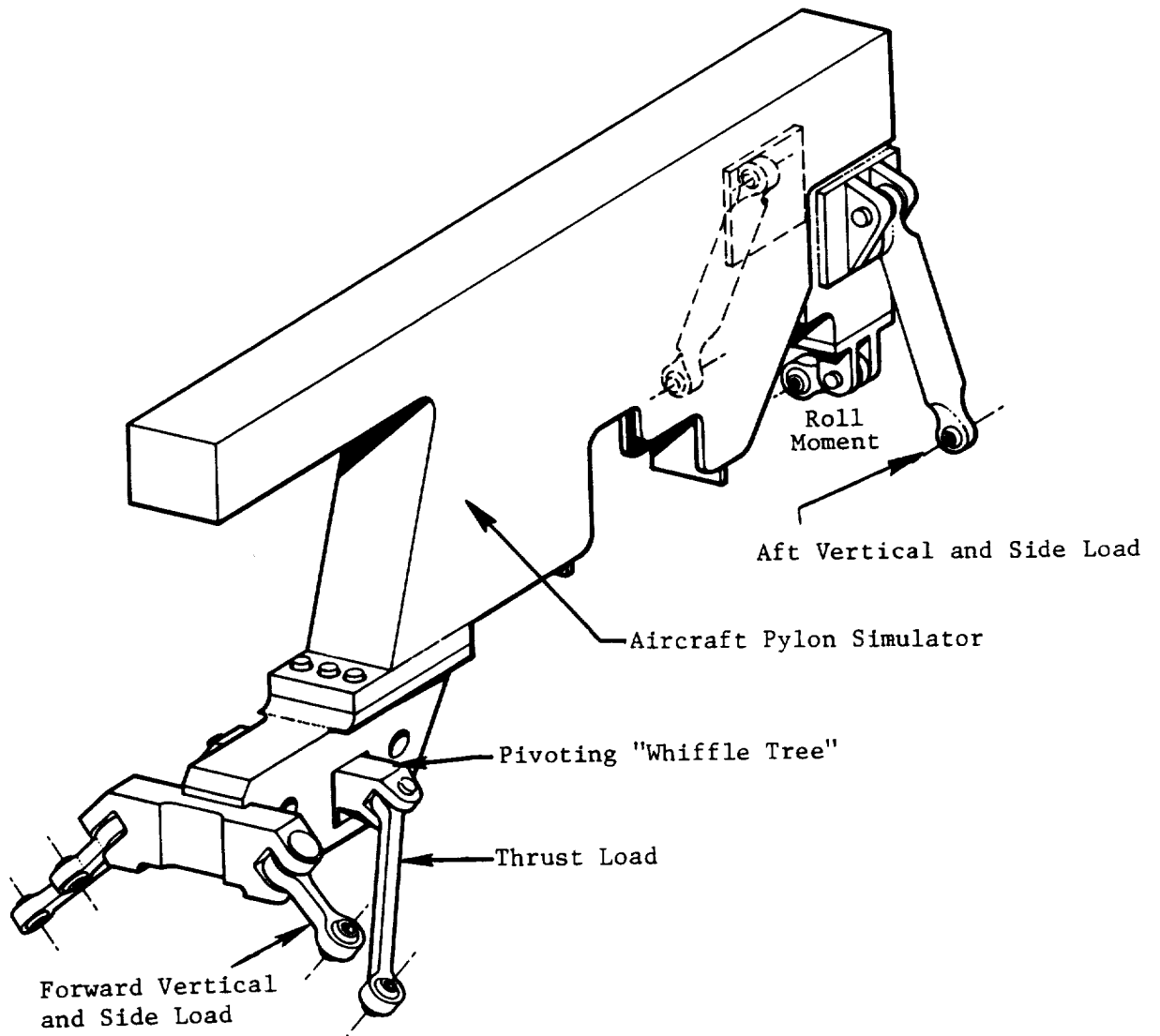


Figure 44. Mount Links.

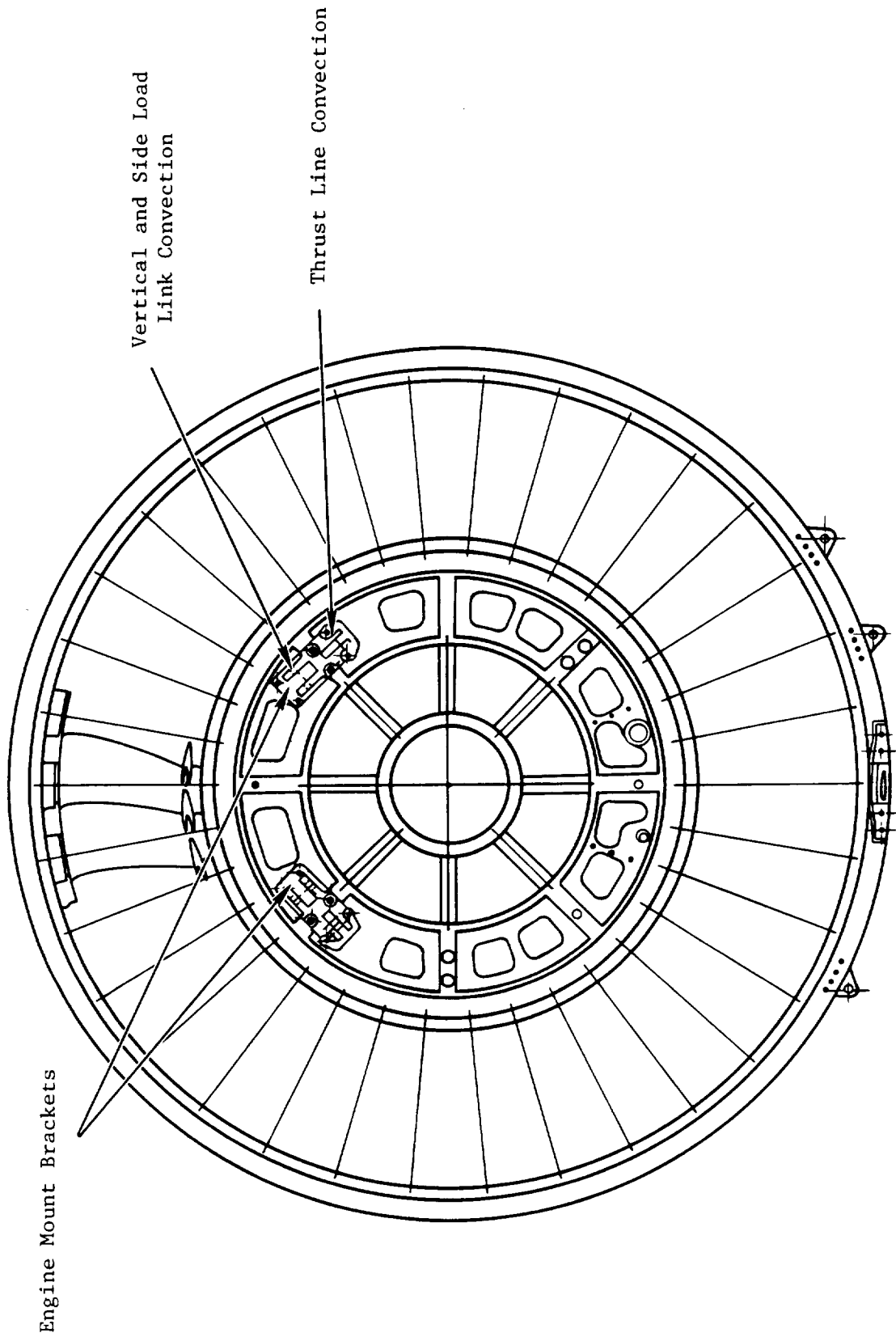


Figure 45. Forward Mount Brackets/Fan Frame.

5.9.3 Accessory Package

The accessory package location for the FPS was selected to reduce fuel consumption and DOC. The principal choices for accessory arrangement were as follows:

- Fan-case-bottom-mounted aircraft and engine accessories.
- Core-component-mounted aircraft and engine accessories, thermally isolated in a shielded and vented compartment.
- Pylon-mounted aircraft accessories with engine accessories in the core compartment.

Evaluation of these systems included consideration of differences in installation drag and pressure losses, weight, maintenance cost, and the impact of these on mission fuel and DOC. Summaries of the results are shown in Tables XXIV and XXV. Because these results tended to favor the core-compartment arrangement, this was chosen as the baseline configuration for the E³. However, the engine design retains the ability to be modified to the other arrangements if desired by users. Figure 46 shows the core-mounted accessory package chosen for the E³ FPS.

5.10 CONTROL SYSTEM

A Full Authority Digital Electronic Control (FADEC) utilizes digital electronic computation and associated control and accessory elements to control fuel flow, fuel distribution, compressor variable stators, active clearance control air, and the thrust reverser. Requirements for the control system are outlined below and are followed by a description of the system and its elements.

5.10.1 Design

Most of the basic control system functional requirements evolve from the engine design definition; this establishes the variables to be controlled and the fundamental control characteristics required. The major control system functional requirements thus established are to:

- Modulate fuel flow to control thrust
- Divide the fuel flow into the two zones of the double annular combustor as required to meet exhaust emission goals

Table XXIV. Accessory Gearbox Location Trade Study Results.

Location	Pylon (Aircraft Accessories) Core (Engine Accessories)	Fan Case (All)	Core Mount (All)
Δ Weight, kg (lbm)	+22.7 (+50)	+34.0 (+75)	0
Δ Maintenance Estimated \$/EFH	+1.84 \rightarrow +2.69	-0.42 \rightarrow -1.27	0
Δ SFC (Drag, ΔP), %	-0.1	+0.65	0
Δ DOC, % ⁽¹⁾	+0.26	+0.13	0
ΔW_f , %	0	+0.72	0

⁽¹⁾Evaluated using 7.9¢ to 13.2¢/liter (30¢ to 50¢/gal) fuel price.

Table XXV. Qualitative Factors in Accessory Package Selection.

Fan Case Mount

- Must be Designed to Comply with FAA Wheels-Up Landing Regulation
- Accessory Fairing Tends to Block Reverser if Side-Mounted
- Aircraft Asymmetry or Left-Hand/Right-Hand Engines if Side-Mounted
- Best Accessibility of Candidate Configurations

Core Compartment Mount

- Some Airline Disfavor from Maintenance, Accessibility Aspect

Pylon Mount

- Airline Disfavor from Accessibility Aspect
- May Have Significant Drag Penalty in Close Nacelle/Wing Placement
- Access and Mounting Problem with DACO-Type Tail Engine Installation

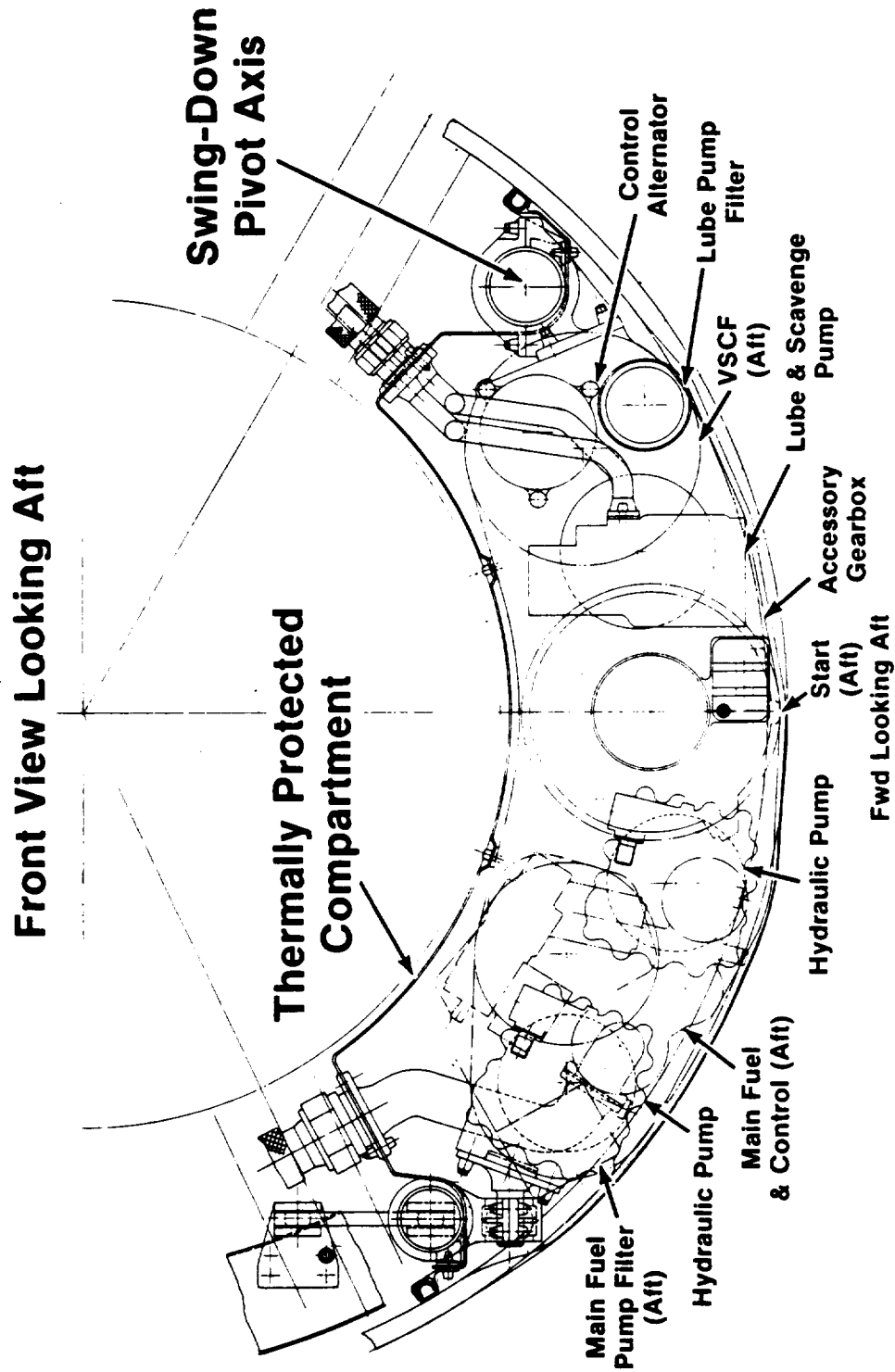


Figure 46. E3 FPS Accessory Package.

- Position the compressor variable stators for best compressor performance
- Position the air valves in the three separate active clearance control systems (compressor, high pressure turbine, and low pressure turbine) to achieve the minimum rotor clearances possible at important operating conditions and to prevent rubbing at any condition
- Control thrust reverser actuation and integrate it with other controlled variables on the engine
- Sense, process, and transmit engine and control system data for engine condition monitoring.

A simplified schematic of the control is shown in Figure 47. The main element in the system is the digital control. The control is designed basically for single channel operation with the intent that in-service development will eventually result in a digital control equal in reliability to current hydromechanical controls which have extensive military and commercial operational development. However, for initial service, redundant controls are considered necessary to achieve the desired operational reliability. The two units will be functionally identical; software logic will cause one to serve as the primary control and the other as an active standby which is brought on line automatically if a primary unit malfunction is detected by self-test within that unit. When satisfactory in-service digital control reliability has been demonstrated, the standby unit will be eliminated from the system.

The system will be designed to operate with input commands and data from the aircraft in the form of multiplexed, digital, electronic signals. Because of the critical nature of the input commands, it is anticipated that these signals will be generated using power from the top-priority aircraft electrical bus, that dual (redundant) signals will be supplied, that the signals will be transmitted over separate lines, and that the signals will include a periodic test word to identify signal malfunctions. It is further anticipated that these signals will be in the form dictated by the applicable specification for aircraft avionics digital data transfer. The controls also receive a number of inputs from electrical sensors on the engine. Most of these will be dual element devices with separate elements supplying each control.

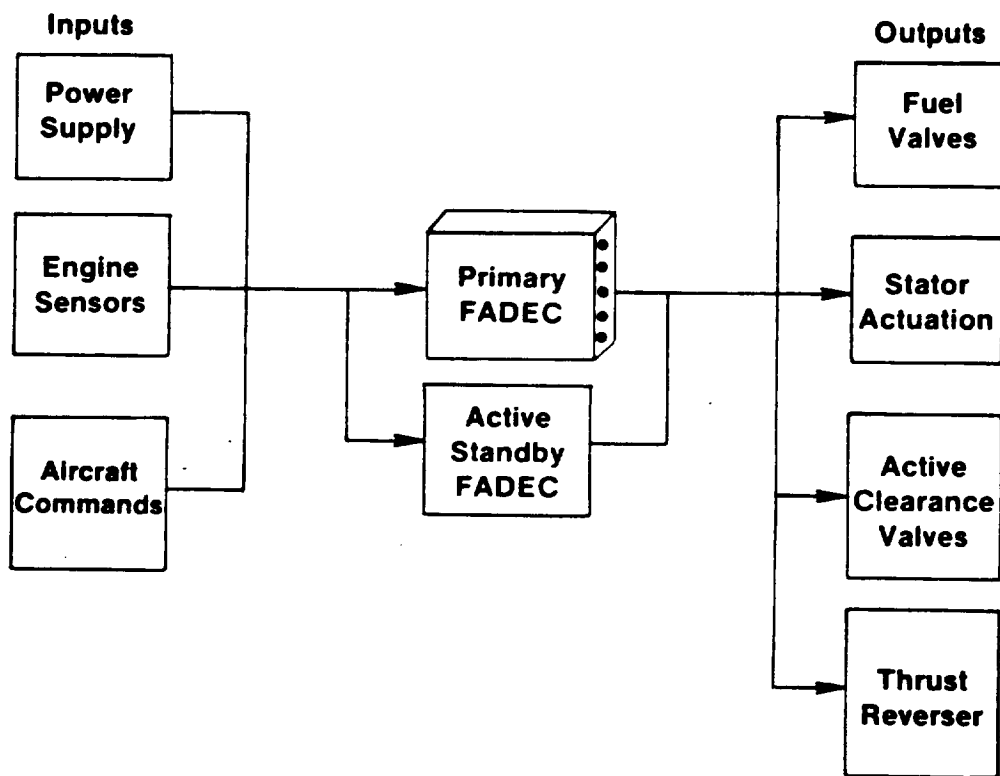


Figure 47. Full Authority Digital Electronic Control (FADEC).

An additional protective feature in the control system is the Failure Indication and Corrective Action (FICA) strategy. FICA detects engine sensor failures and substitutes signals calculated by the FADEC, thus permitting continued operation with a failed sensor. A simplified engine model is incorporated into the FADEC software along with sensor failure detection logic. A mathematical filter technique (extended Kalman filter) is used to continuously update the engine model using data from all unfailed sensors.

An engine-driven control alternator will be the primary source of electrical power for the digital controls. Aircraft power from the 28-volt d.c. system will serve as a backup and will provide power for static control checkout and for engine starts. Use of aircraft power for starts reduces the design speed range of the control alternator and results in a smaller, more efficient design.

Outputs from the digital control operate servovalves which, in turn, control the actuation of the various controlled elements in the system. The servovalves will be multiple-coil electrohydraulic or electropneumatic devices incorporating a fail-safe design feature which causes the element being controlled to remain fixed, or to drift slowly in a safe direction, if the signal from the digital control fails to zero or to maximum current.

The basic engine cycle inputs to the control system are shown pictorially on Figure 48. T_{12} , P_{T0} , and T_{25} serve primarily as control scheduling parameters, but N_1 , N_2 , and T_{42} serve primarily as feedback in the fuel control loop. T_3 and P_{S3} are involved in a turbine inlet temperature calculation, and P_{S3} is also used in transient fuel scheduling. The inputs will also be used for condition monitoring and for the sensor failure accommodation feature.

Two types of temperature sensors are used: resistance temperature detectors for the fan and core inlets, and thermocouples for the compressor discharge and LPT inlet. Pressures are sensed by probes or static taps at appropriate locations and are converted to variable-frequency electrical signals by transducers in the digital control. Fan speed (rpm) is sensed by a magnetic pickup in conjunction with a multitoothed disk on the fan shaft to provide a pulsing signal, with a frequency proportional to fan speed, to the digital control. Core rpm is sensed by measuring the frequency of the FADEC power

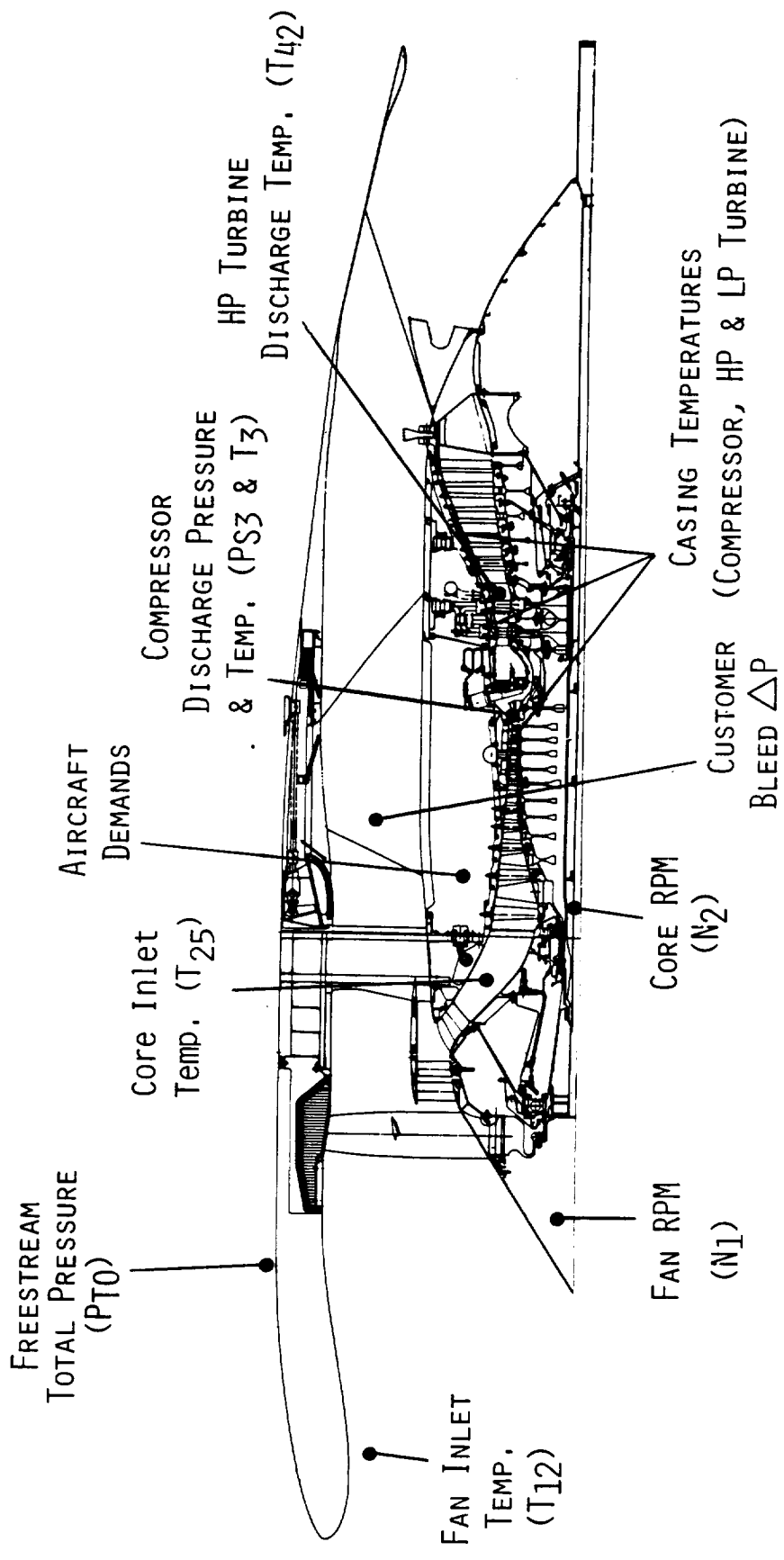


Figure 48. Control System Inputs.

supply from the control alternator, which rotates at a constant multiple of core speed.

The outputs controlled by the system are shown pictorially on Figure 49. The boxes on Figure 49 indicate additional controlled outputs beyond those incorporated on a typical, current, transport engine; namely, the CF6-50C.

The digital control for this engine is a solid-state electronic device designed specifically as an aircraft engine control. The design incorporates a single, time-shared, digital microprocessor operating in conjunction with solid-state memory elements to perform essentially all of the computation and logic required for the various control functions of the engine. Also included are timing and control elements which control processor/memory operation and circuit elements which handle input/output signal functions. The basic clock rate of the computer is 3.5 megahertz, and program running time is approximately 0.010 second.

The digital control design is tailored for operation in an aircraft engine environment and incorporates features aimed at reducing the effects of factors which are known to be major sources of problems. Extensive experience on General Electric military engines with limited authority electrical controls has shown that most problems are associated with mechanical interconnection failures between electrical elements, caused by thermal and vibratory stresses, or with electrical element degradation caused by high temperature. In the digital control, extensive use is made of integrated circuit chips to reduce the number of elements required for interconnection. In addition, most circuit elements are mounted on ceramic, multilayer circuit boards; this further reduces the number of interconnections exposed to vibration and atmospheric effects. Figure 50 is a schematic of this circuit board design. The materials used (namely, Kovar leads, tungsten circuit runs, and alumina boards) all have low and well matched thermal-expansion coefficients to reduce thermal stresses. The circuit boards are mounted to a fuel-cooled aluminum plate to reduce the effects of environmental and internally generated heat.

Digital engine control technology at General Electric has evolved over a period of years, beginning with off-engine units in the early 1970's and proceeding to refined on-engine designs for the NASA/GE QCSEE program and the U.S. Navy/GE FADEC program. The E³ control is an extension of this design,

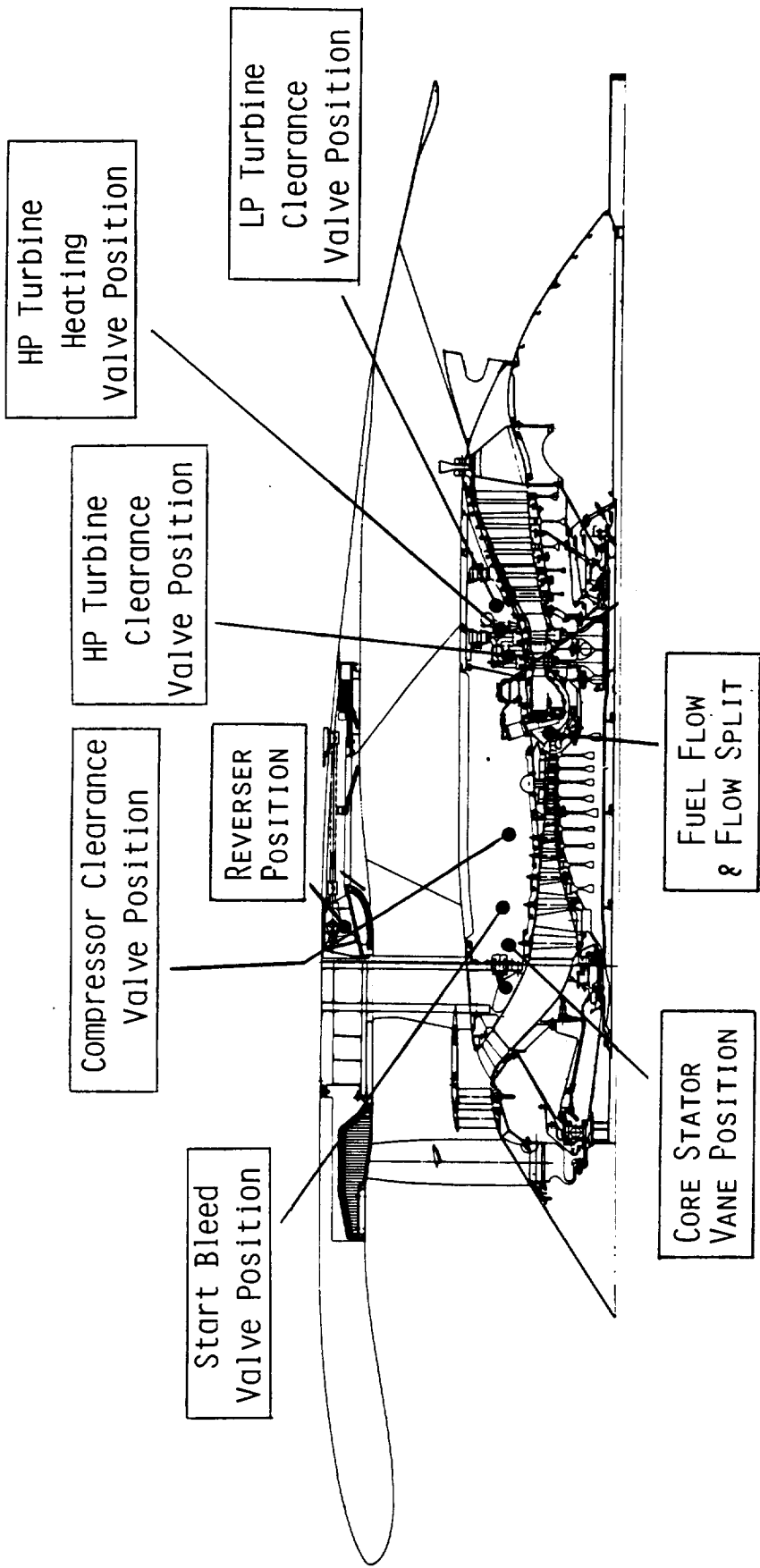
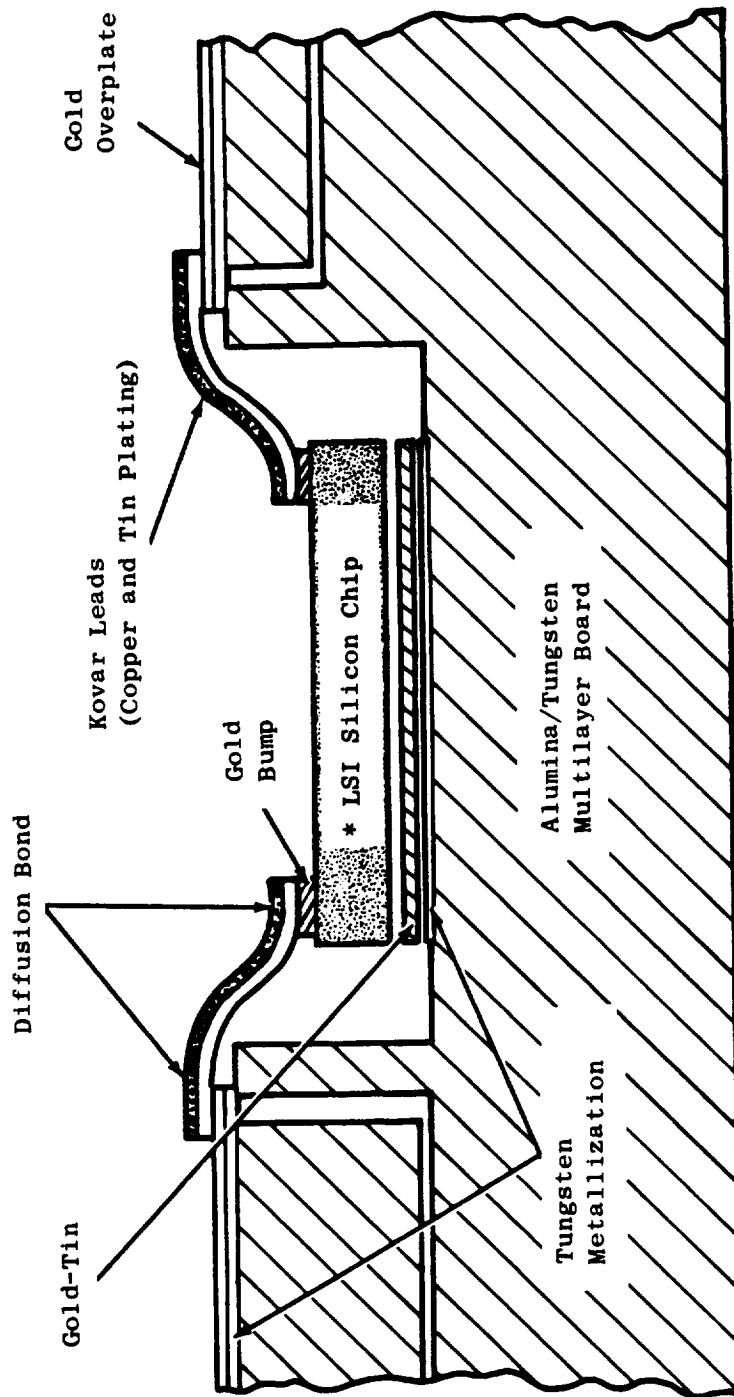


Figure 49. Control System Outputs.



* LSI = Large Scale Integration

Figure 50. Hybrid Electronics.

incorporating a self-contained power supply that eliminates the external voltage regulation required with earlier designs and including input circuitry that accepts signals from thermocouples and engine condition monitoring sensors. An off-engine version of the control was used on the E³ core engine, and an on-engine version (see Figure 51) was used on the ICLS engine. Both controls proved very successful, providing full authority control of the engines and incorporating software that provided extensive adjustability over a digital link from the control room that allowed thorough and efficient exploration of engine characteristics. Engine testing is reported in the Core Design and Performance Report, Reference 8, and the ICLS Design and Performance Report, Reference 9.

5.10.2 Fuel Control System

A schematic of the fuel system is shown in Figure 52. The system uses a positive displacement fuel pump with integral centrifugal boost. Fuel from the positive displacement pump element enters the fuel valve where a metering valve/bypass valve combination meters fuel to the engine and bypasses surplus fuel back to the pump. Metering valve position and, thus, fuel flow are controlled by the digital control by means of an electrohydraulic metering servovalve and an electrical metering valve position feedback transducer. The fuel valve includes a mechanical core-overspeed governor that operates on the bypass valve, a fuel shutoff valve, and a pressurizing valve to maintain sufficient fuel pressure to operate servos at low flow conditions.

Control of fuel flow is basically achieved by modulating flow to set thrust in response to the thrust-command input from the aircraft. Because no practical method is available to sense thrust directly, a study was performed comparing 14 engine variables which can be sensed or computed by the control system and used as a measure of thrust. Included among the candidate parameters were fan rpm, core rpm, a fuel flow related parameter, and various parameters computed from pressure and/or temperature at various points in the engine flowpath. The potential thrust parameters were compared by using a special computer model that operated the engine with each parameter (taken one at a time) in control and applied typical engine and control component tolerances at key operating conditions to define thrust setting accuracy.

ORIGINAL PAGE IS
OF POOR QUALITY

ORIGINAL PAGE
BLACK AND WHITE PHOTOGRAPH

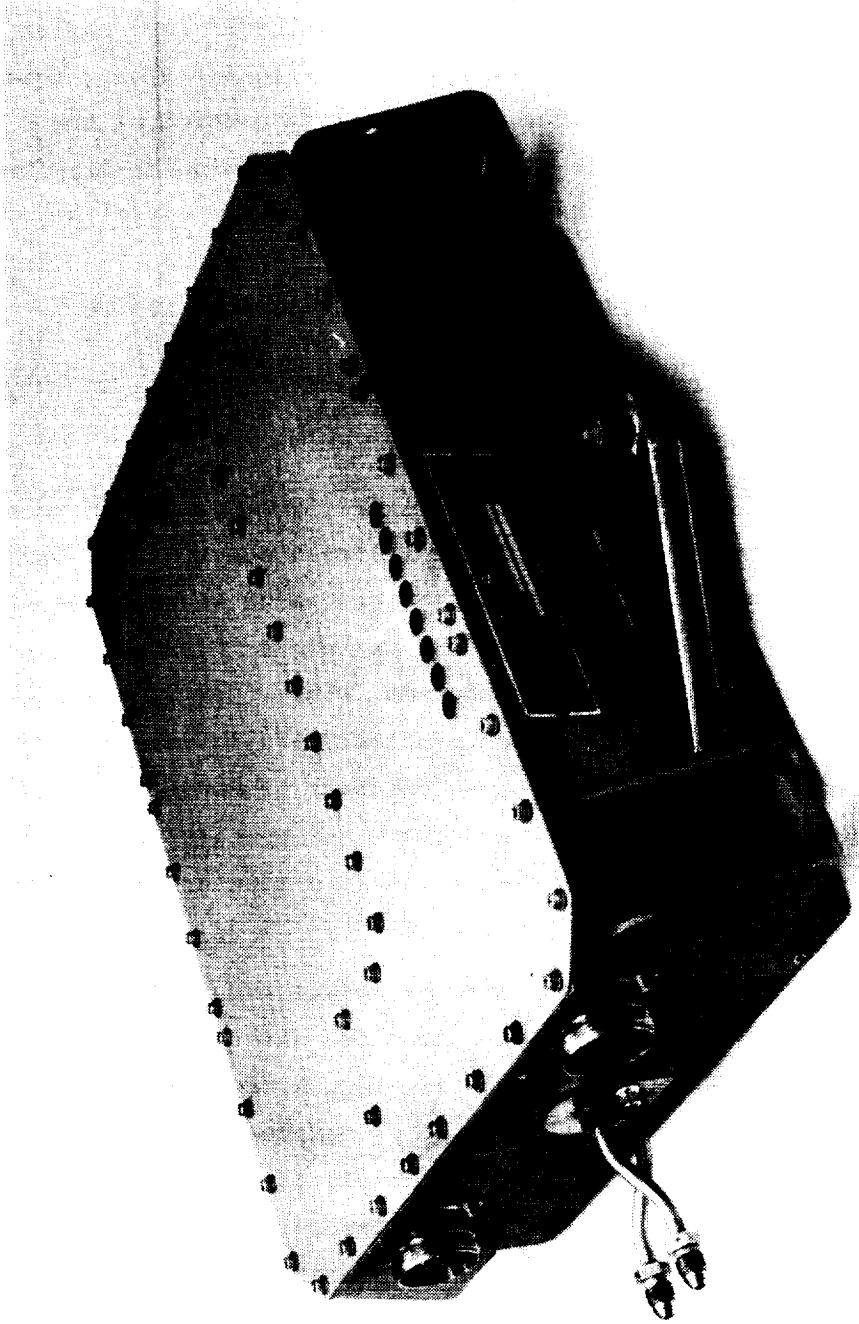


Figure 51. ICLS Full Authority Digital Electronic Control.

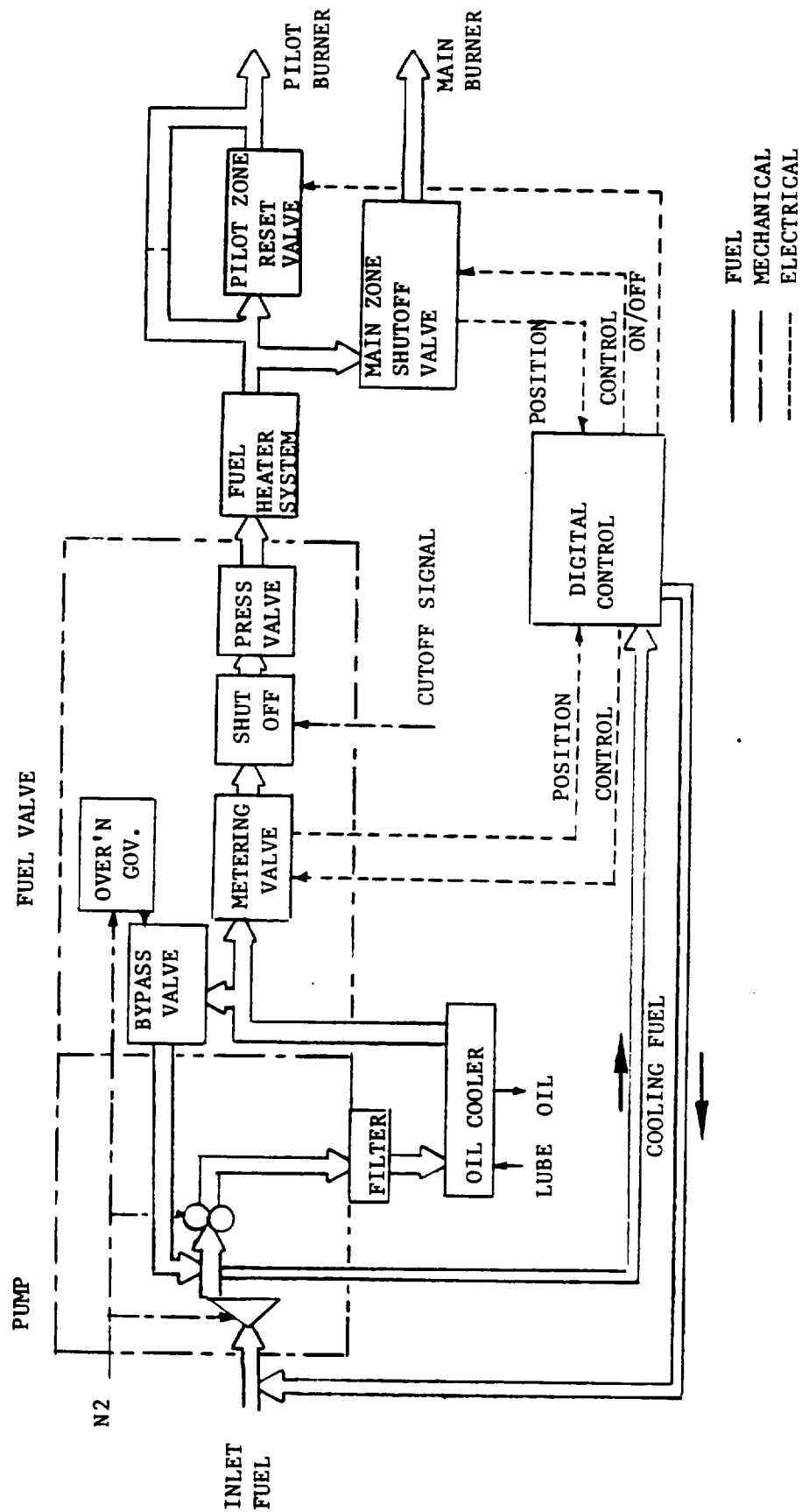


Figure 52. E³ Fuel System.

Of the 14 thrust parameters compared, corrected fan rpm provided the best thrust setting accuracy, and it was selected as the primary fuel controlling parameter. Thus, during normal steady-state operation, fuel flow is modulated to control corrected fan rpm. Fuel flow limits are applied by the digital control to prevent overspeed, overtemperature, compressor stall, or combustor blowout. The flow is then split for the two zones of the combustor, with pilot-zone flow only for starting, ground idle, and flight idle, and with flow in both zones at higher power levels.

The fuel flow split is established primarily by the characteristics of the fuel nozzles, with the digital control selecting and controlling the transition between single- and double-annular combustion by positioning the Main Zone Shutoff Valve (MZSOV) and the Pilot Zone Reset Valve (PZRV). The transition to double annular is made by first opening the MZSOV a small amount so that the empty fuel nozzle injection tubes fill without starving the pilot zone. Dwell time at this intermediate position is controlled as a function of total fuel flow rate. Once this time has elapsed, the MZSOV opens fully and the PZRV is temporarily closed to enrich the main zone for better ignition. The PZRV is reopened after sufficient time has elapsed to assure main zone ignition has occurred. Transition back to single-annular combustion is made by simply closing the MZSOV.

5.10.3 Stator Control System

The core compressor stator control system is shown schematically in Figure 53. A pair of fuel-driven ram actuators operates the stator-actuation system of levers and annular rings around the compressor case. Fuel to the actuators is controlled by an electrohydraulic servovalve on one of the actuators. The servovalve control signal is supplied by the digital control. A position transducer in one actuator provides a feedback signal to the digital control.

The digital control schedules variable stator vane (VSV) position in accordance with a basic corrected core speed schedule, much the same as is done on the CF6-50C, but it also applies a number of compensating biases to exploit the capabilities of variable compressor stators to accommodate the engine transients and widely varying steady-state operating conditions. The

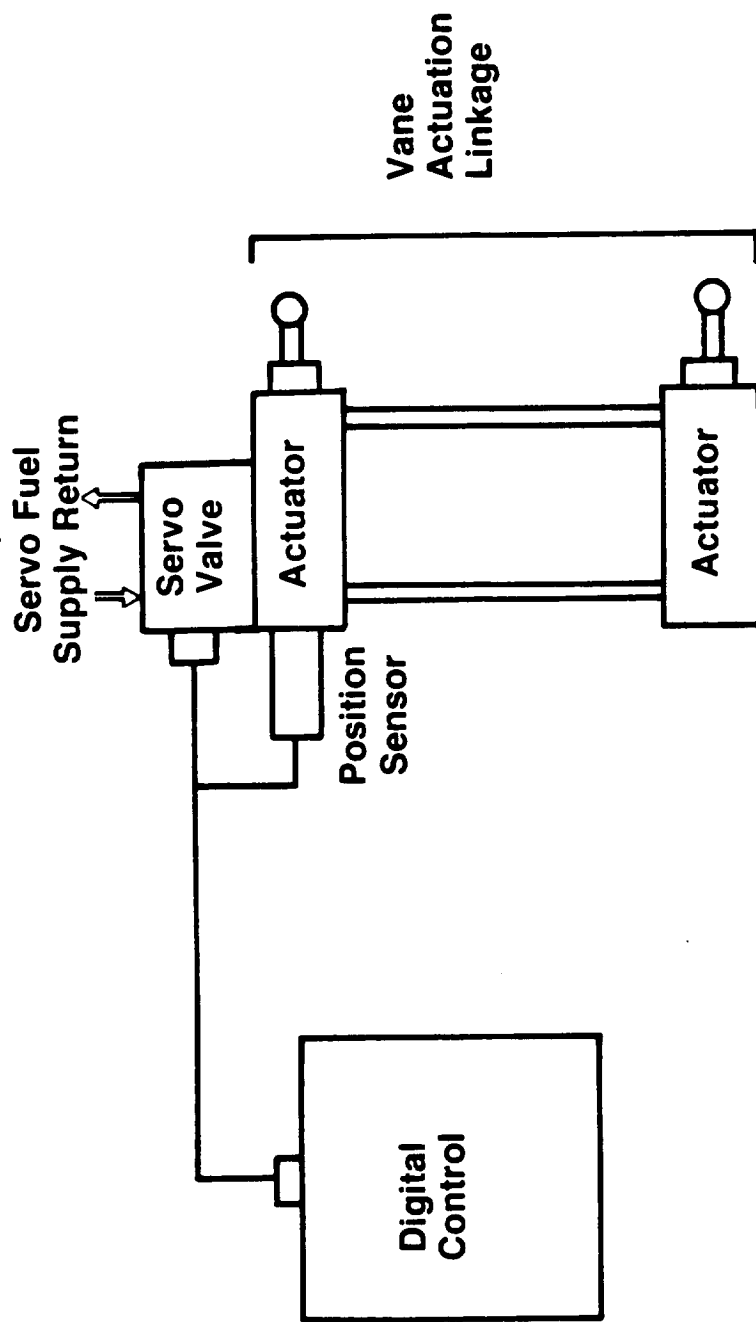


Figure 53. Compressor Stator Vane Control.

exact nature of these biases would be determined during engine development testing. Some of the potential stator biases are listed below.

Rain Reset - Heavy rain causes reduction in core inlet temperature (T_{25}), and termination of rain, combined with the T_{25} sensing lag, can cause compressor stall. This bias is applied in the closing direction when sensed T_{25} is less than calculated T_{25} (as it will be in heavy rain), thus increasing stall margin.

Stall Avoidance - CF6 experience has shown that the optimum stator setting in the cruise corrected speed region is different than the optimum setting in this region on the ground. This schedule modification can be accomplished with a power demand reset of the stators.

Stall Recovery - Experience has shown that recovery from a compressor stall can often be accomplished by temporarily shifting the stators in the closed direction. When a rapid drop in compressor discharge pressure occurs, as it will during a stall, this function creates a temporary stator closure and, simultaneously, a fuel flow reduction. If recovery does not occur, shutdown or power reduction by the pilot will be required as on current engines. If recovery does occur and then the engine stalls a second time, the stator closing bias would be reapplied and left on to provide additional stall margin until the engine is shut down.

Reverse Reset - Experience has shown that it is desirable to bias the stators in the closed direction to accommodate the inlet disturbances that can accompany thrust reverser operation.

Deterioration Compensation - Experience has shown that engine deterioration results in a change in the core speed/fan speed relationship. Stator reset can restore the original relationship and regain some lost internal efficiency.

Bleed Compensation - A stator reset might be used to adjust the compressor operating point and improve efficiency when customer bleed air is being extracted. Such a reset is being shown in the preliminary control system design.

Transient Compensation - It is quite probable that some adjustment to the basic stator schedule would improve transient operation of the compressor

and thereby improve transient response. Also, as demonstrated successfully in the NASA/GE QCSEE Program, transient response at approach conditions can be improved by resetting the stator schedule in the closed direction so that core rpm is higher than normal at approach, and maximum thrust can be reestablished with less rpm change than normally required. Development testing would be required to determine if this could be done without causing aeromechanical compressor instability or unsatisfactory engine efficiency changes.

5.10.4 Active Clearance Control System

As noted in previous sections, this engine has three separate active clearance control systems. Clearance control in compressor Stages 6 through 10 is achieved by modulating the flow of fifth stage bleed air over the aft compressor casing. Clearance control in the turbines is achieved by modulating the flow of air extracted from the fan duct into separate annular manifolds surrounding the HPT and LPT casings.

The control system elements involved in active clearance control are shown schematically in Figure 54. The compressor clearance control air is regulated by a modulating valve actuated by fuel and controlled by an electrohydraulic servovalve operated by a signal from the digital control. An electrical position transducer supplies feedback to the digital control.

The air to each turbine clearance control system is regulated by a two-way, fuel-operated, modulating butterfly valve. Separate valves are included for the HPT and LPT. The digital control operates both valves through electrohydraulic servovalves. Position feedback transducers are included on both valves.

The strategy for controlling clearances is based on casing temperatures. The FADEC senses casing temperatures, calculates target casing temperatures, and modulates cooling air valves to make the sensed casing temperatures match the target temperatures. Target casing temperatures are calculated using a schedule of fan inlet air temperature and core corrected rpm. There is an inherent time delay which gives extra clearance margin on takeoff and initial climb. Clearances for the compressor, HPT, and LPT are controlled independently. A decel modifier shuts off ACC cooling until casing temperature drops

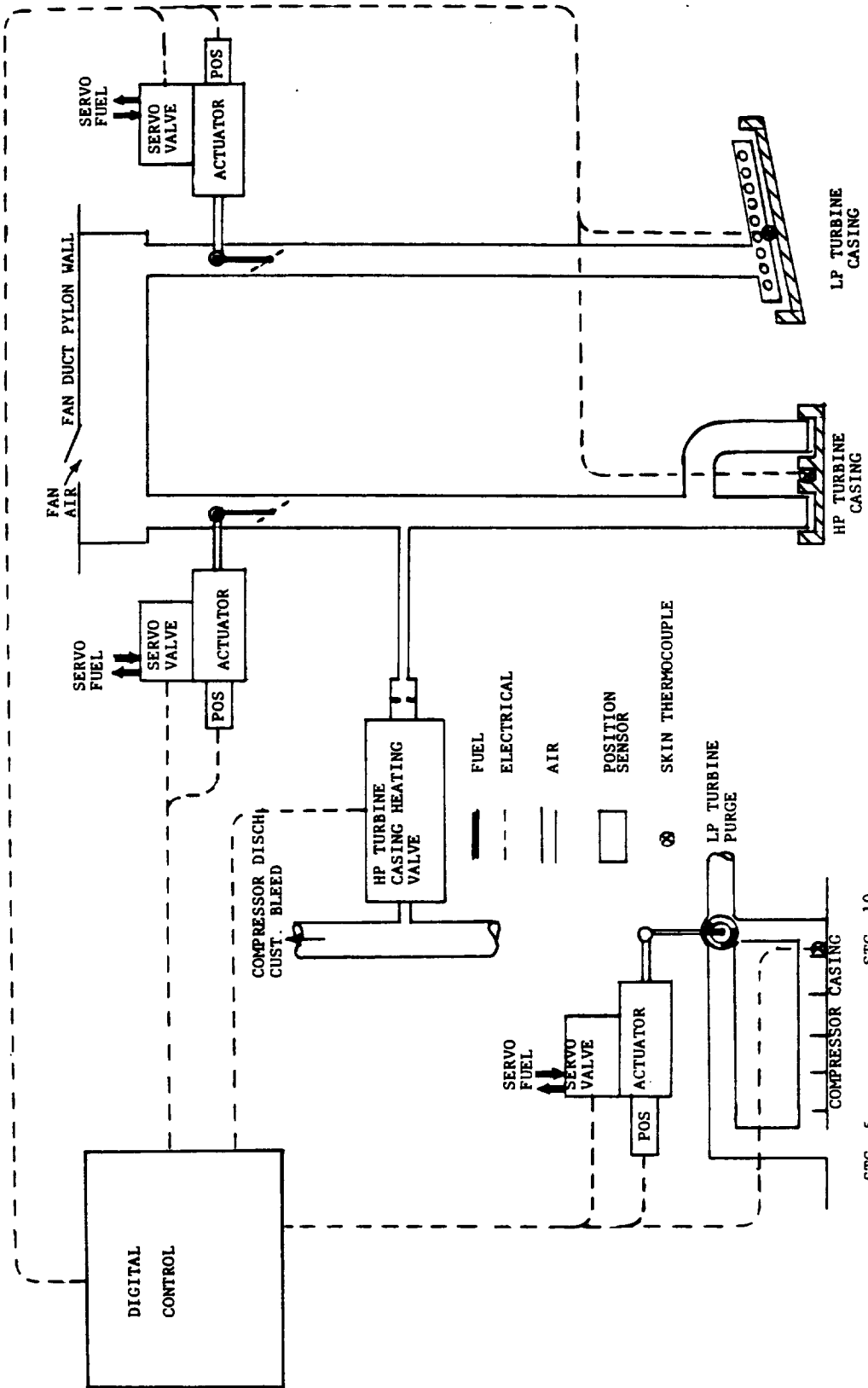


Figure 54. Clearance Control System.

to the scheduled level. This feature acts independently for the compressor, HPT, and LPT.

As discussed in the HPT section, an active clearance control heating circuit warms the casings quickly following startup. This circuit is included in Figure 54. The control keeps a heating air valve open until measured casing temperatures reach normal steady-state idle temperatures.

5.10.5 Fuel Heater/Regenerator System

The FPS uses a fuel heating system to improve fuel consumption. The aircraft environmental control system (ECS) air was selected as the heat source. Heat is transferred from the ECS air to the fuel. This recovers otherwise wasted energy. At idle, the lower fuel flow does not provide an adequate heat sink; therefore, fan air cooling of the ECS air must be used at idle. At takeoff, climb, and cruise, the fuel flow provides a more than adequate heat sink. Above idle, ECS air temperature is controlled by bypassing a portion of the air around the ECS air cooler. The fuel heating system avoids the loss of fan air during aircraft flight, which ordinarily is used to cool ECS air, and then is dumped overboard. The fuel heater/regenerator system is shown schematically in Figure 55.

5.10.6 Performance

ICLS testing provided an extensive final test of the E³ control system. The ICLS results are listed below. More detailed information is available in Reference 9.

- Speed Governing - Both core (up to 30% thrust) and fan (above 30%) speed controls were stable. The switchover from core to fan control was smooth.
- Transition - Transitions between single- and double-annular combustion were smooth and reliable.
- Fuel Flow Limits - T_{42} , P_{S3} , and T_{41} calculated limits on fuel flow were demonstrated.
- Stator Scheduling - A maximum deviation of only ± 0.5 degree was achieved during fast transients.

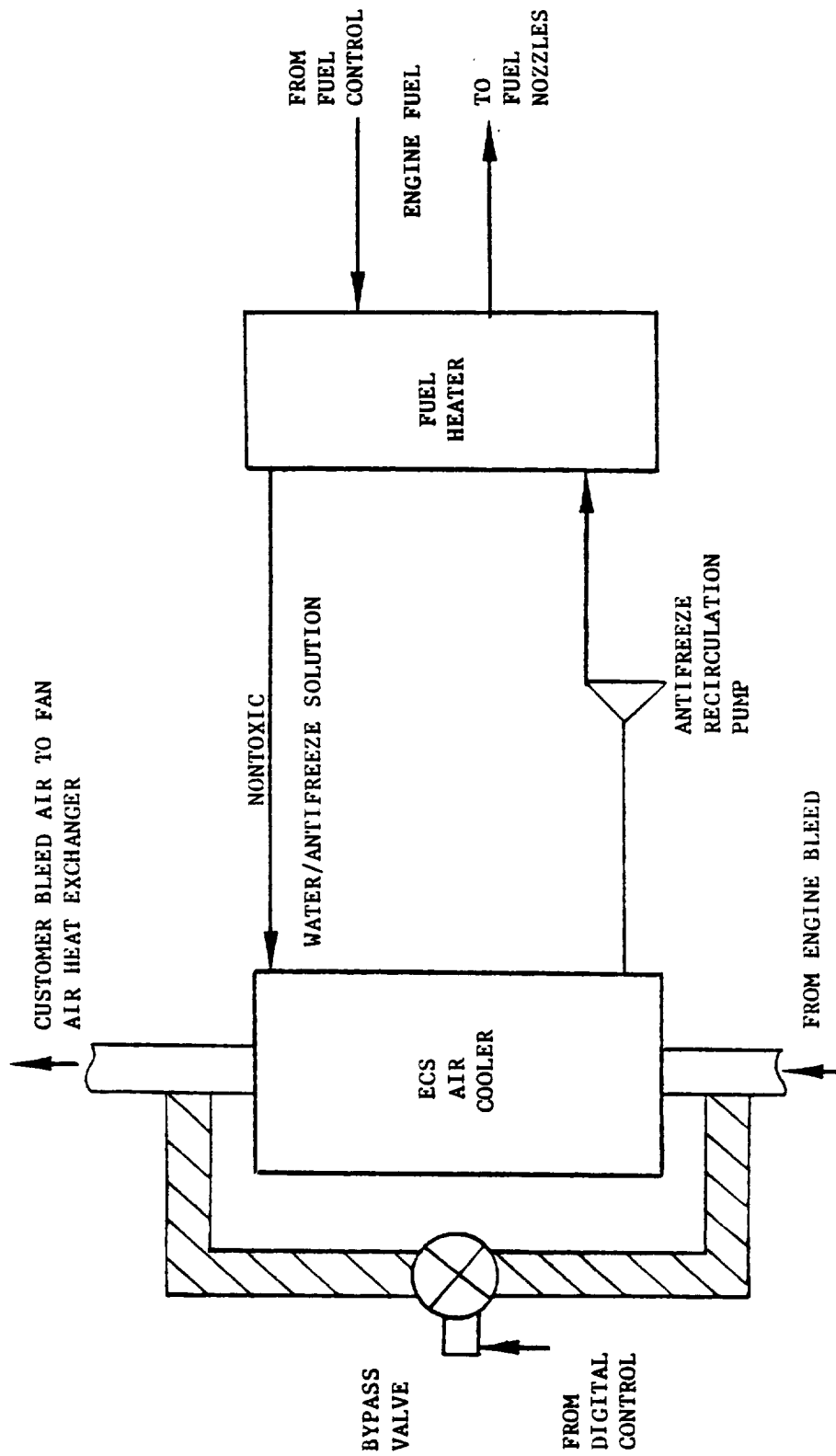


Figure 55. Fuel Heater/Regenerator Schematic.

- Accel/Decel Transients - The control functioned properly. Minimum demonstrated time from flight idle to 90% thrust was approximately 5.5 seconds. No stalls or blowouts occurred during transient testing.
- Active Clearance Control - Closed loop ACC was demonstrated for the compressor and LPT. Closing off ACC air during a deceleration was demonstrated. FADEC control of ACC was not used for the HPT because the HPT ACC system had been modified and used to correct an eccentricity problem.
- FICA - Failures of T_3 , T_{42} , T_{25} , fan speed, core speed, P_{S3} , fan speed plus T_3 , fan speed plus T_{42} , and fan speed plus T_{25} were simulated. All simulated sensor failures except core speed produced normal operation, both steady state and transiently. The core speed failure operation was marginally acceptable. Time did not permit developing a solution. However, with more work, core speed failure FICA would be resolved for FPS.
- Reliability - The FADEC was mounted on the fan case. No problems were encountered during the 65 hour test.

5.11 DYNAMIC SYSTEM

5.11.1 Design

A high load squeeze film damper has been designed as an integral part of the FPS engine system. This damper is configured to provide effective vibration control over a broad unbalance range that includes low-to-abusive unbalance levels. The design incorporates a tuned core rotor bearing support arrangement combined with a multiple film squeeze film damper located at the core rotor forward bearing (No. 3 bearing). The damper-suspension system reduces the dynamic response levels by driving the bending strain energy associated with core rotor bending into the tuned bearing supports. This allows the squeeze film damper that is in parallel with the forward tuned bearing support to provide an efficient energy sink to dissipate the energy of vibration through the action of viscous damping. Figure 56 shows the bearing support system and the damper. The bearing supports are "squirrel cage" structures that provide relatively soft load paths through spring elements machined integrally with the cylindrical structural portions. It was established that a 5.254×10^7 N/m (3×10^5 lb/in) spring rate for each squirrel cage would provide the required rotor centering action for maneuver loads (based on requirements for the flight propulsion system configuration) and also permit

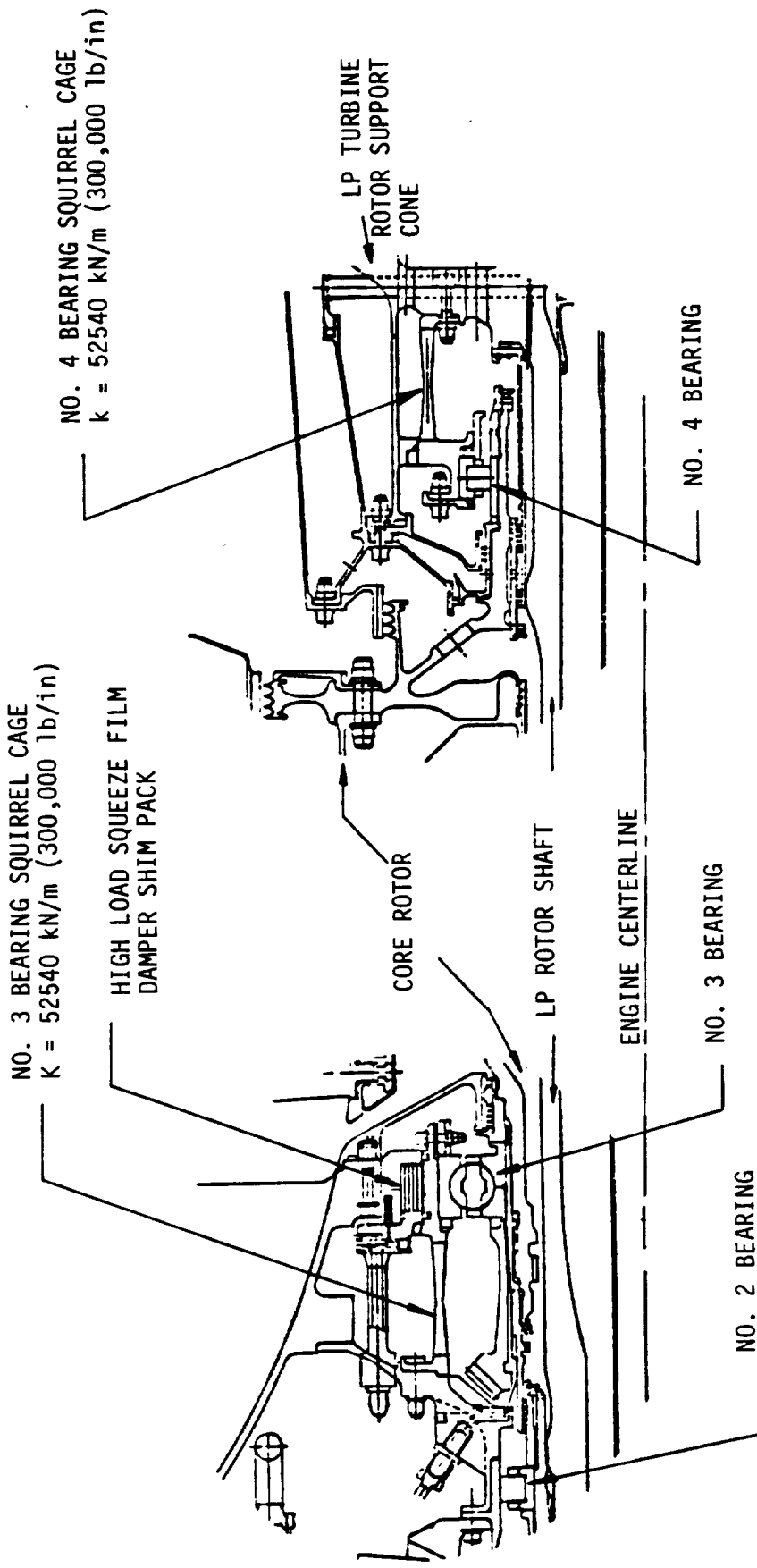


Figure 56. Core Rotor Soft Support and Squeeze-Film Damper System.

the squeeze film damper to provide the desired vibration control. As shown in Figure 56 and in greater detail in Figure 57, the damper consisted of a sealed squeeze film damper with sleeves or shims inserted in the damper annulus. The insertion of the sleeves into the squeeze film resulted in small clearance annuli and the sum of the individual clearances provided a relatively large overall clearance. The combination of small clearance annuli and circumferential flow results in high damping and the large overall clearance allows large deflections to occur with a low spring rate.

5.11.2 Performance

The FPS rotor support system was evaluated in ICLS testing. The test results demonstrated excellent system vibration characteristics with an absence of speed avoidance zones over the complete operating range. Engine vibration levels were well behaved and the vibration response characteristics showed good agreement with pretest calculations. Maximum synchronous vibration levels were recorded at the No. 3 bearing accelerometer located on the soft side (rotor side) of the forward squirrel cage; 0.104 mm-DA (4.1 mils-DA) 1/core at 3,200 rpm N_F /12,420 rpm N_C and 0.127 mm-DA (5 mils-DA) 1/fan at 2,600 rpm N_F /11,900 rpm N_C . As predicted, the core synchronous response levels indicated very highly damped behavior characterized by a basically flat response curve over the core operating speed range. The No. 3 bearing high load damper (multifilm sealed configuration) in conjunction with the soft-mounted core rotor provided this expected vibration control. It will be noted that in addition to a static squirrel cage spring support at the forward core rotor bearing, this engine employs a unique rotating squirrel cage spring support at the aft core rotor bearing. Fan synchronous vibration response was associated with rigid body motion of the core rotor off of the soft suspension system. No trace of the fan nodding mode (coupled fan rotor/fan frame) was detected in the fan operating speed range. This was consistent with the pretest analysis which predicted the fan nodding mode to be well above the operating speed range. As expected, there was no evidence of whirl instability, which was consistent with the highly damped core rotor mounting.

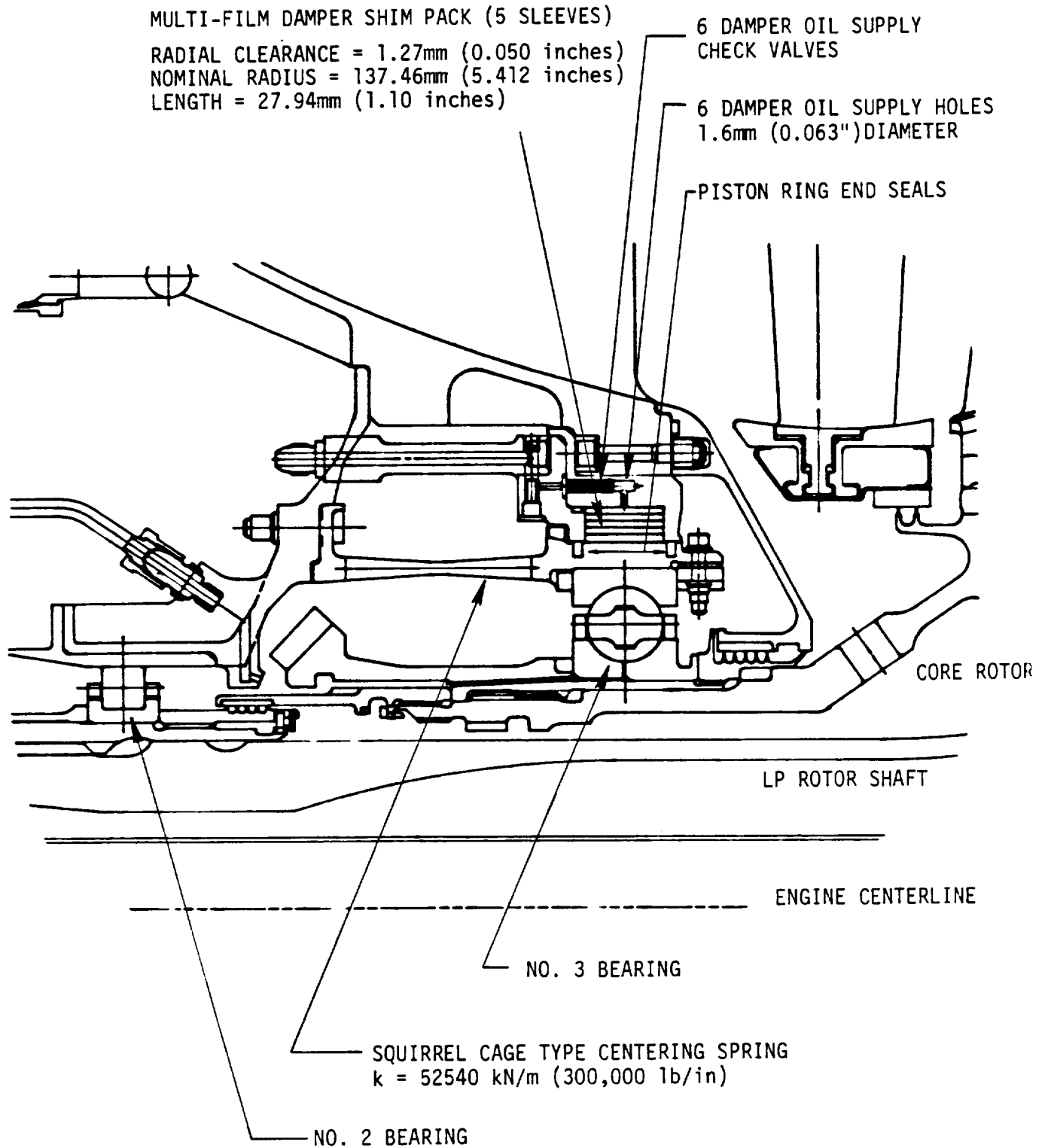


Figure 57. Number 3 Bearing Soft Support and High Load Damper.

5.12 WEIGHT

The FPS is a 211-cm (83-in) diameter fan engine with a core sized for 54.4 kg/sec (120 lbm/sec) corrected flow. Takeoff thrust was originally 162.4 kN (36,500 lbf). Because of component efficiency improvements and a rematched cycle using those components, takeoff thrust for the final FPS has increased to 175.3 kN (39,000 lbf). The component weight breakdown for this engine is detailed in Table XXVI.

5.13 COST

The estimated purchase costs for the various components that make up the FPS are provided in Table XXVII. These costs are for the 250th production engine and are expressed in 1980 dollars.

Maintenance costs are \$90.64 per engine flight hour, also expressed in 1980 dollars.

Table XXVI. FPS Weight Summary.

<u>Fan & Booster Module</u>	<u>kg</u>	<u>lbm</u>
Rotor	481	1,061
Frame & Stators	622	1,370
Subtotal	1,103	2,431
<u>LPT Module</u>		
Rotor	260	573
Stator	257	567
Frame, Mixer, & Centerbody	221	488
Shaft, Cone	99	218
Subtotal	837	1,846
<u>Core Module</u>		
Compressor Rotor	214	472
Compressor Stator	235	518
Combustor, Casing & Diffuser	137	303
HPT Rotor	283	623
HPT Stator	132	290
Subtotal	1,001	2,206
<u>Miscellaneous</u>		
Configurations	123	272
Lube Hardware	24	53
Control & Accessories	65	143
Sumps, Driver, & Seals	320	705
Subtotal	532	1,173
<u>Basic Engine Total</u>	3,473	7,656
<u>Installation</u>		
Inlet	162	358
Reverser	379	835
Cowl, Pylon & Exhaust	181	400
Engine Buildup	270	595
Total	992	2,188
<u>Installed Engine Total</u>	4,465	9,844

Table XXVII. FPS Cost Summary.

Purchase cost, 250th engine in 1980 dollars

Bare Engine	
Fan Module	\$ 559,000
LPT Module	440,000
Core Module	1,045,000
Miscellaneous	598,000
Total	2,642,000
Installation	
Inlet	217,000
Fan Reverse and Duct	450,000
Core Cowl and Tailpipe	122,000
Engine Buildup	236,000
Total	\$1,033,000
Installed Engine	\$3,675,000

6.0 ENGINE/AIRCRAFT INTEGRATION

In order to ensure that the FPS represented a practical design fully capable of installation on advanced aircraft, a substantial effort early in the program concentrated on aircraft/engine integration studies. Through subcontracts with the major commercial aircraft companies (Boeing, Douglas, and Lockheed), mission evaluations of E³ versus current (CF6-50C) technology were performed in advanced study aircraft. An important part of the subcontract effort dealt with review and critique of the installation design to establish suitability of the E³ engine for installation on advanced commercial aircraft. Elements of the installation such as the inlet, thrust reverser, mount system, accessory package, and aft cowling were reviewed and, in many cases, changed to reflect aircraft company input regarding aerodynamic and structural design of the installation. Another important part of the effort dealt with the evaluation of the fuel burned and direct operating cost (DOC) benefits of the FPS installed in advanced aircraft.

The engine/aircraft integration results are presented in Reference 2. An updated assessment of the economic payoff due to E³ is presented in the following discussions.

6.1 SENSITIVITY FACTORS

Each airframe company established relationships between changes in engine specifications and the service payoff. Changes in engine sfc, weight, maintenance cost, and purchase cost were related to changes in aircraft fuel burned and DOC. General Electric also established these relationships, called sensitivity factors or trade factors. These factors were used for optimization studies and for economic payoff analysis.

The original airframe company work was for very low fuel prices, in the 7.9¢ to 13.2¢ per liter (30¢ to 50¢/gallon) range. Since then, a composite set of sensitivity factors was generated from the airframe data, and this has been adjusted to current fuel prices.

The sensitivity factors are for "rubber aircraft," meaning that a change in engine weight or sfc is reflected in a change in the aircraft design and weight, and fuel load.

The airframe data were for two-, three-, and four-engine aircraft, flying from 926 to 12,038 km (500 to 6,500 nmi), and carrying 196 to 500 seats. Distinctions were made between "design" flights and "typical" flights. However, this distinction was less than the considerable scatter between the different sources, so no distinction between design and typical flights is made in the updated sensitivity factors.

The sensitivity factors are presented in terms of 1980 dollars and are for the FPS size engine. The aircraft fuel burned trades are as follows:

- A 1% change in sfc yields 1.3% change in fuel burned.
- A 340 kg (750 lbm) change in weight yields a 1.3% change in fuel burned.

The DOC sensitivity factors are presented in Table XXVIII.

6.2 ECONOMIC EVALUATION

Once a system has met its basic operating requirements such as longevity, environmental considerations, safety, etc., the bottom line measure of the value of the system is its productivity per dollar expenditure. The FPS is measured in terms of an improvement in DOC compared to the CF6-50C reference engine.

The three contributing airframe companies evaluated the early form of the FPS in their advanced aircraft. Since then, the FPS has changed slightly, sfc has improved, and fuel price has increased substantially. The final FPS has been reevaluated with these changes.

The economic analysis of the final FPS is presented in Table XXIX and Figure 58. It is presented as an improvement in DOC for a variety of advanced aircraft using the FPS, compared to similar aircraft using the CF6-50C.

The E³ economic program goal is to achieve a 5% reduction in DOC from a typical current production engine, taken as the CF6-50C. The DOC reduction achieved by the E³ FPS exceeds the goal on all study aircraft, and ranges from 8.6% to 16.1%, based on a fuel price of \$0.396/liter (\$1.50/gallon) in 1980 dollars.

Table XXVIII. Direct Operating Cost Sensitivity Factors.

1980 \$'s

	<u>% Change In DOC</u>			
	For			
	1% ΔSFC	181kg (400#) Δ Weight	\$5.95 Δ Maintenance Flight Hour	\$213,000 Δ Purchase Cost
For \$0.13/liter (\$0.48/Gallon)				
Flying 926 km (500 N Mi)	0.50	.50	.50	.51
1,232 km (665)	.50	.50	.50	.50
1,852 km (1,000)	.51	.50	.50	.49
3,704 km (2,000)	.52	.50	.49	.48
5,556 km (3,000)	.54	.50	.48	.47
12,038 km (6,500)	.58	.52	.45	.45
For \$0.40/liter (\$1.50/Gallon)				
Flying 926 km (500 N Mi)	.75	.56	.35	.35
1,232 km (665)	.76	.56	.35	.35
1,852 km (1,000)	.77	.57	.34	.34
3,704 km (2,000)	.79	.57	.33	.32
5,556 km (3,000)	.81	.57	.32	.31
12,038 km (6,500)	.86	.59	.28	.29
For \$0.66/liter (\$2.50/Gallon)				
Flying 926 km (500 N Mi)	.88	.60	.27	.28
1,232 km (665)	.89	.60	.27	.28
1,852 km (1,000)	.90	.60	.27	.27
3,704 km (2,000)	.92	.61	.26	.25
5,556 km (3,000)	.94	.61	.25	.24
12,038 km (6,500)	.99	.62	.22	.21

Table XXIX. DOC Improvements.

	E ³ Improvements in DOC Over CF6-50C	
	\$0.396/l (\$1.50/g) Fuel Price in 1980 Dollars	\$0.661/l (\$2.50/g) Fuel Price in 1980 Dollars
Boeing, 2 Engines, 196 Passengers 3,704 km (2,000 nmi) Design Flight 1,232 km (665 nmi) Typical Flight	10.9% 8.6%	13.0% 10.9%
Lockheed, 3 Engines, 500 Passengers 5,556 km (3,000 nmi) Design Flight 2,593 km (1,400 nmi) Typical Flight	12.0% 10.3%	13.9% 12.3%
Lockheed, 4 Engines, 500 Passengers 12,038 km (6,500 nmi) Design Flight 5,556 km (3,000 nmi) Typical Flight	16.2% 14.1%	18.3% 16.1%
Douglas, 3 Engines, 458 Passengers 5,556 km (3,000 nmi) Design Flight 1,852 km (1,000 nmi) Typical Flight	13.1% 11.5%	15.3% 13.8%

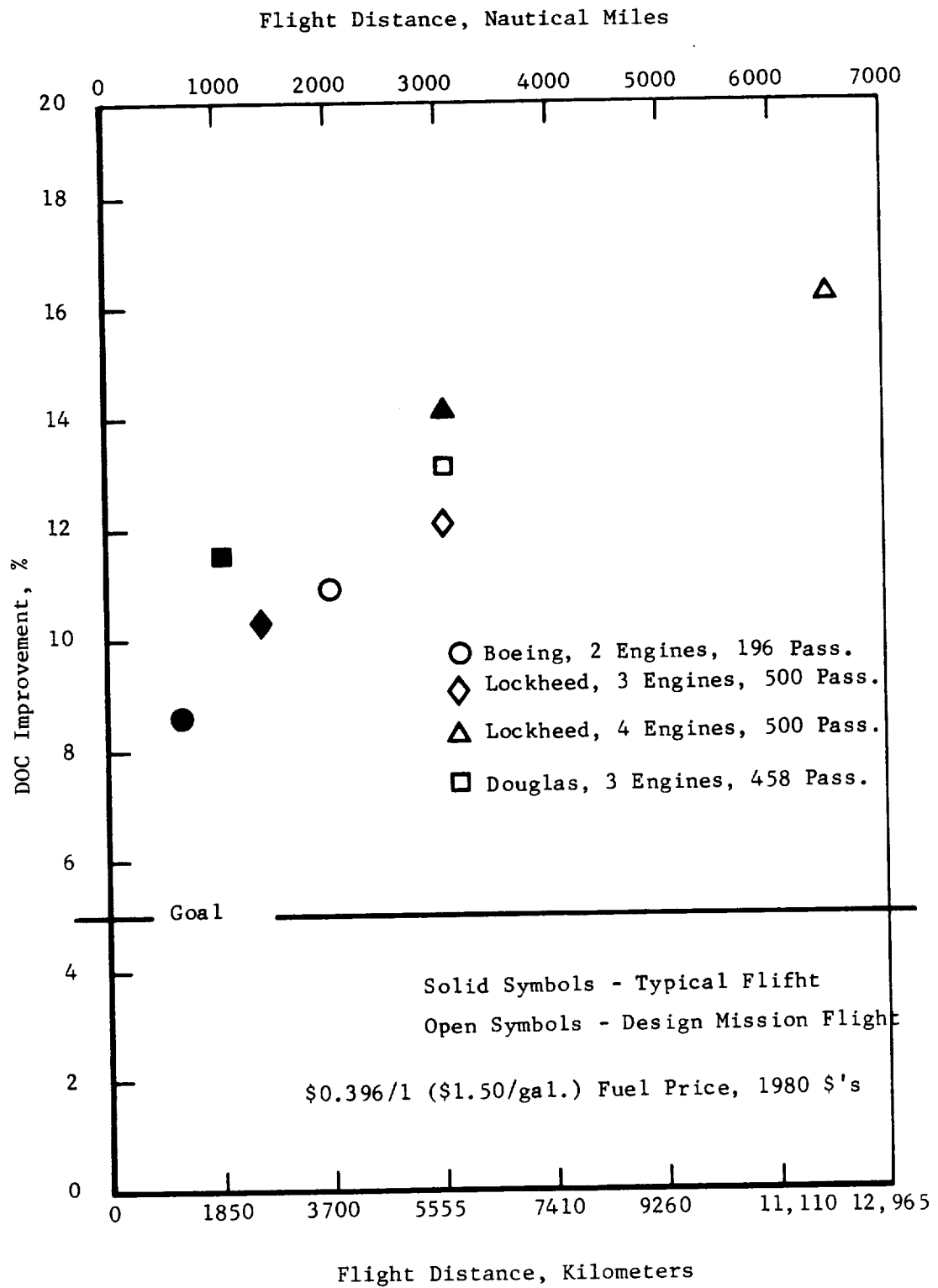


Figure 58. E³ DOC Improvements Relative to CF6-50C.

7.0 CONCLUSIONS

The General Electric E³ FPS incorporates advanced technology for direct transfer into engines of today and of the future.

The goals established at E³ program inception have been met or exceeded by the NASA/GE E³ FPS. A summary of these goals versus achievements follows.

Specific Fuel Consumption

Goal - To reduce installed sfc at least 12% relative to that of the CF6-50C, evaluated at maximum cruise.

Achievement - 16.9% reduction.

Performance Retention

Goal - To experience no more than half of the service performance deterioration of a CF6-50C.

Achievement - Goal met.

Direct Operating Cost

Goal - To reduce aircraft DOC by at least 5% from that for similar CF6-50C powered aircraft.

Achievement - A 8.6% to 16.2% lower DOC, depending on the aircraft used and the flight length.

Noise

Goal - To comply with FAR 36 (March 1978) noise standards.

Achievement - Goal met with margin.

Emissions

Goal - To meet EPA proposed standards for engines certified after January 1981.

Achievement - Goal met.

8.0 RECOMMENDATIONS

While the technology demonstrated in the NASA/GE E³ program is being transferred to current and future product line aircraft engines, substantial additional technology awaits demonstration of readiness for such transfer.

With today's commercial airline fleet burning 10 billion dollars worth of fuel per year, an improvement in the fuel efficiency of this fleet's engines of only 1% would pay for the entire NASA/GE E³ program in one year, and the NASA/GE E³ achieved a 16.9% improvement.

Such tremendous returns on investment are rare, and it is highly recommended that such technology programs as the NASA/GE E³ program continue to receive Government support in the future.

9.0 REFERENCES

1. Johnston, R.P., et al., "Energy Efficient Engine - Flight Propulsion System Preliminary Analysis and Design," NASA-Lewis Research Center, NASA CR-159583, November 1979.
2. Patt, R.F., "Energy Efficient Engine - Flight Propulsion System Aircraft/Engine Integration Evaluation," NASA-Lewis Research Center, NASA CR-159584, June 1980.
3. Stearns, E.M., "Energy Efficient Engine - Flight Propulsion System Preliminary Analysis and Design Update," NASA-Lewis Research Center, NASA CR-167980, August 1976.
4. Neitzel, R.E., Hirschcron, R., and Johnston, R.P., "Study of Turbofan Engine Designed for Low Energy Consumption," NASA-Lewis Research Center, NASA CR-135053, August 1976.
5. Neitzel, R.E., Hirschcron, R., and Johnston, R.P., "Study of Unconventional Engine Designed for Low Energy Consumption," NASA-Lewis Research Center, NASA CR-135136, December 1976.
6. Wisler, D.C., Koch, C.C., and Smith, L.H. Jr., "Preliminary Design Study of Advanced Multistage Axial Flow Core Compressors," NASA-Lewis Research Center, NASA CR-135133, February 1977.
7. Johnston, R.P., et al., "Energy Efficient Engine - Preliminary Design and Integration Study," NASA-Lewis Research Center, NASA CR-135444, September 1978.
8. Stearns, E.M., et al., "Energy Efficient Engine - Core Design and Performance Report," NASA-Lewis Research Center, NASA CR-168069, December 1982.
9. Stearns, E.M., et al., "Energy Efficient Engine - Integrated Core/Low Spool Design and Performance Report," NASA-Lewis Research Center, NASA CR-168211, August 1983.

DISTRIBUTION LIST

NASA Headquarters
600 Independence Avenue, SW
Washington, DC 20546
Attn: R/R. S. Colladay
RJ/C. C. Rosen
RP/J. Facey (2 copies)
RS/L. Harris

NASA Lewis Research Center
21000 Brookpark Road
Cleveland, OH 44135

Attn: J. A. Ziemianski	MS 86-1
C. C. Ciepluch	MS 100-3
J. E. Rohde	MS 86-7
P. G. Batterton	MS 86-7
G. K. Sievers	MS 86-7
M. J. Hartmann	MS 3-7
L. J. Kiraly	MS 23-2
J. F. Groeneweg	MS 86-7
J. C. Williams	MS 500-211
A. Strazisar	MS 5-9
H. E. Rohlik	MS 86-7
R. G. Willoh	MS 77-9
J. J. Reinmann	MS 86-7
L. J. Bober	MS 86-7
A. G. Powers	MS 86-4
R. E. Coltrin	MS 86-7
C. L. Ball	MS 5-9
E. A. Willis	MS 500-212
E. J. Graber	MS 86-7
E. T. Meleason	MS 86-7
D. A. Sagerser	MS 86-7
R. D. Hager	MS 86-7 (10 copies)
Library	MS 60-3 (2 copies)
Report Control Office	MS 60-1
Tech. Utilization Office	MS 7-3
J. R. Mihalow	MS 77-8
L. Reid	MS 5-9
AFSC Liaison Office	MS 501-3
Army R&T Propulsion Lab	MS 302-2

NASA Ames Research Center
Moffett Field, CA 94035
Attn: M. H. Waters 202-7

DISTRIBUTION LIST (Continued)

NASA Langley Research Center
Langley Field, VA 23365
Attn: R. Leonard
D. Maiden
L. J. Williams

NASA Scientific and Technical Information Facility
P. O. Box 8757
B. W. I. Airport, MD 21240
Attn: Accession Dept. (20 copies)

NASA Dryden Flight Research Center
P. O. Box 273
Edwards, CA 93523
Attn: J. A. Albers

Department of Defense
Washington, DC 20301
Attn: R. Standahar 3D1089 Pentagon

Wright-Patterson Air Force Base
Dayton, OH 45433
Attn: APL Chief Scientist AFWAL/PS
E. E. Abell ASD/YZE
H. I. Bush AFWAL/POT
R. P. Carmichael ASD/XRHI
R. Ellis ASD/YZN
W. H. Austin, Jr. ASD/ENF

Eustis Directorate
U. S. Army Air Mobility
R&D Laboratory
Fort Eustis, VA 23604
Attn: J. Lane, SAVDL-EU-Tapp

Navy Department
Naval Air Systems Command
Washington, DC 20361
Attn: W. Koven AIR-03E
J. L. Byers AIR-53602
E. A. Lichtman AIR-330E
G. Derderian AIR-5362C

Naval Air Propulsion Test Center
Trenton, NJ 08628
Attn: J. J. Curry
A. A. Martino

DISTRIBUTION LIST (Continued)

U. S. Naval Air Test Center
Code SY-53
Patuxent River, MD 20670
Attn: E. A. Lynch

USAVRAD Command
P. O. Box 209
St. Louis, MO 63166
Attn: Robert M. Titus

Department of Transportation
NASA/DOT Joint Office of Noise
Abatement
Washington, DC 20590
Attn: C. Foster

Federal Aviation Administration
Noise Abatement Division
Washington, DC 20590
Attn: E. Sellman AEE-120

Engine Manufacturers

Curtiss Wright Corporation
Woodridge, NJ 07075
Attn: S. Lombardo
S. Moskowitz

Cummins Engine Company
Technical Center
500 S. Poplar
Columbus, IN 47201
Attn: J. R. Drake

Detroit Diesel Allison Division
of General Motors Corporation
P. O. Box 894
Indianapolis, IN 46206
Attn: W. L. McIntire

AVCO Lycoming
550 S. Main Street
Stratford, CT 06497
Attn: H. Moellmann

DISTRIBUTION LIST (Continued)

Detroit Diesel Allison Division
of General Motors Corporation
333 West First Street
Dayton, OH 45402
Attn: F. H. Walters

AiResearch Manufacturing Company
111 South 34th Street
P. O. Box 5217
Phoenix, AZ 85010
Attn: C. E. Corrigan (93-120/503-4F)

The Garrett Corporation
AiResearch Manufacturing Company
Torrance, CA 90509
Attn: F. E. Faulkner

Williams Research Company
2280 West Maple Road
Walled Lake, MI 48088
Attn: R. VanNimwegen
R. Horn

The Garrett Corporation
AiResearch Manufacturing Company
402 S. 36th Street
Phoenix, AZ 85034
Attn: Library

Teledyne CAE, Turbine Engines
1330 Laskey Road
Toledo, OH 43612
Attn: R. H. Gaylord

General Electric Company/AEBG
One Neumann Way
Evendale, OH 45215
Attn: K. W. Schuning (3 copies) MD H-42
T. F. Donohue MD H-44

General Electric Company/AEBG
1000 Western Avenue
Lynn, MA 01910
Attn: R. E. Neitzel

DISTRIBUTION LIST (Continued)

Pratt & Whitney
Engineering Division
P. O. Box 2691
West Palm Beach, FL 33402
Attn: B. A. Jones MS 713-11

Pratt & Whitney
Engineering Division
400 Main Street
East Hartford, CT 06108
Attn: W. Gardner (3 copies) MS 162-13
I. Mendelson MS 162-31

Airframe Manufacturers

Boeing Commercial Airplane Company
P. O. Box 3707
Seattle, WA 98124
Attn: P. E. Johnson MS 9H-46
D. C. Nordstrom MS 73-01

Boeing Aerospace Company
P. O. Box 3999
Seattle, WA 98124
Attn: D. S. Miller MS 40-26
H. Higgins

The Boeing Company, Wichita Division
Wichita, KS 67210
Attn: D. Tarkelson

Gates Learjet Corporation
P. O. Box 7707
Wichita, KS 67277
Attn: E. Schiller

Douglas Aircraft Company
McDonnell Douglas Corporation
3855 Lakewood Boulevard
Long Beach, CA 90846
Attn: R. T. Kawai Code 36-41
M. Klotzsche

Douglas Aircraft Company
McDonnell Douglas Corporation
P. O. Box 516
St. Louis, MO 63166
Attn: F. C. Claser Dept. 243

DISTRIBUTION LIST (Continued)

Lockheed California Company
Burbank, CA 91502
Attn: J. F. Stroud Dept. 75-42
R. Tullis Dept. 75-21

Lockheed Georgia Company
Marietta, GA 30060
Attn: H. S. Sweet

General Dynamics Convair
P. O. Box 80847
San Diego, CA 92138
Attn: S. Campbell MZ 632-00

Grumman Aerospace Corporation
South Oyster Bay Road
Bethpage, NY 11714
Attn: C. Hoeltzer

Rockwell International
International Airport
Los Angeles Division
Los Angeles, CA 90009
Attn: A. W. Martin

Airlines

American Airlines
Maintenance & Engineering Center
Tulsa, OK 74151
Attn: W. R. Neeley

Delta Airlines, Inc.
Hartsfield-Atlanta
International Airport
Atlanta, GA 30320
Attn: C. C. Davis

Eastern Airlines
International Airport
Miami, FL 33148
Attn: A. E. Fishbein

Transworld Airlines
605 Third Avenue
New York, NY 10016
Attn: A. E. Carrol

DISTRIBUTION LIST (Continued)

Pan American World Airways, Inc.
JFK International Airport
Jamaica, NY 11430
Attn: A. MacLarty

United Airlines
San Francisco International Airport
Maintenance Operations Center
San Francisco, CA 94128
Attn: J. J. Overton

Others

Hamilton Standard
Bradley Field
Windsor Locks, CT 06096
Attn: P. J. Dumais MS 1A-3-1

Westinghouse Electric Corporation
P. O. Box 5837
Beulah Road
Pittsburgh, PA 15236
Attn: Library

Fluidyne Engineering Corporation
5900 Olson Memorial Highway
Minneapolis, MN 55422
Attn: J. S. Holdhusen

University of Tennessee Space
Institute
Tullahoma, TN 37388
Attn: Dr. V. Smith

Rohr Corporation
P. O. Box 878
Foot & H Street
Chula Vista, CA 92012
Attn: Library

TRW Equipment Group
TRW, Inc.
23555 Euclid Avenue
Cleveland, OH 44117
Attn: I. Toth

DISTRIBUTION LIST (Continued)

Solar Division
International Harvester
2200 Pacific Highway
San Diego, CA 92112
Attn: Library

Aerospace Corporation
R&D Center
Los Angeles, CA 90045
Attn: Library

Gas Dynamics Laboratories
Aerospace Engineering Building
University of Michigan
Ann Arbor, MI 48109
Attn: Dr. C. W. Kaufmann

Massachusetts Institute of Technology
Department of Astronautics & Aeronautics
Cambridge, MA 02139
Attn: Library

Brunswick Corporation
2000 Brunswick Lane
Deland, FL 32720
Attn: A. Erickson

Massachusetts Institute of Technology
Department of Structural Mechanics
Cambridge, MA 02139
Attn: J. Mar
A. Epstein

Drexel University
College of Engineering
Philadelphia, PA 19104
Attn: A. M. Mellor

Penn State University
Department of Aerospace Engineering
233 Hammond Building
University Park, PA 16802
Attn: Dr. B. Lakshminarayana



